

SYNTHESIS OF HALOGENATED FLAVONOIDS AS ANTI-DENGUE AGENTS



A Thesis Submitted in Partial Fulfillment of the Requirements  
for the Degree of Master of Science in Chemistry

Department of Chemistry

Faculty of Science

Chulalongkorn University

Academic Year 2018

Copyright of Chulalongkorn University

การสังเคราะห์แฮไลเจนเทตเฟลไวโนอยด์เพื่อเป็นสารต้านไข้เลือดออก



วิทยานิพนธ์นี้เป็นส่วนหนึ่งของการศึกษาตามหลักสูตรปริญญาวิทยาศาสตรมหาบัณฑิต

สาขาวิชาเคมี ภาควิชาเคมี

คณะวิทยาศาสตร์ จุฬาลงกรณ์มหาวิทยาลัย

ปีการศึกษา 2561

ลิขสิทธิ์ของจุฬาลงกรณ์มหาวิทยาลัย

Thesis Title	SYNTHESIS OF HALOGENATED FLAVONOIDS AS ANTI-DENGUE AGENTS
By	Miss Thao Huynh Nguyen Thanh
Field of Study	Chemistry
Thesis Advisor	Assistant Professor WARINTHORN CHAVASIRI, Ph.D.

---

Accepted by the Faculty of Science, Chulalongkorn University in Partial Fulfillment of the Requirement for the Master of Science

..... Dean of the Faculty of Science  
(Professor POLKIT SANGVANICH, Ph.D.)

THESIS COMMITTEE

..... Chairman  
(Associate Professor VUDHICHAJ PARASUK, Ph.D.)

..... Thesis Advisor  
(Assistant Professor WARINTHORN CHAVASIRI, Ph.D.)

..... Examiner  
(Tanatorn Khotavivattana, Ph.D.)

..... External Examiner  
(Assistant Professor Wimolpan Rungprom, Ph.D.)

จุฬาลงกรณ์มหาวิทยาลัย  
CHULALONGKORN UNIVERSITY

เถา ฮุน เหวียน ธานท์ : การสังเคราะห์แฮโลจีนเทตเฟลโวนอยด์เพื่อเป็นสารต้าน  
ไข้เลือดออก. ( SYNTHESIS OF HALOGENATED FLAVONOIDS AS ANTI-DENGUE  
AGENTS) อ.ที่ปรึกษาหลัก : ผศ. ดร.วรินทร์ ชวศิริ

เฟลโวนอยด์แสดงฤทธิ์ทางชีวภาพหลากหลาย อนุพันธ์เฟลโวนอยด์บางชนิดแสดงฤทธิ์  
ดีกว่าสารเริ่มต้น เมื่อไม่นานมานี้ มีรายงานว่าแฮโลจีนเทตเฟลโวนอยด์แสดงฤทธิ์ต้านไข้เลือดออก  
ในการศึกษานี้ ได้สังเคราะห์อนุพันธ์โบรมิเนตและไอโอดิเนตเฟลโวนอยด์ยี่สิบสองตัว และ  
ศึกษาฤทธิ์ทางชีวภาพ พบว่าเป็นการรายงานการศึกษาของอนุพันธ์สิบเจ็ดชนิดเป็นครั้งแรก 8-  
bromobaicalein, 6,8-dibromopinocembrin, 6,8-dibromopinostrobin และ 6,8-  
diiodopinostrobin มีศักยภาพเป็นสารต้านไข้เลือดออกและไม่มีความเป็นพิษ สารเหล่านี้แสดงค่า  
EC<sub>50</sub> ต่ำและค่า CC<sub>50</sub> สูง ซึ่งสามารถพิจารณาได้ว่าเป็นสารออกฤทธิ์ในการรักษาที่มีศักยภาพ  
นอกจากนี้ได้ศึกษาสารในกลุ่ม brominated O<sup>7</sup>-ether chrysin เบื้องต้น พบว่า 6,8-dibromo-  
O<sup>7</sup>-butylchrysin และ 6,8-dibromo-O<sup>7</sup>-hexylchrysin แสดงฤทธิ์ที่น่าสนใจ อย่างไรก็ตาม  
ภายใต้ภาวะของการทดลองนี้สารบางตัวไม่ละลาย แม้ว่าความสัมพันธ์ระหว่างความยาวของสายโซ่  
และฤทธิ์ทางชีวภาพไม่สอดคล้องกัน เพอร์เซ็นต์การยับยั้งพริกซ์เพิ่มขึ้น จากสายโซ่ที่มีหมู่เอทิลถึง  
หมู่เฮกซิล

จุฬาลงกรณ์มหาวิทยาลัย  
CHULALONGKORN UNIVERSITY

สาขาวิชา เคมี  
ปีการศึกษา 2561

ลายมือชื่อนิสิต .....

ลายมือชื่อ อ.ที่ปรึกษาหลัก .....



# # 6072054423 : MAJOR CHEMISTRY

KEYWORD: Halogenated flavonoids, brominated *O*<sup>7</sup>-ether chrysin, anti-dengue agents

Thao Huynh Nguyen Thanh : SYNTHESIS OF HALOGENATED FLAVONOIDS AS ANTI-DENGUE AGENTS. Advisor: Asst. Prof. WARINTHORN CHAVASIRI, Ph.D.

Flavonoids have been recognized as promising compounds with various bioactivities. Certain flavonoid derivatives exhibited more potent activities than their parent compounds. Recently, halogenated flavonoids have been addressed for their anti-dengue activity. In this research, a series of twenty-two brominated and iodinated flavonoid derivatives were synthesized and explored for dengue infection inhibition. Seventeen derivatives have been investigated for the first time. 8-Bromobaicalein, 6,8-dibromopinocembrin, 6,8-dibromopinostrobin, 6,8-diiiodopinostrobin were disclosed as effective and non-toxic anti-dengue agents. These compounds displayed remarkably low  $EC_{50}$  as well as high  $CC_{50}$ , which could be considered as potent therapeutic agents. Moreover, the preliminary screening on brominated *O*<sup>7</sup>-ether chrysin discovered some noticeable compounds, for example, 6,8-dibromo-*O*<sup>7</sup>-butylchrysin and 6,8-dibromo-*O*<sup>7</sup>-hexylchrysin; nonetheless, some synthesized brominated *O*<sup>7</sup>-ether chrysin were insoluble under tested conditions. Though the relationship between the length of side chain and bioactivity were inconsistent, there was a gradually increasing in percentage of plaque inhibition from ethyl to hexyl in case of 6,8-dibromo *O*<sup>7</sup>-ether chrysin.

Field of Study: Chemistry

Student's Signature .....

Academic Year: 2018

Advisor's Signature .....

## ACKNOWLEDGEMENTS

The author wants to express her grateful and special appreciation to her advisor, Assistant Professor Dr. Warinthorn Chavasiri for his patient instruction, generous support and dedication during her Master study. Thanks to his lessons, the author can nourish her desires in science.

It would be the author's honor to have Associate Professor Dr. Vudhichai Parasuk, Assistant Professor Dr Wimolpun Rungprom and Dr. Tanatorn Khotavivattana as her committees, as well as having their comments, suggestions and advice to complete her thesis.

The author wishes to thank for the supporting from the 90th Anniversary of Chulalongkorn University Fund and Natural Products Research Unit (NPRU) for supplement of chemicals and laboratory equipment through her research.

Moreover, the author wants to give a sincere thankfulness to PhD students Kieu Van Nguyen, Trang Hoang Thuy Thuy Le, Master students Nha Thanh Tran, Truc Thi Hong Phan and other Vietnamese friends as well as Thai and Indonesia friends for their physical and mental supporting through her study. Without these things, the author could not be strong enough to get over difficulties last two years.

Specially, the author wants to say an honest thank to Nhung Thi Tuyet Ngo, the one who has helped her since the beginning of application, and for her good and bad times. No matter how long the time passes, the author will never forget what they have been through together. The author wishes all the best for Nhung's life.

Last but not least, the author wants to express her deepest grateful to her parents and sister in Viet Nam, who always encourage, motivate and believe in her ability since she was a child. No words can describe their sacrifices for her success. From the bottom of her heart, they are the precious relationships she has in her life.

Thao Huynh Nguyen Thanh

## TABLE OF CONTENTS

	Page
ABSTRACT (THAI).....	iii
ABSTRACT (ENGLISH).....	iv
ACKNOWLEDGEMENTS .....	v
TABLE OF CONTENTS .....	vi
LIST OF TABLES.....	ix
LIST OF FIGURES .....	x
LIST OF ABBREVIATIONS .....	xiv
Chapter 1 Introduction.....	1
1.1 Dengue.....	1
1.1.1 Introduction.....	1
1.1.2 Clinical therapies.....	2
1.2 Flavonoids.....	3
1.2.1 Introduction.....	3
1.2.2 Anti-dengue activity of flavonoids.....	5
1.3 Halogenated flavonoid derivatives.....	8
1.3.1 Halogenation of flavonoids.....	8
1.3.2 Anti-dengue activity of halogenated flavonoids.....	10
1.3.3 Review of other bioactivities of halogenated flavonoids.....	11
Chapter 2 Experimental .....	15
2.1 Instruments and equipment.....	15
2.2 Chemicals.....	15

2.3 Synthesis of halogenated flavonoids.....	16
2.3.1 Hydrolysis of hesperetin (15) and baicalein (18) from their corresponding glycosides.....	16
2.3.2 Brominated flavonoids.....	17
2.3.3 Iodinated flavonoids.....	18
2.3.4 Brominated $O^7$ -ether chrysin.....	18
2.4 Anti-dengue activity study.....	25
2.4.1. Preliminary screening.....	25
2.4.2. Cytotoxicity of compounds with cell lines.....	26
2.4.3. Effective concentration ( $EC_{50}$ ).....	26
2.4.4. Cytotoxic concentration ( $CC_{50}$ ).....	27
Chapter 3 Results and discussion.....	28
3.1 Halogenation of flavonoids.....	28
3.1.1 Preliminary study on the halogenation of chrysin (34).....	28
3.1.2 Halogenation of selected flavonoids.....	30
3.1.3 Anti-dengue evaluation of halogenated flavonoids.....	39
3.2 Brominated $O^7$ -ether chrysin as anti-dengue agents.....	46
3.2.1 Literature review of $O^7$ -ether chrysin.....	46
3.2.2 Synthesis of brominated $O^7$ -ether chrysin.....	49
3.2.3 Anti-dengue activity of brominated $O^7$ -ether chrysin.....	59
Chapter 4 Conclusions.....	63
REFERENCES.....	65
APPENDIX.....	70
VITA.....	101



จุฬาลงกรณ์มหาวิทยาลัย  
**CHULALONGKORN UNIVERSITY**

## LIST OF TABLES

<b>Table 1.1</b> Percentage inhibition of DENV-2 NS2B-NS3 virus protease cleavage <sup>a</sup> of compounds <b>7</b> and <b>9</b> . [14] .....	6
<b>Table 1.2</b> Half maximal inhibitory concentration (IC <sub>50</sub> ) and selective index (SI) of naringenin ( <b>12</b> ) for anti – DENV activity in Huh7.5 cells.[18].....	8
<b>Table 1.3</b> EC <sub>50</sub> and SI values of halogenated chrysin ( <b>19</b> ) and ( <b>20</b> ). [24].....	11
<b>Table 2.1</b> Structures of flavonoids derivatives <b>19</b> , <b>42</b> - <b>62</b> .....	19
<b>Table 3.1</b> Screening of halogenation of chrysin ( <b>34</b> ).....	29
<b>Table 3.2</b> Halogenation of selected flavonoids.....	32
<b>Table 3.3</b> Tentative <sup>1</sup> H NMR spectral assignment and exact mass of compounds <b>44</b> - <b>50</b> .....	37
<b>Table 3.4</b> Anti-dengue results of brominated and iodinated flavonoids.....	39
<b>Table 3.5</b> Bromination of O <sup>7</sup> - ether chrysin series <b>53</b> - <b>62</b> . ....	53
<b>Table 3.6</b> Tentative <sup>1</sup> H NMR spectral assignment and exact mass of compounds <b>53</b> - <b>62</b> .....	57
<b>Table 3.7</b> % plaque inhibition and % cell viability of brominated O <sup>7</sup> - ether chrysin series. ....	59

## LIST OF FIGURES

Figure 1.1 Classification of flavonoids. ....	4
Figure 1.2 Flavonoids from Mexican Tephrosia species. ....	5
Figure 1.3 Structures of 6-11. ....	6
Figure 1.4 Structures of 12 - 17. ....	7
Figure 1.5 Structures of baicalein (18). ....	8
Figure 1.6 Structures of 19 - 24. ....	10
Figure 1.7 Structures of 25 - 27. ....	12
Figure 1.8 Structure of 8-chloro-5,7,3', 4'-tetramethoxyepicatechin (28). ....	13
Figure 1.9 Structures of 29 - 33. ....	14
Figure 3.1 Preliminary screening of halogenation of chrysin (34). ....	28
Figure 3.2 Proposed mechanism of bromination of chrysin (34). ....	29
Figure 3.3 Halogenation of selected flavonoids. ....	31
Figure 3.4 Apigenin (63) and luteolin (64). ....	35
Figure 3.5 EC <sub>50</sub> , CC <sub>50</sub> and TI value of flavonoids and their halogenated derivatives... ..	43
Figure 3.6 Structures of 65, 38, 40. ....	47
Figure 3.7 IC <sub>50</sub> value of $\alpha$ -glucosidase inhibitory activity of chrysin and its derivatives. ....	47
Figure 3.8 Structure of O <sup>7</sup> -hexylchrysin (39). ....	48
Figure 3.9 Two proposed synthetic pathways of dibromo O <sup>7</sup> - ether chrysin 53, 55, 57, 59, 61. ....	49
Figure 3.10 Hydrogen bonding of hydroxyl group and adjacent carbonyl group. ....	50
Figure 3.11 Synthetic scheme of dibromo O <sup>7</sup> - ether chrysin 53, 55, 57, 59, 61. ....	51

Figure 3.12 Synthetic scheme of monobromo O <sup>7</sup> - ether chrysin	54, 56, 58, 60, 62	52
Figure 3.13 Regioselectivity of NBS to position 6 of O <sup>7</sup> - ether chrysin		52
Figure 3.14 Correlation of proton 8 with carbon 9 on HMBC of 56 (Expansion)		54
Figure 3.15 Correlation of proton 8 with carbon 9 on HMBC of 60 (Expansion)		55
Figure A1 The <sup>1</sup> H NMR spectrum (DMSO-d <sub>6</sub> , 400 MHz) of 18		71
Figure A2 The <sup>1</sup> H NMR spectrum (DMSO-d <sub>6</sub> , 400 MHz) of 15		71
Figure A3 The <sup>1</sup> H NMR spectrum (DMSO-d <sub>6</sub> , 400 MHz) of 19		72
Figure A4 The <sup>1</sup> H NMR spectrum (MeOD, 400 MHz) of 42		72
Figure A5 The <sup>1</sup> H NMR spectrum (Acetone-d <sub>6</sub> ) of 43		73
Figure A6 The HR-ESI-MS of 44		73
Figure A7 The <sup>1</sup> H NMR spectrum (Acetone-d <sub>6</sub> , 400 MHz) of 44		74
Figure A8 The <sup>13</sup> C NMR spectrum (Acetone-d <sub>6</sub> , 100 MHz) of 44		74
Figure A9 The <sup>1</sup> H NMR spectrum (CDCl <sub>3</sub> , 400 MHz) of 45		75
Figure A10 The <sup>13</sup> C NMR spectrum (CDCl <sub>3</sub> , 100 MHz) of 45		75
Figure A11 The HR-ESI-MS of 46		76
Figure A12 The <sup>1</sup> H NMR spectrum (CDCl <sub>3</sub> , 400 MHz) of 46		76
Figure A13 The <sup>13</sup> C NMR spectrum (CDCl <sub>3</sub> , 100 MHz) of 46		77
Figure A14 The HR-ESI-MS of 47		77
Figure A15 The <sup>1</sup> H NMR spectrum (Acetone-d <sub>6</sub> , 400 MHz) of 47		78
Figure A16 The <sup>13</sup> C NMR spectrum (Acetone-d <sub>6</sub> , 100 MHz) of 47		78
Figure A17 The <sup>1</sup> H NMR (Acetone-d <sub>6</sub> , 400 MHz) of 48		79
Figure A18 The <sup>13</sup> C NMR (Acetone-d <sub>6</sub> , 100 MHz) of 48		79
Figure A19 The <sup>1</sup> H NMR spectrum (Acetone-d <sub>6</sub> , 400 MHz) of 49		80
Figure A20 The <sup>13</sup> C NMR spectrum (Acetone-d <sub>6</sub> , 100 MHz) of 49		80



Figure A21	The $^1\text{H}$ NMR spectrum (DMSO- $d_6$ , 400 MHz) of <b>50</b> .....	81
Figure A22	The $^{13}\text{C}$ NMR spectrum (DMSO- $d_6$ , 100 MHz) of <b>50</b> .....	81
Figure A23	The $^1\text{H}$ NMR spectrum (Acetone- $d_6$ , 400 MHz) of <b>51</b> .....	82
Figure A24	The $^1\text{H}$ NMR spectrum (Acetone- $d_6$ , 400 MHz) of <b>52</b> .....	82
Figure A25	The HR-ESI-MS of <b>53</b> .....	83
Figure A26	The $^1\text{H}$ NMR spectrum ( $\text{CDCl}_3$ , 400 MHz) of <b>53</b> .....	83
Figure A27	The $^{13}\text{C}$ NMR spectrum ( $\text{CDCl}_3$ , 100 MHz) of <b>53</b> .....	84
Figure A28	The HR-ESI-MS of <b>54</b> .....	84
Figure A29	The $^1\text{H}$ NMR spectrum ( $\text{CDCl}_3$ , 400 MHz) of <b>54</b> .....	85
Figure A30	The $^{13}\text{C}$ NMR spectrum ( $\text{CDCl}_3$ , 100 MHz) of <b>54</b> .....	85
Figure A31	The HR-ESI-MS of <b>55</b> .....	86
Figure A32	The $^1\text{H}$ NMR spectrum ( $\text{CDCl}_3$ , 400 MHz) of <b>55</b> .....	86
Figure A33	The $^{13}\text{C}$ NMR spectrum ( $\text{CDCl}_3$ , 100 MHz) of <b>55</b> .....	87
Figure A34	The $^1\text{H}$ NMR spectrum ( $\text{CDCl}_3$ , 400 MHz) of <b>56</b> .....	87
Figure A35	The $^{13}\text{C}$ NMR spectrum ( $\text{CDCl}_3$ , 100 MHz) of <b>56</b> .....	88
Figure A36	The HSQC correlation ( $\text{CDCl}_3$ ) of <b>56</b> .....	88
Figure A37	The HMBC correlation ( $\text{CDCl}_3$ ) of <b>56</b> .....	89
Figure A38	The HMBC (expansion) correlation ( $\text{CDCl}_3$ ) of <b>56</b> .....	89
Figure A39	The HR-ESI-MS of <b>57</b> .....	90
Figure A40	The $^1\text{H}$ NMR spectrum ( $\text{CDCl}_3$ , 400 MHz) of <b>57</b> .....	90
Figure A41	The $^{13}\text{C}$ NMR spectrum ( $\text{CDCl}_3$ , 100 MHz) of <b>57</b> .....	91
Figure A42	The $^1\text{H}$ NMR spectrum ( $\text{CDCl}_3$ , 400 MHz) of <b>58</b> .....	91
Figure A43	The $^{13}\text{C}$ NMR spectrum ( $\text{CDCl}_3$ , 100 MHz) of <b>58</b> .....	92
Figure A44	The HSQC correlation ( $\text{CDCl}_3$ ) of <b>58</b> .....	92

Figure A45 The HMBC correlation (CDCl <sub>3</sub> ) of <b>58</b> .....	93
Figure A46 The HMBC (expansion) correlation (CDCl <sub>3</sub> ) of <b>58</b> .....	93
Figure A47 The <sup>1</sup> H NMR spectrum (CDCl <sub>3</sub> , 400 MHz) of <b>59</b> .....	94
Figure A48 The <sup>13</sup> C NMR spectrum (CDCl <sub>3</sub> , 100 MHz) of <b>59</b> .....	94
Figure A49 The <sup>1</sup> H NMR spectrum (CDCl <sub>3</sub> , 400 MHz) of <b>60</b> .....	95
Figure A50 The <sup>13</sup> C NMR spectrum (CDCl <sub>3</sub> , 100 MHz) of <b>60</b> .....	95
Figure A51 The HSQC correlation (CDCl <sub>3</sub> ) of <b>60</b> .....	96
Figure A52 The HMBC correlation (CDCl <sub>3</sub> ) of <b>60</b> .....	96
Figure A53 The HMBC (expansion) correlation (CDCl <sub>3</sub> ) of <b>60</b> .....	97
Figure A54 The HR-ESI-MS of <b>61</b> .....	97
Figure A55 The <sup>1</sup> H NMR spectrum (CDCl <sub>3</sub> , 400 MHz) of <b>61</b> .....	98
Figure A56 The <sup>13</sup> C NMR spectrum (CDCl <sub>3</sub> ) of <b>61</b> .....	98
Figure A57 The HR-ESI-MS of <b>62</b> .....	99
Figure A58 The <sup>1</sup> H NMR spectrum (CDCl <sub>3</sub> ) of <b>62</b> .....	99
Figure A59 The <sup>13</sup> C NMR spectrum (CDCl <sub>3</sub> ) of <b>62</b> .....	100

## LIST OF ABBREVIATIONS

calcd	calculated
CC	Cytotoxic concentration
CH <sub>2</sub> Cl <sub>2</sub>	dichloromethane
concd	concentrated
d	doublet (NMR)
dd	doublet of doublets (NMR)
DENV	dengue virus
DF	dengue fever
DHF	dengue hemorrhagic fever
DMD	dimethyl dioxirane
DMF	<i>N,N</i> -dimethylformamide
DMSO	dimethyl sulfoxide
EC	Effective concentration
equiv.	equivalent
EtOAc	Ethyl acetate
g	gram (s)
HMBC	Heteronuclear multiple bond correlation

HR-ESI-MS High resolution-electrospray ionization mass

HSQC Heteronuclear single quantum correlation

m multiplet (NMR)

MHz Mega Hertz

mL milliliter (s)

mm millimeter (s)

mmol millimole (s)

NBS *N*-bromosuccinimide

NMR Nuclear Magnetic Resonance

ppm part per million

s singlet (NMR)

SI Selective Index

rt room temperature

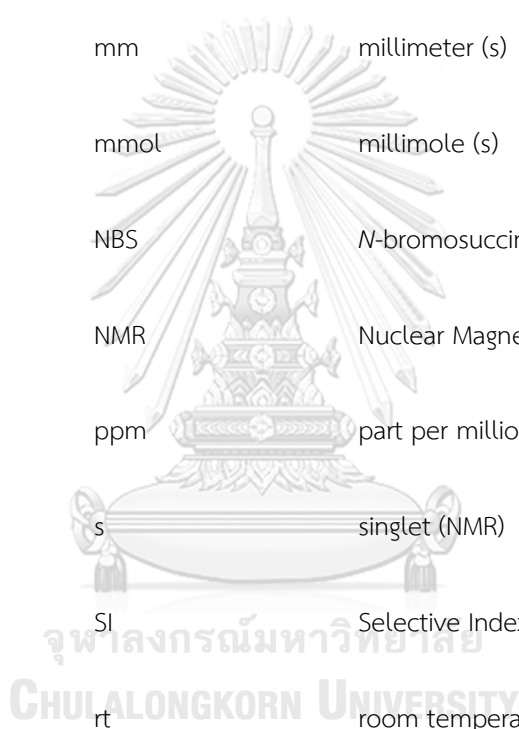
TI Therapeutic Index

TLC Thin layer chromatography

$[M+Na]^+$  pseudomolecular ion

$[M+ 2Na - H]^+$  pseudomolecular ion

$\alpha$  alpha



$\delta$  chemical shift

$\delta_{\text{H}}$  chemical shift of proton

$\mu\text{g}$  microgram (s)

$\mu\text{L}$  microliter (s)

$\mu\text{M}$  micromolar (s)

2-D NMR 2-dimensional nuclear magnetic resonance



# Chapter 1

## Introduction

### 1.1 Dengue

#### 1.1.1 Introduction

Dengue is mosquito-borne viral disease, caused by the four dengue virus serotypes 1-4. The dengue virus (DENV) belonging to the genus *Flavivirus* (family Flaviviridae), is considered as one of the most widely-spreading and endangered pathogen in the tropics. The virus is transmitted by the vector *Aedes* mosquitoes, commonly *Aedes aegypti* species. The infective symptoms can vary from asymptomatic to dengue fever (DF) and dengue hemorrhagic fever (DHF).[1] Typically, dengue fever symptoms include sudden onset of high fever, headaches, muscle and joint pains, which generally misleading with common flu, and can be recovered after two to seven days.[2] However, when the disease develops to DHF, the patient can suffer severe capillary leakage, hemorrhage, thrombocytopenia and fatality.[2]

Nowadays, the affected areas have been spreading out more than hundred countries in Southeast Asia, the Western Pacific, the Americas and Eastern Mediterranean.[3] Noticeably, the most seriously threatened regions are Southeast Asia and the Western Pacific.[3] The first reported case of dengue in Thailand was in 1949; infrequent cases was discovered through 1950s later on and the first epidemic DHF in Bangkok was stated in 1958.[4-7] Moreover, before 2004, Thailand announced the highest number of annual infected patients in Southeast Asia, with an average of

almost 69,000 cases every years in the period 1985-1999.[8] These data warned the emergent situation of this global illness and the urgency of long-term medical treatments.

### 1.1.2 Clinical therapies

Up to now, diagnosis is principally clinical while medical therapies is supportive and the disease control mainly target on the vector. Briefly, up to now, there are three major elements in dengue analysis[3]:

- Development of ELISAs for dengue-specific IgM detection
- Mosquito cell lines and monoclonal antibody development for viral isolation and identification.
- Reverse transcriptase-polymerase chain reaction (RT-PCR)

These methods considered the serological, virological and molecular diagnosis of dengue.[9]

So far, treatment of dengue infection consists of four methods which can either succeed or fail:

- Vaccination: there are four different serotypes of DENV 1-4, therefore, an effective vaccine must be tetravalent and provides a permanent protection for human. However, the accomplished vaccine has not been disclosed.[3]

- Medication/Treatment: there are no special antiviral therapies currently existing for dengue fever. Other supportive cares can be used to overcome the DF symptoms as well as lessen the severe DHF.[3]
- Natural treatment: Some of herbal cures can be listed such as *Boesenbergia rotunda*, *Kaempferia parviflora*, *Carica papaya*, etc. due to their activity against *Aedes aegypti*. [3]
- Prevention: The practical and simple protection from dengue is to avoid being bitten by the vector.[3] In addition, the elimination of vectors should be considered properly in order to limit the transmission of dengue virus in community.

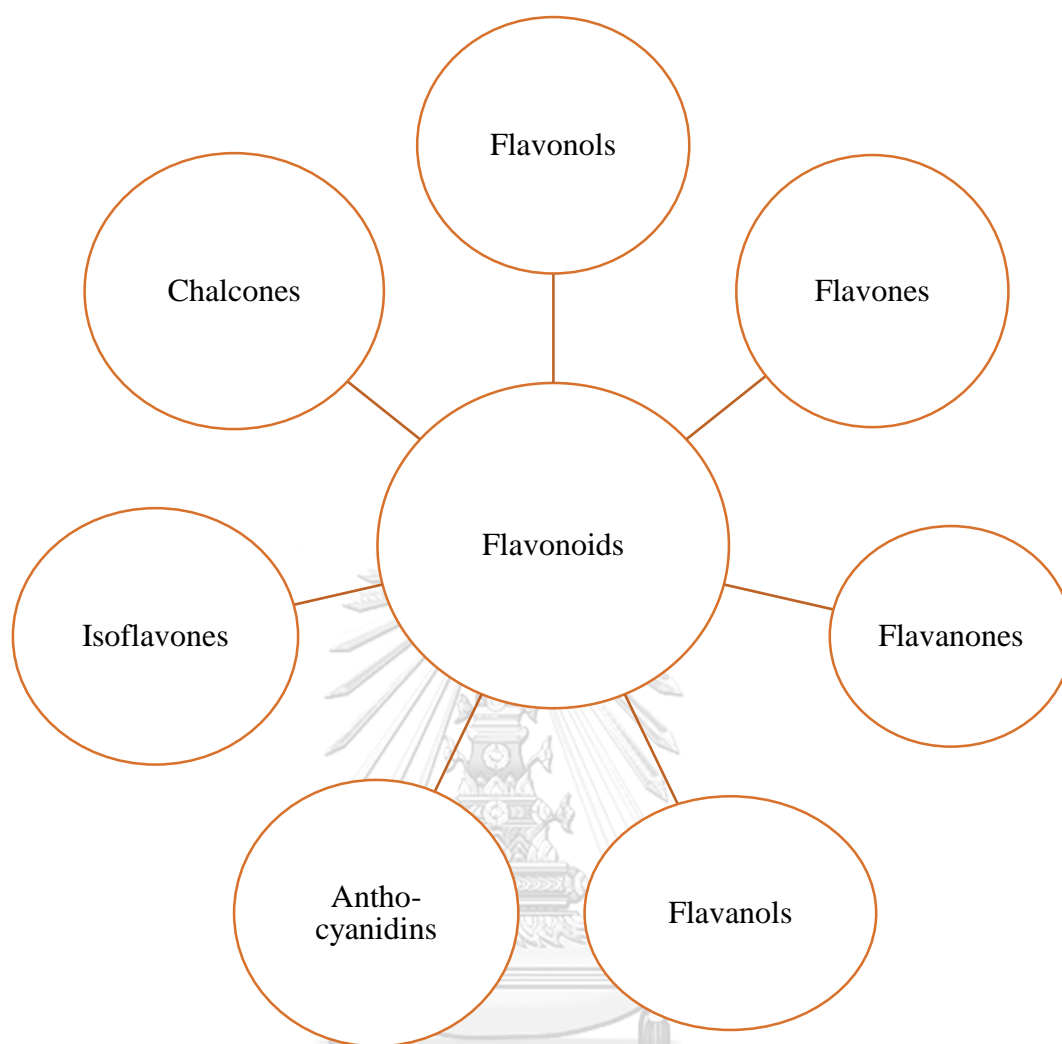
The shortage of medicinal treatments for dengue infection has been received a huge attraction of scientists in several years. In the effort to look for the promising agents, thousands of antiviral research on different targets have been conducting from all over the world.

## 1.2 Flavonoids

### 1.2.1 Introduction

Flavonoids are well-known secondary metabolites existing in a variety of plants. The basic skeleton of this class consists of fifteen carbons with two fused six-membered rings and one benzene ring. This enormous type of natural products is classified into many sub-divisions by the degree of oxidation of ring C or the positions of ring B (**Figure 1.1**).





จุฬาลงกรณ์มหาวิทยาลัย  
**Figure 1.1** Classification of flavonoids.  
CHULALONGKORN UNIVERSITY

Up to now, flavonoids were reported to possess a wide range of bioactivities such as anti-oxidant, anti-inflammatory, anti-bacterial, anti-cancer, *etc.*[10] Daidzein, a representative of isoflavone, is dominant in soybean and proved to have anti-cancer, anti-cardiovascular disease, anti-diabetic activity, *etc.*[11] Another example is chrysin, a flavone which is abundantly contributed as one of main ingredients in honey, propolis and blue passion flower (*Pasiflora caerulea*).[12] Chrysin is convinced of its

anti-oxidant, anti-inflammatory, neuroprotective activity in several studies.[12] Because of their diverse bioactivities and natural sources, a hundred of researches have been conducted continuously on different flavonoids.

### 1.2.2 Anti-dengue activity of flavonoids

Recently, the intensive investigation of flavonoids as anti-dengue agents has been addressed. In 2000, Sánchez *et al.* evaluated *in vitro* antiviral effect of **1-5**, isolated from Mexican *Tephrosia* species, using LLC-MK2 cells and DENV-2 serotype (**Figure 1.2**).[13] Only glabranine (**1**) and 7-O-methylglabranine (**2**) exhibited notable inhibition of 70% virus infection at 25  $\mu\text{M}$ .

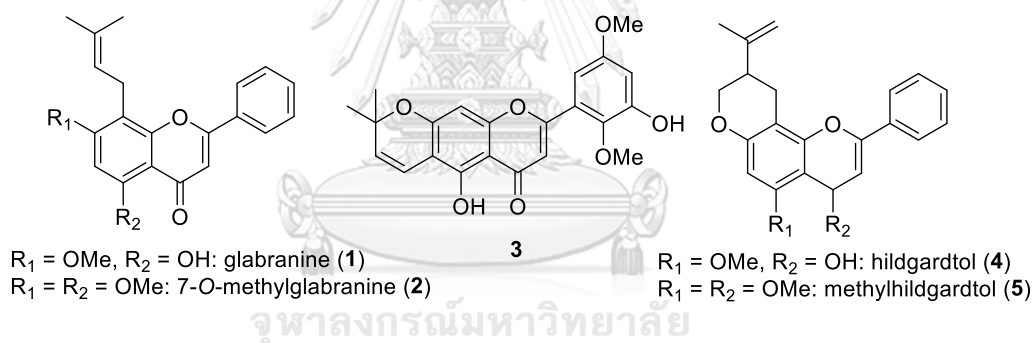


**Figure 1.2** Flavonoids from Mexican *Tephrosia* species.

Tan *et al.* worked on three flavanones **6-8**, a phenylpropanoid **9** and two cyclohexenyl chalcone derivatives **10-11** derived from *Boesenbergia rotunda* (L.), a familiar spice of the ginger family (Zingiberaceae), testing against DENV-2 virus NS2B-NS3 protease by enzymatic assay (**Figure 1.3**).[14] Even though pinocembrin (**7**) and cardamonin (**9**) acted as inactive components, there was an interesting synergetic effect when these compounds were mixed (**Table 1.1**).

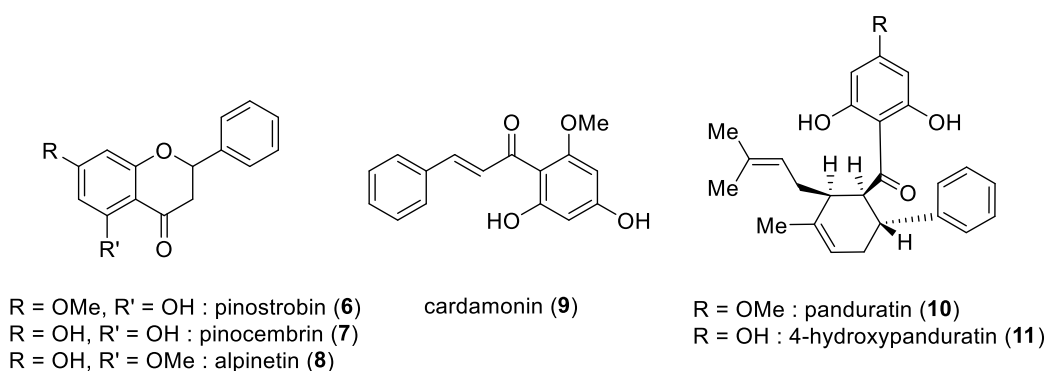


Figure 1.3 Structures of 6-11.

Table 1.1 Percentage inhibition of DENV-2 NS2B-NS3 virus protease cleavage<sup>a</sup> of compounds 7 and 9. [14]

Compound(s)	Percentage Inhibition of DENV-2 NS2B-NS3 Protease; Concentration Used (ppm)		
	120	240	400
7	30.1 ± 0.5	47.3 ± 0.5	56.1 ± 0.4
9	39.4 ± 0.6	50.1 ± 0.4	71.3 ± 0.3
7 + 9	52.6 ± 0.4	63.5 ± 0.5	81.8 ± 0.3

<sup>a</sup> The substrate cleaved by NS2B-NS3 protease used in the experiment corresponded to the peptide Boc-Gly-Arg-Arg-MCA. ± corresponds to standard deviation.

Researches developed in 2011 released some noticeable results of anti-dengue activity of flavonoids. In two separately different scope of tested compounds of Zandi and co-workers, naringenin (**12**), quercetin (**13**), daidzein (**14**), and hesperetin (**15**) were evaluated against DENV-2 serotype infection *in vitro* utilizing Vero cells,[15] whilst naringenin (**12**), rutin (**16**) and fisetin (**17**) were examined *in vitro* on antiviral effects at

the different stages of DENV-2 (NGC strain) infection (Figure 1.4).[16] **13** presented significant inhibitory activity ( $IC_{50}$  35.7  $\mu\text{g/mL}$ ) against DENV-2 infection, and **17** inhibited virus replication ( $IC_{50}$  55  $\mu\text{g/mL}$ ) after virus adsorption on Vero cells. However, the mechanism of affecting or interaction of these compounds remained unknown.

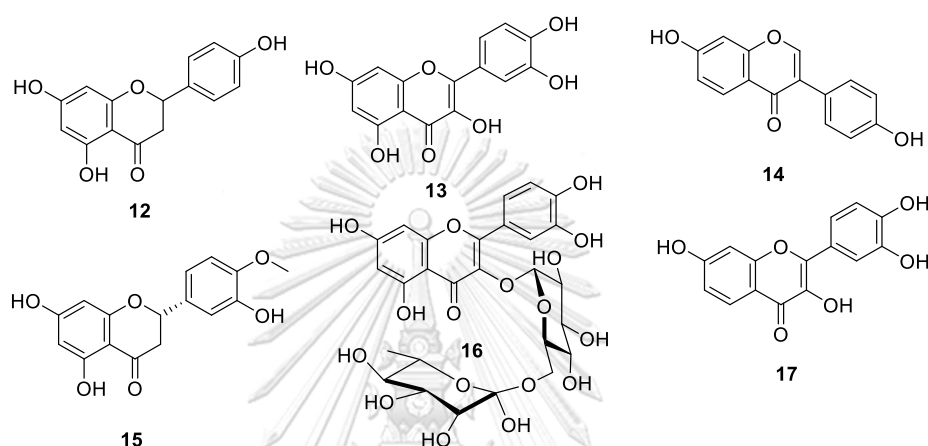
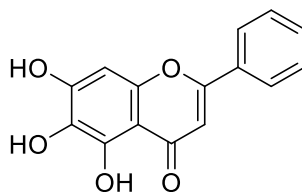


Figure 1.4 Structures of **12** - **17**.

Baicalein (**18**) (Figure 1.5) is usually extracted from the root of *Scutellaria baicalensis*, a traditional Chinese medicinal herb in the Lamiaceae family.[17] Zandi *et al.* studied on *in vitro* assay using Vero cells and Foci Forming Unit Reduction Assay (FFURA) to assess antiviral activity of **18** against DENV-2.[17] This flavone displayed  $IC_{50}$  value of 6.46  $\mu\text{g/mL}$  affecting on DENV-2 serotype replication in Vero cells when it was added after adsorption to the cells. Moreover, **18** also possessed direct virucidal ( $IC_{50}$  1.55  $\mu\text{g/mL}$ ) as well as anti-adsorption ( $IC_{50}$  7.14  $\mu\text{g/mL}$ ) effects against DENV-2.



**Figure 1.5** Structures of baicalein (**18**).

An investigation on naringenin (**12**) in 2017 by Frabasile and co-workers demonstrated the anti-dengue virus activity as well as its ability to inhibit the replication of four DENV serotypes in Huh7.5 cells (**Table 1.2**).<sup>[18]</sup> This result supported the potential use of **12** for the development of specific dengue virus treatment.

**Table 1.2** Half maximal inhibitory concentration ( $IC_{50}$ ) and selective index (SI) of naringenin (**12**) for anti – DENV activity in Huh7.5 cells.<sup>[18]</sup>

DENV	$IC_{50}$	SI
DENV-1/FGA	35.81	8.60
DENV-2/ICC265	17.97	17.32
DENV-3/5532	117.1	2.66
DENV-4/TVP360	177.5	1.75

$$SI = CC_{50}/IC_{50}$$

### 1.3 Halogenated flavonoid derivatives

#### 1.3.1 Halogenation of flavonoids

Since the beginning of the 21<sup>st</sup> century, researchers have been fond of studying on halogenation of flavonoids. At that time, halogenation of aromatic compounds normally used molecular halogens ( $Cl_2$ ,  $Br_2$ ,  $I_2$ ) in chlorinated solvents such as  $CCl_4$ ,

which caused several drawbacks on environment. Toxic reagents (chlorine gas or bromine liquid) and solvents, pollutant wastes as by-products were considered as limitations of this method. Other methods, including NBS-amberlyst, metal-oxo-catalyzed  $\text{KBr-H}_2\text{O}_2$ ,  $\text{KBr-NaBO}_3$ , required strict conditions or complicated work-up steps.[19-21] To overcome these problems, in 2002, Bovicelli *et al.* reported a mild, efficient and regioselective method by DMD/NaX or Oxone®/acetone/water/NaX applied on selected flavanones.[22] The results showed that the mixture of substrate, DMD or Oxone® and NaX in an appropriate proportion achieved high yield of products with regioselectivity depending on the structures of starting materials.

After a decade since Bovicelli's investigation, in 2015, Bernini and partners revealed a new ecofriendly method of halogenation by making use of aqueous solution of hydrogen peroxide ( $\text{H}_2\text{O}_2$ ), sodium halides ( $\text{NaCl}$  or  $\text{NaBr}$ ) and acetic acid on different classes of flavonoids.[23] The regioselectivity on products was controlled by the effects of ethereal oxygen on ring C endowed with the methoxy groups existing on ring B. Moreover, this method solved the disadvantages of general halogenation, such as non-toxic reagents and by-product, facile procedure and conditions.

These studies opened a new application of halogenation method on flavonoids with environmental friendliness.

### 1.3.2 Anti-dengue activity of halogenated flavonoids

In a past few years, the examination of halogenated flavonoids as anti-dengue candidate has been attracted interests. The first report of Suroengsit *et al.* in 2017 on 8 selected flavonoid derivatives (**Figure 1.6**) showed that two halogenated chrysin **19**-**20** strongly inhibited virus production with >99%.<sup>[24]</sup> These compounds also exhibited broad spectrum activities against all dengue serotypes and Zika virus. Both halogenated chrysin were relatively non-toxic with cell-viability over 80% (**Table 1.3**).

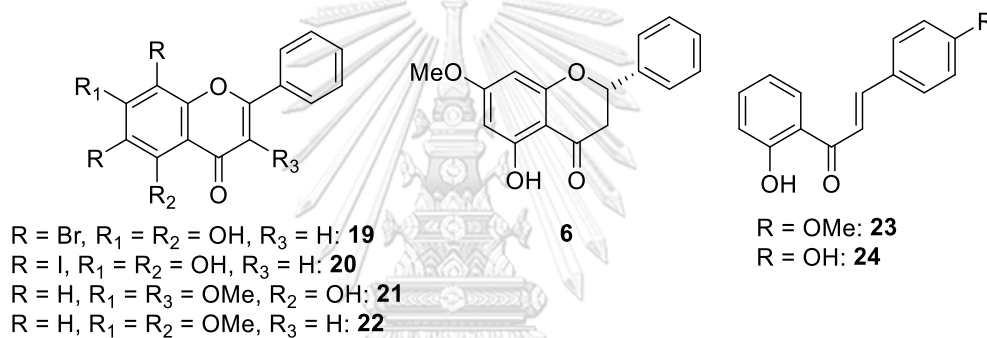


Figure 1.6 Structures of **19** - **24**.

**Table 1.3** EC<sub>50</sub> and SI values of halogenated chrysin (**19**) and (**20**). [24]

Serotypes	Compounds			
	<b>19</b>		<b>20</b>	
	EC <sub>50</sub> (μM) <sup>a</sup>	SI <sup>c</sup>	EC <sub>50</sub> (μM) <sup>a</sup>	SI <sup>c</sup>
DENV1 (16007)	2.30 ± 1.04	19.42	2.30 ± 0.92	19.39
DENV2 (NGC)	1.47 ± 0.86	30.43	2.19 ± 0.31	20.37
DENV3 (16562)	2.32 ± 1.46	19.22	1.02 ± 0.31	43.64
DENV4 (c0036)	1.78 ± 0.72	25.12	1.29 ± 0.60	34.50
ZIKV (SV0010/15) <sup>b</sup>	1.65 ± 0.86	27.02	1.39 ± 0.11	32.14

<sup>a</sup>EC<sub>50</sub> were determined by plaque assay in 96-well plates. <sup>b</sup>EC<sub>50</sub> was determined by plaque assay in 24-well plates. <sup>c</sup>Selectivity index (CC<sub>50</sub>/EC<sub>50</sub>). Mean ± standard error of the means (SEM) of two independent experiments, in which each experiment was performed in triplicate.

### 1.3.3 Review of other bioactivities of halogenated flavonoids

Beside anti-dengue activity, halogenated derivatives of flavonoids have been evaluated for their bio-potentials in many researches since late 20<sup>th</sup> century.

In 1996, halogenated flavones were examined as aryl hydrocarbon (Ah) receptor agonists and antagonists by Lu and co-workers.[25] The halogenated flavones **25-27** (**Figure 1.7**) exhibited competitive Ah receptor binding affinities (IC<sub>50</sub> 0.79 to 2.28 nM) compared with 2,3,7,8-tetrachlorodibenzo-*p*-dioxin (TCDD) (1.78 nM). In addition, these compounds also induced transformation of the rat cytosolic Ah receptor and induced CYP1A1 gene expression in MCF-7 human breast cancer cells.



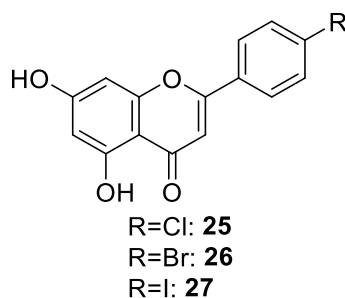


**Figure 1.7** Structures of **25** - **27**.

In 2005, Park *et al.* synthesized 6,8-disubstituted chrysin derivatives and tested for inhibition of PGE<sub>2</sub> production.[26] Two halogenated chrysin derivatives **19** and **20** expressed strong inhibitory activities with 99.93 and 98.41% of inhibition of COX-2 catalyzed PGE<sub>2</sub> production from LPS-induced RAW 264.7 cells, respectively. Four years later, these two compounds were also investigated for *in vitro* and *in vivo* anti-inflammatory effect in a study of Do and colleagues.[27] Despite of an increasing of six to seven folds comparing with chrysin in *in vitro* anti-inflammatory activity, there were no remarkable difference between the halogenated derivatives and chrysin in *in vivo* test. This result implied an important role of molecular size affecting on the penetration of compounds into body. Lastly, Krongkan and partners examined brominated and iodinated chrysin derivatives **19** and **20** on anti-bacterial activity against *Propionibacterium acnes*, *Staphylococcus aureus*, *Streptococcus sobrinus*, *Salmonella typhi* and *Streptococcus mutans*.[28] These compounds exhibited excellent inhibition zone on five tested strains in a range of 18 to 21 mm. Furthermore, **19** and **20** were bacteriostatic agents toward *P. acnes*, *S. aureus*, and bactericidal agents for others. The combination of **19** and streptomycin

displayed the most synergetic effect with sixteen-fold increasing in activity, compared to individual antibiotics, against *P. acnes*, *S. sobrinus* and *S. mutans*, meanwhile the synergetic effect only showed on *P. acnes* when mixing **20** with streptomycin. In conclusion, **19** and **20** have been reported as new potent anti-inflammatory and anti-bacterial agents.

In addition, Bernini and his group reported anti-fungal activity of synthesized chlorinated and brominated flavonoids on *Trichoderma koningii*, *Fusarium oxysporum* and *Cladosporium cladosporioides*. [23] 8-Chloro-5,7,3',4'-tetramethoxyepicatechin (**28**) (Figure 1.8) was the most active compounds against all types of fungi, compared to other tested derivatives.

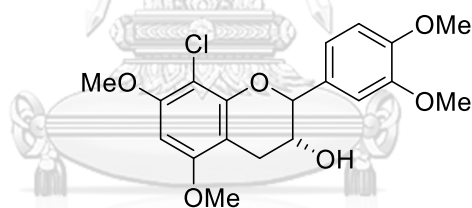
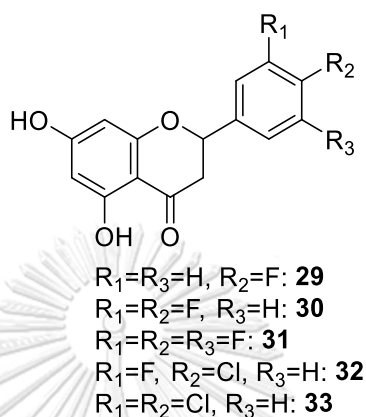


Figure 1.8 Structure of 8-chloro-5,7,3',4'-tetramethoxyepicatechin (**28**).

A study published in 2016 of Zhang and co-workers conducted on 5,7-dihydroxyflavanone derivatives including halogenated compounds **29-33** (Figure 1.9), evaluating their antimicrobial efficacy on Gram-positive, Gram-negative and yeast. [29] Most of halogenated compounds showed better antimicrobial activity than their natural analogs: **33** exhibited the lowest MIC value of 10  $\mu\text{g}/\text{mL}$  towards Gram-positive strains *Bacillus anthracis*, *Bacillus cereus* and 20  $\mu\text{g}/\text{mL}$  towards *Bacillus subtilis*,

*Staphylococcus aureus*; **29** expressed 30  $\mu\text{g/mL}$  of MIC towards all tested Gram-positive strains. Moreover, dichloro derivative **33** also inhibited the growth of *Saccharomyces cerevisiae* with MIC 10  $\mu\text{g/mL}$ .



**Figure 1.9** Structures of **29** - **33**.

Literature review has given out strong evidences to support the possibility of halogenated flavonoids as new bioactive agents, such as anti-fungal, anti-bacteria, anti-microbial activity. In addition, the promising dengue inhibition of di-halogenated chrysin suggested that halogenated flavonoids could be investigated as new anti-dengue agents.

Thus, the objective of this research was focused on these targets:

1. To synthesize a series of halogenated flavonoid derivatives under mild, effective and ecofriendly conditions.
2. To evaluate and investigate the inhibition of dengue infection of synthesized compounds.

## Chapter 2

### Experimental

#### 2.1 Instruments and equipment

Thin layer chromatography (TLC) was performed on aluminum sheet precoated with silica gel, Kieselgel 60 F<sub>254</sub> (Merck, Germany), column chromatography was conducted on silica gel no. 7734 (Merck, Germany). All NMR spectra (<sup>1</sup>H and <sup>13</sup>C NMR) were recorded in deuterated chloroform (CDCl<sub>3</sub>), acetone-*d*<sub>6</sub>, methanol-*d*<sub>4</sub> (MeOD) or dimethylsulfoxide-*d*<sub>6</sub> (DMSO-*d*<sub>6</sub>) on a Bruker AV400 and Varian Mercury 400 plus spectrometer at 400 MHz for <sup>1</sup>H NMR and at 100 MHz for <sup>13</sup>C NMR. The chemical shifts ( $\delta$ ) are assigned in comparison with residual solvent protons.

#### 2.2 Chemicals

Chrysin (**34**), naringenin (**12**) and quercetin hydrate (**13**) were purchased from Tokyo Chemical Industry company and used without further purification. Pinostrobin (**6**) and pinocembrin (**7**) isolated from *Boesenbergia rotunda* were received as a gift from Mr. Pablo Chourreu Alba. Hesperetin (**15**) and baicalein (**18**) were hydrolyzed from their corresponding *O*-glycosides: hesperidin (**35**) and baicalin (**36**).[30, 31] A series of *O*<sup>7</sup>-ether chrysin **37-41** with variation of chain length was obtained from Ms. Krongkan Kingkaew *et al.*[28] Other synthetic reagents were purchased from Merck chemical company or otherwise stated. All solvents used in this study were purified by standard methods except for those which were reagent grades.

## 2.3 Synthesis of halogenated flavonoids

### 2.3.1 Hydrolysis of hesperetin (**15**) and baicalein (**18**) from their corresponding glycosides

#### Hydrolysis of hesperetin (**15**) from hesperidin (**35**) [30]

To a flask containing 0.5 g of hesperidin (**35**), 500 mL of hydrolysis system concd.  $\text{H}_2\text{SO}_4:\text{CH}_3\text{COOH}:\text{C}_2\text{H}_5\text{OH}$  (1:1:9) were carefully poured and well-stirred at  $80^\circ\text{C}$  for 8.5 h. The reaction mixture was extracted with EtOAc until the organic phase was neutralized. The solvent was evaporated by reduced evaporation and hesperetin (**15**) (206 mg, 83% yield) was isolated by column chromatography with mobile phase hexane:EtOAc 6:4.

#### Hydrolysis of baicalein (**18**) from baicalin (**36**) [31]

98%  $\text{H}_2\text{SO}_4$  (2.0 mL, 0.037 mmol) was added dropwise to a round flask (100 mL) containing baicalin (**36**) (50 mg, 0.11 mmol) and stirred on magnetic stirrer at room temperature, following by slowly dropped 2.0 mL of water. After the evolution of heat terminated, one portion of water (15 mL) was poured directly to the mixture and the yellow powder was achieved by suction filtration and washed with water.

Hesperetin (**15**): yellow powder (83%)  $^1\text{H}$  NMR (100MHz,  $\text{DMSO-d}_6$ )  $\delta$  12.13 (s, 1H), 10.8 (b, 1H), 9.10 (s, 1H), 6.94-6.87 (m, 3H), 5.88 (d,  $J = 3.5$  Hz, 2H), 5.42 (dd,  $J = 12.4$ , 3.1 Hz, 1H), 3.77 (s, 3H), 3.19 (dd,  $J = 17.1$ , 12.4 Hz, 1H), 2.70 (dd,  $J = 17.1$ , 3.1 Hz, 1H).

Baicalein (**18**): yellow powder (81%)  $^1\text{H}$  NMR (400 MHz,  $\text{DMSO-d}_6$ )  $\delta$  8.06 (m, 2H), 7.59 (m, 3H), 6.92 (s, 1H), 6.63 (s, 1H).

### 2.3.2 Brominated flavonoids

#### General procedure for bromination by NaBr/H<sub>2</sub>O<sub>2</sub>/CH<sub>3</sub>COOH [23]

A 30% aqueous solution of H<sub>2</sub>O<sub>2</sub> (3.0 equiv.) was added to the flask of flavonoid (0.1 mmol) and an appropriate amount of NaBr (2.0-4.0 equiv.) in CH<sub>3</sub>COOH (2.5 mL); then, the mixture was stirred at room temperature for 24 h. The reaction was monitored by TLC. At the end, the crude was treated with Na<sub>2</sub>S<sub>2</sub>O<sub>3</sub> and extracted with EtOAc (3×10 mL). The reunited organic fractions were dried over anhydrous Na<sub>2</sub>SO<sub>4</sub>; after filtration, the solvent was evaporated under reduced pressure. Final products were isolated and purified by chromatographic column using hexane: EtOAc: acetone = 60:40:4 as eluent.

#### General procedure for bromination by NaBr/Oxone® [27]

To the solution of chrysin (**34**) (0.1 mmol) in acetone:water 5:1 was added NaBr (0.3 mmol). After cooling, Oxone® (0.3 mmol) was added and the mixture was stirred at room temperature for 2 h. The final solution was treated with Na<sub>2</sub>S<sub>2</sub>O<sub>3</sub> and evaporated under reduced pressure.

#### General procedure for bromination of baicalein (**18**) [32]

A mixture of baicalein (**18**) (35 mg, 0.13 mmol) and NBS (33 mg, 0.19 mmol) in THF (4.0 mL) and concd. H<sub>2</sub>SO<sub>4</sub> (5.0 μL) was stirred at room temperature for 12 h. The reaction mixture was extracted with EtOAc, washed with 10% aqueous NaHSO<sub>4</sub> solution and water, dried over anhydrous Na<sub>2</sub>SO<sub>4</sub>, and then concentrated under reduced

pressure. The residue was recrystallized from MeOH to give the target compound (35%) as yellow powder.

### 2.3.3 Iodinated flavonoids

#### General procedure for iodination by KI/H<sub>2</sub>O<sub>2</sub>/CH<sub>3</sub>COOH

A 30% aqueous solution of H<sub>2</sub>O<sub>2</sub> (3.0 equiv.) was added to the flask of flavonoid (0.1 mmol) and an appropriate amount of KI (2.0-4.0 equiv.) in CH<sub>3</sub>COOH (2.5 mL); then, the mixture was stirred at room temperature for 24 h. The reaction was monitored by TLC. At the end, the crude was treated with Na<sub>2</sub>S<sub>2</sub>O<sub>3</sub> and extracted with EtOAc (3×10 mL). The separated organic fractions were dried over anhydrous Na<sub>2</sub>SO<sub>4</sub>; after filtration, the solvent was evaporated under reduced pressure. Final products were isolated and purified by chromatographic column using hexane: EtOAc: acetone = 60:40:4 as eluent.

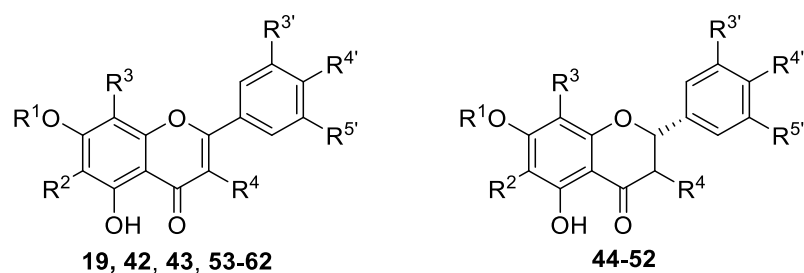
### 2.3.4 Brominated O<sup>7</sup>-ether chrysin

#### General procedure for bromination of O<sup>7</sup>-ether chrysin [33]

A solution of O<sup>7</sup>-ether chrysin **37-41** (0.1 mmol) in CH<sub>2</sub>Cl<sub>2</sub> (10 mL) was added NBS (0.1-0.2 mmol) and stirred for 6 h at room temperature. The solvent then was removed by evaporation and the residues were purified by silica gel column chromatography to obtain the derivatives **53-62**.

Twenty-two synthesized flavonoid derivatives are tabulated in **Table 2.1**.

Table 2.1 Structures of flavonoids derivatives 19, 42 - 62.



Entry	Cpd	R <sup>1</sup>	R <sup>2</sup>	R <sup>3</sup>	R <sup>4</sup>	R <sup>3'</sup>	R <sup>4'</sup>	R <sup>5'</sup>
1	19	H	Br	Br	H	H	H	H
2	42	H	OH	Br	H	H	H	H
3	43	H	Br	Br	OH	H	OH	OH
4	44	H	Br	Br	H	H	H	H
5	45	H	I	H	H	H	H	H
6	46	CH <sub>3</sub>	Br	Br	H	H	H	H
7	47	CH <sub>3</sub>	I	I	H	H	H	H
8	48	CH <sub>3</sub>	I	H	H	H	H	H
9	49	H	Br	Br	H	Br	OH	Br
10	50	H	I	I	H	I	OH	I
11	51	H	Br	Br	H	H	OH	H
12	52	H	Br	Br	H	OH	OCH <sub>3</sub>	H
13	53	C <sub>2</sub> H <sub>5</sub>	Br	Br	H	H	H	H
14	54	C <sub>2</sub> H <sub>5</sub>	Br	H	H	H	H	H
15	55	C <sub>4</sub> H <sub>9</sub>	Br	Br	H	H	H	H
16	56	C <sub>4</sub> H <sub>9</sub>	Br	H	H	H	H	H
17	57	C <sub>6</sub> H <sub>13</sub>	Br	Br	H	H	H	H



Table 2.1 (Continue)

Entry	Cpd	R <sup>1</sup>	R <sup>2</sup>	R <sup>3</sup>	R <sup>4</sup>	R <sup>3'</sup>	R <sup>4'</sup>	R <sup>5'</sup>
18	<b>58</b>	C <sub>6</sub> H <sub>13</sub>	Br	H	H	H	H	H
19	<b>59</b>	C <sub>8</sub> H <sub>17</sub>	Br	Br	H	H	H	H
20	<b>60</b>	C <sub>8</sub> H <sub>17</sub>	Br	H	H	H	H	H
21	<b>61</b>	C <sub>12</sub> H <sub>25</sub>	Br	Br	H	H	H	H
22	<b>62</b>	C <sub>12</sub> H <sub>25</sub>	Br	H	H	H	H	H

6,8-dibromo-5,7-dihydroxyflavone (**19**): yellow powder (92% yield). <sup>1</sup>H NMR (DMSO-*d*<sub>6</sub>) δ 13.74 (s, 1H), 8.14 (dd, *J* = 7.4, 2.2 Hz, 2H), 7.61 (m, 3H), 7.12 (s, 1H). [28]

8-bromo-5,6,7-trihydroxyflavone (**42**): yellow powder (35% yield). <sup>1</sup>H NMR (MeOD) δ 8.04 (m, 2H), 7.56 (m, 3H), 6.77 (s, 1H).[32]

6,8-dibromo-3,5,7,3',4'-pentahydroxyflavone (**43**): light yellow powder (52% yield). <sup>1</sup>H NMR (Acetone-*d*<sub>6</sub>) δ 13.14 (s, 1H), 7.99 (d, *J* = 2.2 Hz, 1H), 7.87 (dd, *J* = 8.5, 2.2 Hz, 1H), 7.03 (d, *J* = 8.5 Hz, 1H).[34]

6,8-dibromo-5,7-dihydroxyflavanone (**44**): light brown powder (93% yield). <sup>1</sup>H NMR (CDCl<sub>3</sub>) δ 12.74 (s, 1H), 7.45 (m, 5H), 5.58 (dd, *J* = 12.2, 3.5 Hz, 1H), 3.15 (dd, *J* = 17.3, 12.2 Hz, 1H), 3.00 (dd, *J* = 17.3, 3.5 Hz, 1H); <sup>13</sup>C NMR (CDCl<sub>3</sub>) δ 195.7, 159.3, 158.0, 157.4, 137.5, 129.1, 126.0, 103.85, 90.6, 89.0, 79.7, 42.6; HR-ESI-MS *m/z* calcd. for C<sub>15</sub>H<sub>9</sub>Br<sub>2</sub>O<sub>4</sub>Na [M + 2Na - H]<sup>+</sup> 456.8663, found 456.8657.

6-iodo-5,7-dihydroxyflavanone (**45**): light brown powder (74% yield).  $^1\text{H}$  NMR ( $\text{CDCl}_3$ )  $\delta$  13.03 (s, 1H), 7.44 (m, 5H), 6.31 (s, 1H), 5.44 (dd,  $J = 12.8, 3.2$  Hz, 1H), 3.25 (dd,  $J = 17.3, 12.8$  Hz, 1H), 2.89 (dd,  $J = 17.3, 3.2$  Hz, 1H);  $^{13}\text{C}$  NMR ( $\text{CDCl}_3$ )  $\delta$  195.4, 163.3, 162.8, 162.7, 137.9, 129.0, 128.9, 126.1, 103.2, 95.3, 79.2, 67.3, 42.7.

6,8-dibromo-5-hydroxy-7-methoxyflavanone (**46**): yellow powder (96% yield).  $^1\text{H}$  NMR ( $\text{CDCl}_3$ )  $\delta$  12.61 (s, 1H), 7.48 (m, 5H), 5.61 (dd,  $J = 12.3, 3.4$  Hz, 1H), 3.98 (s, 3H), 3.18 (dd,  $J = 17.3, 12.3$  Hz, 1H), 3.05 (dd,  $J = 17.3, 3.4$  Hz, 1H);  $^{13}\text{C}$  NMR ( $\text{CDCl}_3$ )  $\delta$  196.3, 162.1, 159.0, 157.7, 137.1, 128.8, 125.7, 105.9, 98.3, 96.6, 79.2, 60.7, 42.4; HR-ESI-MS  $m/z$  calcd. for  $\text{C}_{16}\text{H}_{12}\text{Br}_2\text{O}_4\text{Na}$   $[\text{M} + \text{Na}]^+$  448.90000, found 448.89938.

6,8-diiodo-5-hydroxy-7-methoxyflavanone (**47**): light green crystal (73% yield).  $^1\text{H}$  NMR ( $\text{Acetone-}d_6$ )  $\delta$  13.02 (s, 1H), 7.47 (m, 5H), 5.85 (dd,  $J = 12.6, 3.2$  Hz, 1H), 3.91 (s, 3H), 3.37 (dd,  $J = 17.3, 12.6$  Hz, 1H), 3.14 (dd,  $J = 17.3, 3.2$  Hz, 1H);  $^{13}\text{C}$  NMR ( $\text{Acetone-}d_6$ )  $\delta$  198.2, 167.6, 164.0, 163.0, 139.2, 129.6, 127.1, 106.4, 95.61, 94.7, 80.5, 61.2, 42.6; HR-ESI-MS  $m/z$  calcd. for  $\text{C}_{16}\text{H}_{11}\text{I}_2\text{O}_4\text{Na}$   $[\text{M} + 2\text{Na} - \text{H}]^+$  566.8542, found 566.8525.

6-iodo-5-hydroxy-7-methoxyflavanone (**48**): yellow oil (10% yield).  $^1\text{H}$  NMR ( $\text{Acetone-}d_6$ )  $\delta$  12.95 (s, 1H), 7.53 (m, 5H), 6.33 (s, 1H), 5.68 (dd,  $J = 13.0, 3.1$  Hz, 1H), 3.98 (s, 3H), 3.29 (dd,  $J = 17.4, 13.0$  Hz, 1H), 2.92 (dd,  $J = 17.4, 3.1$  Hz, 1H).  $^{13}\text{C}$  NMR ( $\text{Acetone-}d_6$ )  $\delta$  195.3, 165.6, 164.8, 163.6, 162.2, 137.8, 129.0, 128.9, 126.1, 103.2, 93.2, 91.9, 79.4, 66.0, 42.6.

6,8,3',5'-tetrabromo-5,7,4'-trihydroxyflavanone (**49**): white powder (42% yield).  $^1\text{H}$  NMR (Acetone- $d_6$ )  $\delta$  12.93 (s, 1H), 7.82 (s, 2H), 5.74 (dd,  $J = 12.7, 3.1$  Hz, 1H), 3.38 (dd,  $J = 17.2, 12.7$  Hz, 1H), 3.07 (dd,  $J = 17.2, 3.1$  Hz, 1H);  $^{13}\text{C}$  NMR (Acetone- $d_6$ )  $\delta$  196.1, 159.3, 158.4, 157.3, 151.1, 132.2, 130.6, 128.1, 114.0, 111.9, 102.5, 91.1, 90.0, 77.5, 40.9.

6,8,3',5'-tetraiodo-5,7,4'-trihydroxyflavanone (**50**): yellow powder (48% yield).  $^1\text{H}$  NMR (DMSO- $d_6$ )  $\delta$  12.84 (s, 1H), 7.74 (s, 2H), 5.67 (dd,  $J = 12.8, 3.0$  Hz, 1H), 3.43 (dd,  $J = 17.2, 12.8$  Hz, 1H), 2.95 (dd,  $J = 17.2, 3.0$  Hz, 1H);  $^{13}\text{C}$  NMR (DMSO- $d_6$ )  $\delta$  196.6, 165.9, 165.1, 162.6, 156.3, 138.8, 138.6, 135.9, 135.5, 113.2, 96.7, 84.3, 78.2, 42.6.

6,8-dibromo-5,7,4'-trihydroxyflavanone (**51**): light yellow powder (25% yield).  $^1\text{H}$  NMR (DMSO- $d_6$ )  $\delta$  12.97 (s, 1H), 7.45 (d,  $J = 8.6$  Hz, 2H), 6.92 (d,  $J = 8.6$  Hz, 2H), 5.67 (dd,  $J = 12.6, 3.2$  Hz, 1H), 3.33 (dd,  $J = 17.2, 12.6$  Hz, 1H), 2.95 (dd,  $J = 17.2, 3.2$  Hz, 1H). [35]

6,8-dibromo-5,7,3'-trihydroxy-4'-methoxyflavanone (**52**): yellow powder (61% yield).  $^1\text{H}$  NMR (Acetone- $d_6$ )  $\delta$  12.92 (s, 1H), 7.29 (s, 1H), 7.21 (s, 1H), 7.01 (s, 1H), 5.87 (dd,  $J = 13.1, 3.0$  Hz, 1H), 3.92 (s, 3H), 3.27 (dd,  $J = 17.3, 13.1$  Hz, 1H), 2.94 (dd,  $J = 17.3, 3.0$  Hz, 1H). [35]

6,8-dibromo-7-ethoxy-5-hydroxyflavone or 6,8-dibromo- $O^7$ -ethylchrysin (**53**): yellow powder (86% yield).  $^1\text{H}$  NMR ( $\text{CDCl}_3$ )  $\delta$  13.58 (s, 1H), 8.02 (dd,  $J = 8.0, 3.5$  Hz, 2H), 7.58 (m, 3H), 6.83 (s, 1H), 4.24 (q,  $J = 7.0$  Hz, 2H), 1.57 (t,  $J = 7.0$  Hz, 3H);  $^{13}\text{C}$  NMR (100MHz,  $\text{CDCl}_3$ )  $\delta$  182.1, 164.8, 159.6, 158.0, 152.5, 132.6, 130.4, 129.3, 126.6, 108.6,

105.5, 101.7, 95.8, 70.4, 10.7; HR-ESI-MS  $m/z$  calcd for  $C_{17}H_{12}Br_2O_4Na$   $[M + Na]^+$  460.90000, found 460.90024.

6-bromo-7-ethoxy-5-hydroxyflavone or 6-bromo- $O^7$ -ethylchrysin (**54**): yellow powder (91% yield).  $^1H$  NMR ( $CDCl_3$ )  $\delta$  13.46 (s, 1H), 7.89 (m, 2H), 7.41 (m, 3H), 6.73 (s, 1H), 6.56 (s, 1H), 4.22 (q,  $J = 7.0$  Hz, 2H), 1.55 (t,  $J = 7.0$  Hz, 3H);  $^{13}C$  NMR ( $CDCl_3$ )  $\delta$  181.9, 164.2, 161.0, 158.3, 156.7, 132.0, 131.0, 129.1, 126.3, 105.9, 94.8, 91.5, 65.5, 14.4; HR-ESI-MS  $m/z$  calcd for  $C_{17}H_{13}BrO_4Na$   $[M + Na]^+$  389.98949, found 389.98970.

6,8-dibromo-7-butoxy-5-hydroxyflavone or 6,8-dibromo- $O^7$ -butylchrysin (**55**): yellow powder (82% yield).  $^1H$  NMR ( $CDCl_3$ )  $\delta$  13.57 (s, 1H), 8.01 (m, 2H), 7.58 (m, 3H), 6.82 (s, 1H), 4.15 (q,  $J = 6.5$  Hz, 2H), 1.94 (m, 2H), 1.62 (m, 2H), 1.03 (t,  $J = 6.5$  Hz, 3H);  $^{13}C$  NMR ( $CDCl_3$ )  $\delta$  182.2, 164.8, 160.0, 158.0, 152.5, 132.6, 130.4, 129.3, 126.6, 108.6, 105.5, 101.7, 95.7, 74.2, 32.1, 29.7, 13.9; HR-ESI-MS  $m/z$  calcd for  $C_{19}H_{16}Br_2O_4Na$   $[M + Na]^+$  488.93130, found 488.93206.

6-bromo-7-butoxy-5-hydroxyflavone or 6-bromo- $O^7$ -butylchrysin (**56**): yellow powder (90% yield).  $^1H$  NMR ( $CDCl_3$ )  $\delta$  13.46 (s, 1H), 7.88 (m, 2H), 7.54 (m, 3H), 6.69 (s, 1H) 6.54 (s, 1H), 4.12 (q,  $J = 6.4$  Hz, 2H), 1.89 (m, 2H), 1.58 (m, 2H), 1.02 (t,  $J = 6.4$  Hz, 3H);  $^{13}C$  NMR ( $CDCl_3$ )  $\delta$  182.0, 164.3, 161.3, 158.5, 156.8, 132.2, 131.2, 129.3, 126.5, 106.0, 95.1, 91.6, 69.7, 31.0, 19.3, 13.9.

6,8-dibromo-7-hexyloxy-5-hydroxyflavone or 6,8-dibromo- $O^7$ -hexylchrysin (**57**): yellow powder (87% yield).  $^1H$  NMR ( $CDCl_3$ )  $\delta$  13.57 (s, 1H), 8.00 (d,  $J = 7.2$  Hz, 2H), 7.58

(m, 3H), 6.82 (s, 1H), 4.14 (q,  $J = 6.6$  Hz, 2H), 1.95 (m, 2H), 1.58 (s, 6H), 0.93 (t,  $J = 6.6$  Hz, 3H);  $^{13}\text{C}$  NMR ( $\text{CDCl}_3$ )  $\delta$  182.1, 164.7, 159.6, 157.9, 152.5, 132.6, 130.4, 129.3, 126.6, 108.5, 105.4, 101.7, 95.7, 74.5, 31.6, 30.0, 2.5, 22.6, 14.1; HR-ESI-MS  $m/z$  calcd for  $\text{C}_{21}\text{H}_{20}\text{Br}_2\text{O}_4\text{Na}$   $[\text{M} + \text{Na}]^+$  516.96260, found 516.96247.

6-bromo-7-hexyloxy-5-hydroxyflavone or 6-bromo- $O^7$ -hexylchrysin (**58**): yellow powder (89% yield).  $^1\text{H}$  NMR ( $\text{CDCl}_3$ )  $\delta$  7.89 (m, 2H), 7.54 (m, 3H), 6.71 (s, 1H), 6.55 (s, 1H), 4.12 (q,  $J = 6.4$  Hz, 2H), 1.91 (m, 2H), 1.53 (m, 2H), 1.38 (m, 4H), 0.93 (t,  $J = 6.4$  Hz, 3H);  $^{13}\text{C}$  NMR ( $\text{CDCl}_3$ )  $\delta$  182.0, 164.3, 161.3, 158.5, 156.9, 132.2, 131.2, 129.5, 129.3, 126.5, 106.0, 95.1, 91.7, 70.0, 31.6, 28.9, 25.7, 22.7, 14.1.

6,8-dibromo-7-octyloxy-5-hydroxyflavone or 6,8-dibromo- $O^7$ -octylchrysin (**59**): yellow powder (90% yield).  $^1\text{H}$  NMR ( $\text{CDCl}_3$ )  $\delta$  13.53 (s, 1H), 8.00 (m, 2H), 7.56 (m, 3H), 6.82 (s, 1H), 4.12 (q,  $J = 6.6$  Hz, 2H), 1.92 (m, 2H), 1.56 (m, 2H), 1.34 (m, 8H), 0.93 (t,  $J = 6.5$ , 3H);  $^{13}\text{C}$  NMR ( $\text{CDCl}_3$ )  $\delta$  182.3, 177.7, 164.9, 159.8, 158.1, 152.7, 132.7, 130.6, 129.4, 126.8, 108.7, 105.6, 101.8, 95.9, 74.6, 32.0, 30.2, 29.7, 29.5, 29.4, 26.0, 22.8, 14.2.

6-bromo-7-octyloxy-5-hydroxyflavone or 6-bromo- $O^7$ -octylchrysin (**60**): yellow powder (89% yield).  $^1\text{H}$  NMR ( $\text{CDCl}_3$ )  $\delta$  7.88 (d,  $J = 7.4$  Hz, 2H), 7.54 (m, 3H), 6.70 (s, 1H), 6.55 (s, 1H), 4.11 (q,  $J = 6.4$  Hz, 2H), 1.90 (m, 2H), 1.54 (m, 2H), 1.35 (m, 8H), 0.89 (t,  $J = 6.4$ , 3H);  $^{13}\text{C}$  NMR ( $\text{CDCl}_3$ )  $\delta$  181.8, 164.1, 161.2, 158.3, 156.7, 132.0, 131.1, 129.1, 126.3, 105.9, 105.3, 94.9, 91.5, 69.9, 31.8, 29.2, 28.8, 25.9, 22.6, 14.1.

6,8-dibromo-7-dodecyloxy-5-hydroxyflavone or 6,8-dibromo-*O*<sup>7</sup>-dodecylchrysin (**61**): yellow powder (88% yield). <sup>1</sup>H NMR (CDCl<sub>3</sub>) δ 13.58 (s, 1H), 8.02 (m, 2H), 7.58 (m, 3H), 6.82 (s, 1H), 4.14 (q, *J* = 6.6 Hz, 2H), 1.95 (m, 2H), 1.27 (s, 18H), 0.88 (t, *J* = 6.5 Hz, 3H); <sup>13</sup>C NMR (CDCl<sub>3</sub>) δ 182.3, 165.0, 159.9, 158.2, 152.8, 132.7, 130.7, 129.5, 126.8, 108.8, 105.7, 101.9, 95.9, 74.7, 30.2-14.3 (11C); HR-ESI-MS *m/z* calcd for C<sub>27</sub>H<sub>32</sub>Br<sub>2</sub>O<sub>4</sub>Na [M + Na]<sup>+</sup> 601.0564, found 601.0573.

6-bromo-7-dodecyloxy-5-hydroxyflavone or 6-bromo-*O*<sup>7</sup>-dodecylchrysin (**62**): yellow powder (90% yield). <sup>1</sup>H NMR (CDCl<sub>3</sub>) δ 13.48 (s, 1H), 7.89 (m, 2H), 7.55 (m, 3H), 6.73 (s, 1H), 6.57 (s, 1H), 4.13 (q, *J* = 6.0 Hz, 2H), 1.89 (m, 2H), 1.27 (s, 18H), 0.88 (t, *J* = 6.0 Hz, 3H); <sup>13</sup>C NMR (CDCl<sub>3</sub>) δ 181.8, 164.1, 161.1, 158.3, 156.7, 132.0, 131.0, 129.1, 126.3, 105.9, 96.8, 94.9, 91.5, 69.8, 31.9-14.1 (11C); HR-ESI-MS *m/z* calcd for C<sub>27</sub>H<sub>34</sub>BrO<sub>4</sub> [M + H]<sup>+</sup> 501.16405, found 501.16529.

## 2.4 Anti-dengue activity study

The experiments were conducted under the collaboration with Department of Microbiology, Faculty of Medicine, Chulalongkorn University.

### 2.4.1. Preliminary screening

LLC/MK2 cells (ATCC® CCL-7™) and DENV2 NGC were maintained as previously described.[24] LLC-MK2 (5x10<sup>4</sup> cells) were seeded into each well of 24-well plate and incubated overnight at 37°C under 5% CO<sub>2</sub>. DENV2 was added to the cells at a multiplicity of infection (M.O.I.) of 0.1 and the plate was incubated at 37°C under 5% CO<sub>2</sub> with gentle rocking every 15 min. The plate was washed with phosphate buffer

saline and incubated in maintenance media.[24] Each compound was prepared in DMSO and was introduced into each well to the final concentration of 10  $\mu\text{M}$  during and after infection. One percent DMSO was used as a no-inhibition control and the maintenance media alone was used as a no-virus control. Supernatants were collected at day 3 of incubation and the virus titers were determined by plaque titration. The active compounds were determined by the ability of the compound to inhibit greater than 1-log or 90% of viral titer (plaque forming unit/mL).

#### 2.4.2. Cytotoxicity of compounds with cell lines

The compound toxicity was determined at 10  $\mu\text{M}$  final concentration. LLC/MK2 ( $1 \times 10^4$  cells/well) were seeded into each well of 96-well plates and incubated overnight at 37°C 5%  $\text{CO}_2$ . Compounds were prepared and added to the cells to the final concentration of 10  $\mu\text{M}$ . 1% DMSO was used as a 100% cell viability control. Cells were incubated for 48 h before analyzing their viability by CellTiter 96® AQueous One Solution Cell Proliferation Assay kit (Promega) according to manufacturer's protocol. The plate was read by spectrophotometry at  $A_{450}$  and data were calculated to percent cell viability proportioned to DMSO control.

#### 2.4.3. Effective concentration ( $\text{EC}_{50}$ )

Effective concentration ( $\text{EC}_{50}$ ) was also studied using LLC/MK2  $5 \times 10^4$  cells, which were seeded and infected with DENV2 (M.O.I. of 0.1). Flavonoids were serially diluted in DMSO to the final concentrations as follows; 0, 0.1, 0.25, 0.5, 1, 2, 2.5, 5, 7.5, 10, and 25  $\mu\text{M}$ . DMSO at the concentration of 1% was used as a mock treatment referring to

100% infection. Infected cells were treated with the designated compounds during and post infection. Supernatants were collected at 3 days after infection for analysis of virion production by plaque titration. Non-linear regression analysis was used to determine the effective concentrations. Three independent experiments were performed and results were as means and standard error of the means (SEM). The therapeutic index (TI) was a ratio of  $CC_{50}/EC_{50}$  of the compound.

#### 2.4.4. Cytotoxic concentration ( $CC_{50}$ )

Cytotoxic concentrations ( $CC_{50}$ ) were also studied using LLC/MK2 cells. Briefly, the  $10^4$  cells were seeded into each well of 96-well plates. After an overnight incubation, flavonoids were serially diluted in DMSO to the final concentrations as follows: 1, 5, 7.5, 10, 25, 50, 100, and 250  $\mu$ M. Each concentration was performed in triplicates. DMSO at 1% was used as a mock treatment referring to 100% cell viability. Cells were incubated for 48 h before cell viability was accessed using CellTiter 96® Aqueous One Solution Cell Proliferation Assay kit (Promega, Wisconsin, USA). Non-linear regression analysis was used to determine cytotoxic concentrations ( $CC_{50}$ ) of each experiment. Results were derived from three independent experiments and reported as means and standard error of the means (SEM).



## Chapter 3

### Results and discussion

Structural modification of flavonoids has been investigated for improvement in biological activity along with penetration ability.[36-38] Bioactive halogenated derivatives were proved as promising agents for further study. In this research, halogenation of selected flavonoids was conducted to obtain a range of brominated and iodinated derivatives as new candidates for anti-dengue infection. Moreover, a series of  $O^7$ -ether chrysin was brominated for structure-activity relationship (SAR) evaluation. The inhibition of infection DENV2 was examined on LLC-MK2 cells.

#### 3.1 Halogenation of flavonoids

##### 3.1.1 Preliminary study on the halogenation of chrysin (34)

To find out a suitable method for halogenation of flavonoids, chrysin (34) was chosen as a model (Figure 3.1). Following the reported reaction conditions with suitable modifications, the results are summarized in Table 3.1.[23, 27]

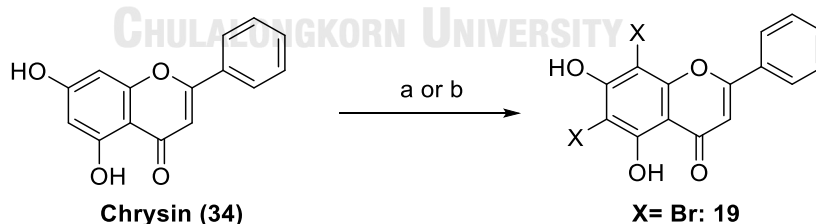


**Figure 3.1** Preliminary screening of halogenation of chrysin (34).

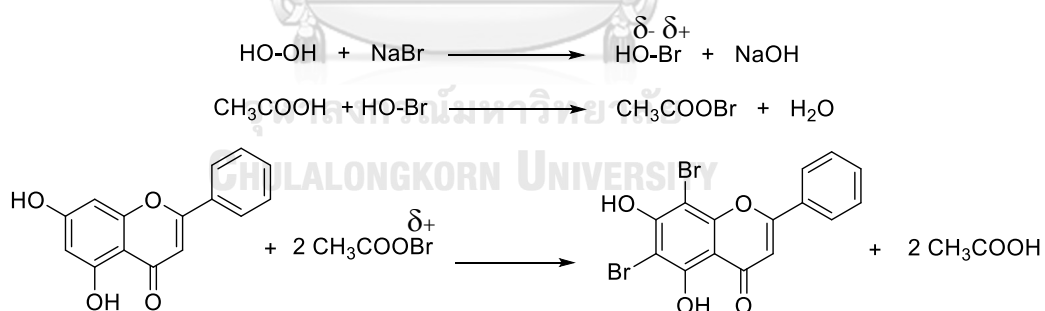
Reagents and conditions: a) NaBr/KI (3.0 equiv.),  $H_2O_2$  (3.0 equiv.),  $CH_3COOH$  (2.5 mL), rt, 24 h; b) NaBr/KI (3.0 equiv.), Oxone® (3.0 equiv.), acetone: $H_2O$ , rt, 2 h.

**Table 3.1** Screening of halogenation of chrysin (**34**).

Entry	Reagent	Oxidant (3.0 equiv.)	Solvent	Time (h)	Note
1	NaBr	H <sub>2</sub> O <sub>2</sub>	CH <sub>3</sub> COOH	24	% yield of <b>19</b> : 92
2	NaBr	Oxone®	acetone:H <sub>2</sub> O	2	% yield of <b>19</b> : 92
3	KI	H <sub>2</sub> O <sub>2</sub>	CH <sub>3</sub> COOH	24	Insoluble product
4	KI	Oxone®	acetone:H <sub>2</sub> O	2	Insoluble product

All the reactions were conducted at rt.

In previous reports, the common electrophilic halides were derived from hydrogen halides or halide salts and the amount was limited to 1.0 equiv. to obtain the monosubstitution as a major component.[22, 23] The proposed mechanism using chrysin as an instance were illustrated below (**Figure 3.2**)

**Figure 3.2** Proposed mechanism of bromination of chrysin (**34**).

In this research, the desired targets are a series of disubstituted flavonoids (**19**, **42-52**) because of their promising bioactive value.[24] The reaction was taken place at rt and checked by TLC every hour. Using an excess of NaBr (3.0 equiv.), 6,8-

dibromochrysin (**19**) was generated as only product in excellent yield (>90%). The expected product was characterized by the absence of signals of 6- and 8- protons at  $\delta_{\text{H}}$  6.50 and 6.21 ppm, and the significant shift of the chelated hydroxyl proton at position 5 from 12.82 ppm of chrysin (**34**) to 13.74 ppm of **42**, due to the effect of bromine atom. The  $^1\text{H}$  NMR spectral data of **19** was also confirmed with those of the previous report.[26] In addition, NaBr/H<sub>2</sub>O<sub>2</sub>/CH<sub>3</sub>COOH or NaBr/Oxone®/acetone:H<sub>2</sub>O 5:1 changed from halogenated solvents to other low toxic solvents and had non-toxic by-product (H<sub>2</sub>O), which could consider as ecofriendly conditions.

6,8-dibromo-5,7-dihydroxyflavone (**19**): yellow powder.  $^1\text{H}$  NMR (DMSO-*d*<sub>6</sub>, Figure A3.)  $\delta_{\text{H}}$  13.74 (s, 1H), 8.14 (dd, *J* = 7.4, 2.2 Hz, 2H), 7.61 (m, 3H), 7.12 (s, 1H).

On the other hand, there was a failure when changing from NaBr to KI, for both oxidants. 6,8-Diiodochrysin (**20**) was synthesized before using I<sub>2</sub> in CH<sub>2</sub>Cl<sub>2</sub> and HNO<sub>3</sub>, and could be dissolved in DMSO.[28] However, in repeated experiments, the insoluble product was received without identifying since it was not able to dissolve in any kind of solvents, leading to the limit of applicability for iodination. Nonetheless, the developed conditions 1.0 equiv. of precursor – 3.0. of NaBr/KI – 3.0 equiv. of H<sub>2</sub>O<sub>2</sub> were applied for other selected flavonoids in this study.

### 3.1.2 Halogenation of selected flavonoids

After applying on chrysin (**34**), the bromination and iodination of selected flavonoids, including flavone: baicalein (**18**); flavanone: pinostrobin (**6**), pinocembrin

(7), naringenin (12), hesperetin (15); flavonol: quercetin (13), were carried out (Figure

3.3). Isolation yields were reported in Table 3.2.

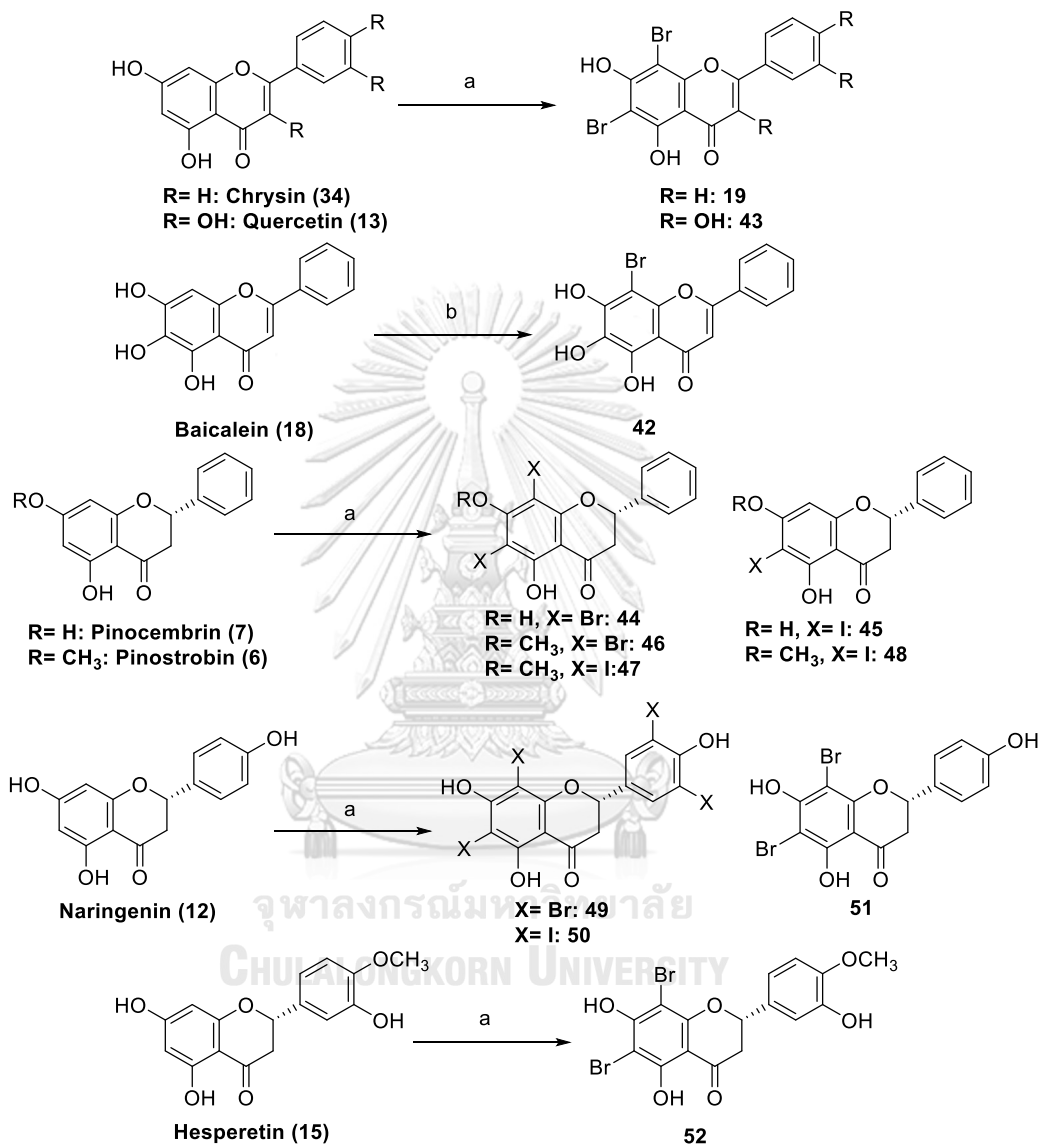


**Figure 3.3** Halogenation of selected flavonoids.

Reagents and conditions: a) NaBr/KI (3.0 equiv.), H<sub>2</sub>O<sub>2</sub> (3.0 equiv.), CH<sub>3</sub>COOH (2.5 mL), rt, 24 h; b) NBS (1.5 equiv.), concd. H<sub>2</sub>SO<sub>4</sub>, THF (4.0 mL), rt, 12 h.

**Table 3.2** Halogenation of selected flavonoids.

Entry	Halogenation	Starting material	% Isolated yield		
			Mono-	Di-	Tetra-
1		Baicalein ( <b>18</b> )			
2		Baicalein ( <b>18</b> ) <sup>a</sup>	35		
3		Pinocembrin ( <b>7</b> )		93	
4		Pinostrobin ( <b>6</b> )		96	
5	Bromination	Naringenin ( <b>12</b> )		25	42
6		Naringenin ( <b>12</b> ) <sup>b</sup>		10	30
7		Naringenin ( <b>12</b> ) <sup>c</sup>		12	21
8		Quercetin ( <b>13</b> )		52	
9		Hesperetin ( <b>15</b> )		61	
10		Pinocembrin ( <b>7</b> )	74		
11		Pinocembrin ( <b>7</b> ) <sup>d</sup>	31		
12	Iodination	Pinostrobin ( <b>6</b> )	10	73	
13		Naringenin ( <b>12</b> )			48
14		Naringenin ( <b>12</b> ) <sup>d</sup>			40
15		Naringenin ( <b>12</b> ) <sup>e</sup>			23

Reaction condition: Precursor (1.0 equiv.), NaBr/KI (3.0 equiv.), H<sub>2</sub>O<sub>2</sub> (3.0 equiv.), rt, 24 h.

<sup>a</sup> NBS (1.5 equiv.), concd. H<sub>2</sub>SO<sub>4</sub>, THF (4.0 mL), rt, 12 h.

<sup>b</sup> NaBr (4.0 equiv.) with H<sub>2</sub>O<sub>2</sub> (3.0 equiv.) in CH<sub>3</sub>COOH (2.5 mL), rt, 24 h.

<sup>c</sup> NaBr (2.0 equiv.) with H<sub>2</sub>O<sub>2</sub> (3.0 equiv.) in CH<sub>3</sub>COOH (2.5 mL), rt, 24 h.

<sup>d</sup> KI (4.0 equiv.) with H<sub>2</sub>O<sub>2</sub> (3.0 equiv.) in CH<sub>3</sub>COOH (2.5 mL), rt, 24 h.

<sup>e</sup> KI (2.0 equiv.) with H<sub>2</sub>O<sub>2</sub> (3.0 equiv.) in CH<sub>3</sub>COOH (2.5 mL), rt, 24 h.

6-Bromobaicalein (**42**) was unsuccessfully generated by using NaBr/H<sub>2</sub>O<sub>2</sub>/CH<sub>3</sub>COOH, but it could be obtained by following previously reported method (entries 1, 2).[32] Compound **42** was confirmed by comparing <sup>1</sup>H NMR spectrum (Figure A4, Appendix) with the reference. In contrast, the bromination of pinocembrin (**7**) and pinostrobin (**6**) was accomplished by using NaBr/H<sub>2</sub>O<sub>2</sub>/CH<sub>3</sub>COOH to gain 6,8-dibromo derivatives in high yield (more than 90%, entries 3, 4). It should be noted here that 6,8-dibromopinocembrin (**44**) and 6,8-dibromopinostrobin (**46**) were synthesized for the first time. These two new compounds were identified from the missing of signals of two protons of 6- and 8-positions at  $\delta_{\text{H}}$  6.07 ppm of pinocembrin (**7**) and  $\delta_{\text{H}}$  5.94 ppm of pinostrobin (**6**). Furthermore, the large shift of chelated hydroxyl proton at position 5 due to the addition of bromine atom was also the characteristic signal of the spectra (Figures A7, A12, Appendix). The bromination of naringenin (**12**) was complicated as the existence of two products with moderate yield (entries 5-7). 6,8,3',5'-Tetrabromonaringenin (**49**) and 6,8-dibromonaringenin (**51**) were similar in the disappearance of signal of two protons at positions 6 and 8 at  $\delta_{\text{H}}$  5.88 ppm and the switch of specific hydroxyl proton at position 5 from  $\delta_{\text{H}}$  12.14 ppm of naringenin (**12**) to 12.93 and 12.98 ppm of **49** and **51**, respectively. Moreover, in the range of aromatic signals of **49**, there is only one signal with integration equal to 2.0 representing for two protons at positions 2' and 6' of ring B. This evidence strongly confirmed for the substitution at 3'- and 5'-positions on phenyl ring B of naringenin (**12**) (Figure A19,

Appendix). In the circumstances of quercetin (**13**) and hesperetin (**15**), the replacement of bromine atom only occurred at activated phenyl ring A, which was proved by the loss of the proton signals at positions 6 and 8 at  $\delta_{\text{H}}$  6.41 and 6.18 ppm of quercetin (**13**) and at  $\delta_{\text{H}}$  5.88 ppm of hesperetin (**15**) (entries 8, 9, Figures A23, A24, Appendix). Compounds **43** and **52** are known compounds and were compared with the reference.[34, 35]

Similarly, the iodination of selected flavonoids gave the same characteristics on the spectra. The obtained products were recognized by the missing of the signals of protons at positions 6 and 8 when collating with their precursors (Figures A9, A15, A17, A21). Besides, these iodinated compounds **45**, **47**, **48** and **50** are firstly reported.

For bromination, there was a noticeable difference in components of the reaction mixture between substituted and unsubstituted phenyl ring B. The parents with plain phenyl ring B gave out dibromo derivatives in excellent yield (>90%). This circumstance could be explained by the inactive reactivity of the unsubstituted benzene ring. 6,8-Dibromochrysin (**19**), 6,8-dibromopinocembrin (**44**) and 6,8-dibromopinostrobin (**46**) were selected as examples for illustration (entries 3, 4). On the contrary, the presence of hydroxyl groups activated the benzene ring, especially at 3' and 5' positions, resulted in tetrabromonaringenin (**49**). In spite of using only 2.0 equiv. of NaBr, the multiple substitution still occurred (entry 7), indicating the crucial role of the hydroxyl group on ring B affecting on its reactivity. Increasing to 4.0 equiv. of NaBr only affected

to the yield, since the percentage yield of each product slightly increased without changing the reaction components (entry 6). Furthermore, there was a regioselectivity occurred on electron-deficient ring A only when applying on quercetin (**13**) and hesperetin (**15**), despite the similarity of ring B structure with naringenin (**12**). The formation of dibromo product in the circumstance of quercetin could be explained by the deprotonation of acidic proton of hydroxyl group at position 7 and the canonical resonance structures of dibromoquercetin quinonemethide,[34] meanwhile hesperetin was still ambiguous. To find out the reasonable explanation, more experiments on similar structures such as apigenin (**63**), luteolin (**64**) are necessitated (Figure 3.4).

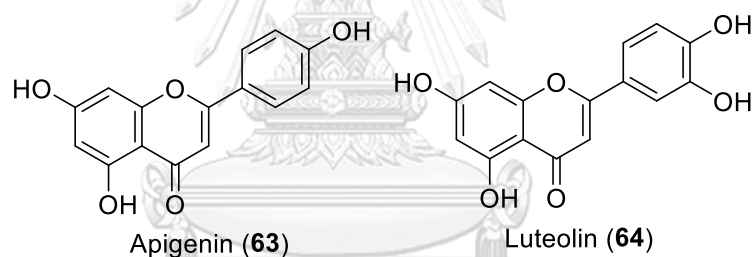


Figure 3.4 Apigenin (**63**) and luteolin (**64**).

Despite of the failure of using KI in iodination of chrysin (**34**), the iodination of pinostrobin (**6**), pinocembrin (**7**) and naringenin (**12**) derivatives were achieved in moderate yields (entries 10-15). This success suggested that the iodination using halide salts as iodinating reagents can be applied on some selected class of flavonoids, in this case is flavanone. Similarly, the iodination of naringenin (**12**) generated tetraiodo derivative (**50**) as a major compound while diiodo one was not achieved (entries 13-



15), which reaffirmed the important role of hydroxyl group on phenyl ring B on activating positions 3' and 5'. In addition, varying the amount of KI did not change the reaction components, but there was a remarkable difference in the yield of reaction (entries 13-15). Interestingly, the regioselectivity on 6-position of ring A could be observed for pinostrobin (**6**) and pinocembrin (**7**) (entries 10-12). There is the difference between two flavanones, *i.e.* the substituent at the 7-position of ring A: pinostrobin (**6**) has a methoxyl group while pinocembrin (**7**) bears a hydroxyl. This observation indicated the role of hydroxyl group at 5-position on the selectivity, which was mentioned in some previous reports.[33, 39]

It should be notified here that this is the first report on the halogenation of pinostrobin (**6**) and pinocembrin (**7**). In addition, tetrahalo-substituted naringenins (**49-50**) have not been addressed before. These new synthesized derivatives were characterized by  $^1\text{H}$  and  $^{13}\text{C}$  NMR and their exact mass were confirmed by HR-ESI-MS (Table 3.3).

**Table 3.3** Tentative <sup>1</sup>H NMR spectral assignment and exact mass of compounds **44-50**.

Cpds	H-2	H-3		5-OH	H-6	H-8	H-2', 6'	H-3', 5'	H-4'	-OCH <sub>3</sub>	Exact mass	
		α	β								Calcd.	Found
	5.58 (dd,	3.15 (dd, <i>J</i>	3.00 (dd, <i>J</i>									
<b>44</b>	<i>J</i> = 12.2, 3.5 Hz)	= 17.3, 12.2 Hz)	= 17.3, 3.5 Hz)	12.74 (s)	-	-	7.45 (m)	-			456.8663	456.8657
	5.44 (dd,	3.25 (dd, <i>J</i>	2.89 (dd, <i>J</i>									
<b>45</b>	<i>J</i> = 12.8, 3.2 Hz)	= 17.3, 12.8 Hz)	= 17.3, 3.2 Hz)	13.03 (s)	-	6.31 (s)	7.44 (m)	-				
	5.61 (dd,	3.18 (dd, <i>J</i>	3.05 (dd, <i>J</i>									
<b>46</b>	<i>J</i> = 12.3, 3.4 Hz)	= 17.3, 12.3 Hz)	= 17.3, 3.4 Hz)	12.61 (s)	-	-	7.48 (m)	3.98 (s)			448.90000	448.89938
	5.85 (dd,	3.37 (dd, <i>J</i>	3.14 (dd, <i>J</i>									
<b>47</b>	<i>J</i> = 12.6, 3.2 Hz)	= 17.3, 12.6 Hz)	= 17.3, 3.2 Hz)	13.02 (s)	-	-	7.47 (m)	3.91 (s)			566.8542	566.8525

**Table 3.3** (Continue)

Cpds	H-3		5-OH	H-8	H-2', 6'	H-3', 5'	H-4'	-OCH <sub>3</sub>	Exact mass	
	$\alpha$	$\beta$							Calcd.	Found
<b>48</b>	5.68 (dd,	3.29 (dd, <i>J</i> = 17.4,	12.95	-	6.33 (s)	7.53 (m)	-	3.98 (s)		
		= 17.4, 3.1	(s)							
	3.1 Hz)	13.0 Hz)								
<b>49</b>	5.74 (dd,	3.38 (dd, <i>J</i> = 17.2,	12.93	-	-	7.82 (s)	-	-		
		= 17.2, 3.1	(s)							
	3.1 Hz)	12.7 Hz)								
<b>50</b>	5.67 (dd,	3.43 (dd, <i>J</i> = 17.2,	12.84	-	-	7.74 (s)	-	-		
		= 17.2, 3.0	(s)							
	3.0 Hz)	12.8 Hz)								

### 3.1.3 Anti-dengue evaluation of halogenated flavonoids

The inhibition of infection DENV2 was conducted under the collaboration with Department of Microbiology, Faculty of Medicine, Chulalongkorn University. The percentage of inhibition, percentage of cell viability, EC<sub>50</sub>, CC<sub>50</sub> and TI value are presented in **Table 3.4**.

**Table 3.4** Anti-dengue results of brominated and iodinated flavonoids.

Entry	Cpds	% Plaque inhibition (at 10 $\mu$ M)	% Cell viability (at 10 $\mu$ M)	EC <sub>50</sub> ( $\mu$ M)	CC <sub>50</sub> ( $\mu$ M)	TI
1	<b>34</b>	86.67 $\pm$ 6.67	79.87 $\pm$ 1.40	N.D	N.D	N.D
2	<b>19</b>	98.82 $\pm$ 0.42	89.08 $\pm$ 7.62	1.47[24]	44.28[24]	N.D
3	<b>18</b>	N.D	N.D	4.04 $\pm$ 1.37	>250	61.88
4	<b>42</b>	N.D	N.D	0.88 $\pm$ 0.14	256.43 $\pm$ 2.90	291.40
5	<b>7</b>	46.67 $\pm$ 9.43	97.84 $\pm$ 3.24	15.45 <sup>a</sup>	>100 <sup>a</sup>	6.47
6	<b>44</b>	99.93 $\pm$ 0.07	101.08 $\pm$ 4.91	2.06 $\pm$ 0.80	67.21 $\pm$ 0.80	32.56
7	<b>6</b>	95.11 $\pm$ 0.38	122.27 $\pm$ 3.12	10.76 $\pm$ 1.63	78.58 $\pm$ 3.29	7.30
8	<b>46</b>	99.90 $\pm$ 0.04	105.14 $\pm$ 1.17	5.83 $\pm$ 0.51	> 100	17.15
9	<b>47</b>	99.84 $\pm$ 0.10	129.51 $\pm$ 5.50	2.8 $\pm$ 1.55	N.A	N.A
10	<b>48</b>	97.11 $\pm$ 3.29	135.24 $\pm$ 1.36	4.1 $\pm$ 1.84	N.A	N.A
11	<b>12</b>	95.33 $\pm$ 0.67	108.02 $\pm$ 2.55	48.17*	311.3*	6.46
12	<b>49</b>	91.82 $\pm$ 2.73	101.98 $\pm$ 2.76	9.36*	39.74*	4.25
13	<b>50</b>	84.55 $\pm$ 1.57	102.07 $\pm$ 3.40	9.62*	35.77*	3.72
14	<b>51</b>	91.11 $\pm$ 3.58	111.40 $\pm$ 6.78	16.65*	92.66*	5.60

Tabl3 3.4 (Continue)

Entry	Cpds	% Plaque inhibition (at 10 $\mu$ M)	% Cell viability (at 10 $\mu$ M)	EC <sub>50</sub> ( $\mu$ M)	CC <sub>50</sub> ( $\mu$ M)	TI
15	<b>13</b>	N.D	N.D	8.34 $\pm$ 0.80	> 100	11.99
16	<b>43</b>	N.D	N.D	8.51 $\pm$ 0.43	> 100	11.75
17	<b>15</b>	N.D	N.D	>25	112.83 $\pm$ 7.59	4.51
18	<b>52</b>	N.D	N.D	6.84 $\pm$ 1.59	47.28 $\pm$ 1.58**	6.91

Data represent means  $\pm$  standard error mean (SEM) of three independent experiment. The results were reported from three independent experiments. Compound **19** was used as positive control.

\* The results were reported from one experiment.

\*\* The results were reported from two independent experiments.

EC<sub>50</sub> = Effective concentrations, the molar concentration of an agonist that produced 50% of the maximal possible effect of that agonist [40];

CC<sub>50</sub> = Cytotoxic concentrations, the concentration of compound required for the reduction of 50% cell viability [41];

TI = Therapeutic Indices;

N.D = Not determine;

N.A = Not available.

<sup>a</sup> Srivarangkul, P. 2018.

The tabular results of biological indices of halogenated flavonoids pointed out some promising candidates for further studying on dengue inhibitors. The first preliminary screening of plaque inhibition at 10  $\mu$ M displayed the efficiency of adding bromine atom into the flavonoid scaffold to the bioactivity. Most derivatives exhibited excellent inhibitory value of more than 90%, especially new compounds **44**, **46** and **47** inhibited approximately more than 99% of virus infection (entries 6, 8 and 9). In comparison with the precursors, derivatization made a significant change for antiviral

activity of flavonoids, except the case of naringenin (**12**). Noticeably, 6,8-dibromopinocembrin (**44**) was doubled of inhibition comparing to its parent (46.67 % of pinocembrin (**7**) *versus* 99.93 % of **44**), which emphasized the contribution of bromine atom to the bioactivity (entries 5, 6). Naringenin (**12**) was previously reported as a promising inhibitor of dengue virus;[18] however, embedded bromine atom did not attain the enhancement of anti-dengue infection as expectation. The percentage of inhibition plaque of tetrabromo-, dibromo-, tetraiodo- derivatives **49-51** were 91.82, 84.55, 91.11, respectively, and lower than that of naringenin (**12**), though the value were still acceptable (entries 11-14). The difference between naringenin (**12**) and chrysin (**34**), baicalein (**18**), pinostrobin (**6**) and pinocembrin (**7**) is the appearance of substituent on phenyl ring B, which might affect the activity. Hesperetin (**15**) and quercetin (**13**) are also have alkoxy groups on phenyl ring B, therefore, they were not screened for inhibition at 10  $\mu$ M. On the other hand, there is a negligible difference among brominated and iodinated derivatives in case of pinostrobin (**6**); however, the activity of 6,8-dibromopinostrobin (**46**) was slightly better than 6,8-diiodopinostrobin (**47**); 6,8-diiodopinostrobin (**47**) is more active than 6-iodopinostrobin (**48**) (entries 8-10).

To estimate the toxicity of tested compounds at 10  $\mu$ M, the percentage of cell viability was accounted. The results showed that the series of halogenated flavonoids are relatively non-toxic with the cell as specific concentration. Most of the cases, more

than 90% of cells were viable, except for chrysin (**34**) and 6,8-dibromochrysin (**19**) (entries 1, 2).

Based on the preliminary screening results, to further evaluate the cytotoxicity and effective concentration of these synthesized products, appropriate experiments were conducted to determine  $EC_{50}$  and  $CC_{50}$  value. The illustration graph of the relationship was showed below (**Figure 3.5**).



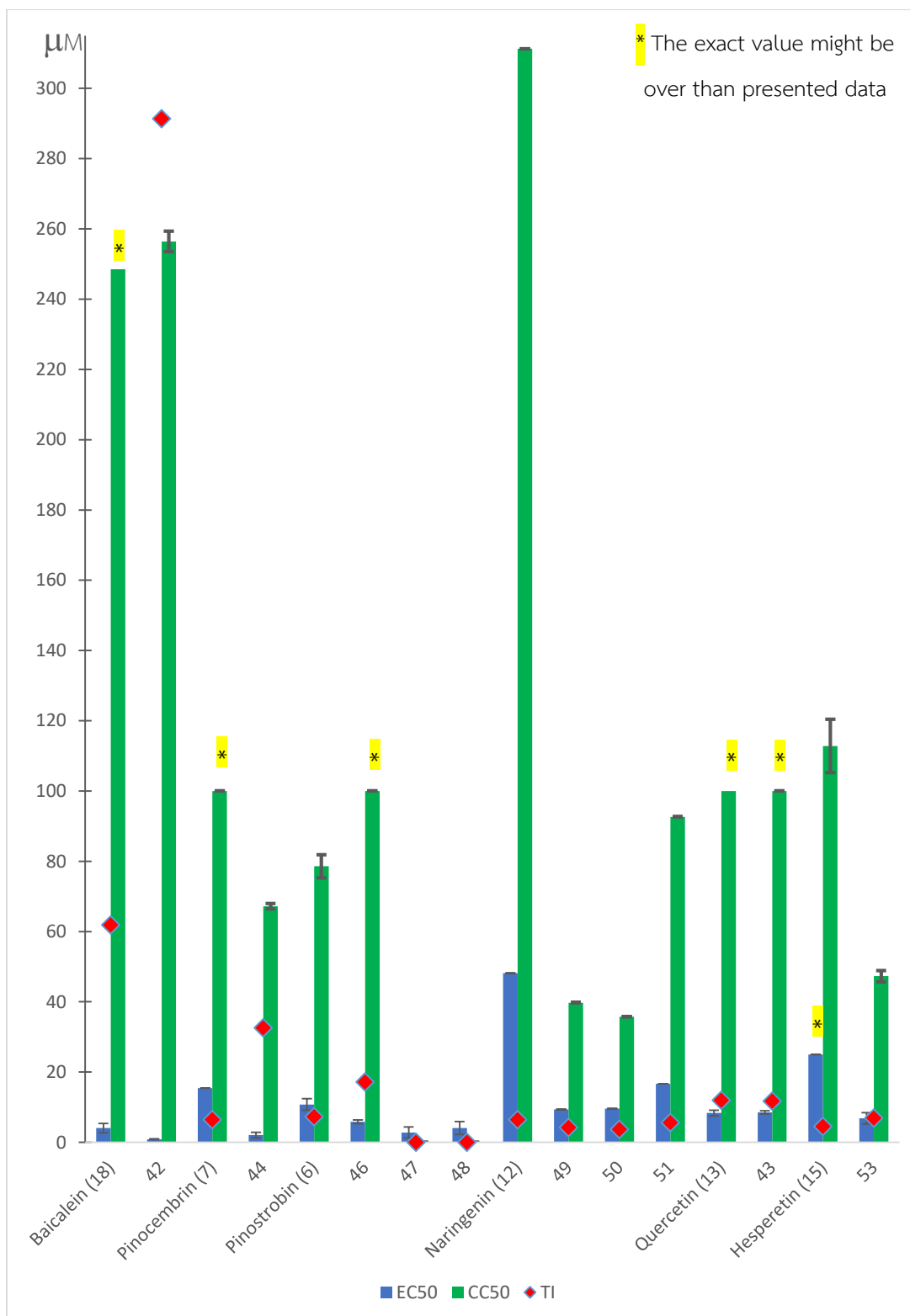


Figure 3.5 EC<sub>50</sub>, CC<sub>50</sub> and TI value of flavonoids and their halogenated derivatives.



In accordance with the inhibitory results, most of the synthesized compounds displayed competitive  $EC_{50}$  and  $CC_{50}$  than the starting materials and could be considered as good anti-dengue agents. Among them, brominated baicalein (**42**) was the most effective compound with  $0.88 \mu\text{M}$  of  $EC_{50}$  (entry 4). In addition, while screening the cytotoxicity concentration  $CC_{50}$ , the result also showed that **42** was less toxic to the cell with the highest  $CC_{50}$  of  $256.43 \mu\text{M}$  in range, consequently TI was 291.40. Though baicalein (**18**) was investigated and proved to have remarkable antiviral effect on multiple stages of dengue virus infection before,[17] bromination made a tremendous enhancement of antiviral effect, along with the promising future as new dengue inhibitor in therapy. Furthermore, 6,8-dibromopinocembrin and pinostrobin (**44**) and (**46**) also possessed noticeably low  $EC_{50}$   $2.064 \mu\text{M}$  and  $5.83 \mu\text{M}$ , respectively, which can be considered as potent anti-dengue agents. On the other hand, the appearance of substituents on the ring B of naringenin (**12**), quercetin (**13**) and hesperetin (**15**) might cause a drawback to the toxicity. The more substituents on ring B, the higher toxicity to the cell, as presented in  $CC_{50}$  of **49** and **50** at  $39.74$  and  $35.77 \mu\text{M}$ , respectively, which made **50** is the most toxic compound to the cell (entries 12, 13). In addition, 6,8-dibromoquercetin (**43**) and 6,8-dibromohesperetin (**52**) though with acceptable  $CC_{50}$ , TI values are unattractive for further study. These suggested that the number of halogen atom need to be controlled and the ring B should be unsubstituted.

When comparing between brominated and iodinated products of pinostrobin (**6**), there is a small dissimilarity in effective concentration  $EC_{50}$  value. Generally, brominated derivatives exhibited better activity than iodinated ones;[24] however, among halogenated pinostrobins, 6,8-diiodopinostrobin (**47**) displayed the lowest  $EC_{50}$  of 2.8  $\mu\text{M}$ , meanwhile the  $EC_{50}$  of 6,8-dibromopinostrobin (**44**) is 5.83  $\mu\text{M}$  (entries 8, 9). Similarly, there is the modest distinction between tetrabromo- and tetraiodonaringenin, disclosing in the higher  $EC_{50}$  value of tetraiodonaringenin (**50**) 9.62  $\mu\text{M}$  than tetrabromonaringenin (**49**) 9.36  $\mu\text{M}$  (entries 12, 13). Nonetheless, the TI values showed that brominated derivative is more potent to be further investigated than iodinated one.

The graphic diagram also revealed the relationship between the  $EC_{50}$ ,  $CC_{50}$  and TI as the important criteria for evaluating the bioactive potential of the compound. Some compounds such as naringenin (**12**), hesperetin (**15**) possessed high  $CC_{50}$  value, which represented for its low toxicity towards to the cells, however, since the  $EC_{50}$  index were relatively high, consequently leading to the low TI value, these compounds were not attractive to investigate deeply. In contrast, baicalein (**18**) and its derivative **42** exhibited either low  $EC_{50}$  or high  $CC_{50}$ , which resulted in extraordinary TI value, and will be considered to study intensely in the future. Besides, the graph could be used for comparison between unsubstituted phenyl ring B flavonoids with substituted ones, since there was a huge distance of baicalein (**18**), pinostrobin (**6**), pinocembrin (**7**) and

their derivatives **42**, **44**, **46**, **47** on the left side of the graph with naringenin (**12**), quercetin (**13**), hesperetin (**15**) and their derivatives **49**, **50**, **51**, **43**, **52** on the right side.

To discover the exact target and understand the important interactions of compound with protein in the cell, other computational calculation and bio-assays are necessary in the future.

### 3.2 Brominated $O^7$ -ether chrysin as anti-dengue agents

#### 3.2.1 Literature review of $O^7$ -ether chrysin

Chrysin (**34**) is famous for its bioactivities such as anti-oxidant, anti-inflammatory, anti-cancer, neuroprotective, *etc.*[12] However, the applications of this compound in biological purposes are restricted because of low absorption and quick excretion in human body.[12] In order to overcome this limitation, a lot of structural modifications were applied like esterification, halogenation, etherification, *etc.*[24, 33, 36, 42] Since 1999, a research done by Shin and partners performed on eighteen chrysin derivatives and examined *in vivo* against the diabetes mellitus.[43] Among them,  $O^7$ -propylchrysin (**65**),  $O^7$ -butylchrysin (**38**),  $O^7$ -octylchrysin (**40**) (**Figure 3.6**) significantly dropped the glucose level in the blood as compared with that of the control, particularly  $O^7$ -butylchrysin (**38**) showed over 50% reduction in the blood glucose level at day-7.

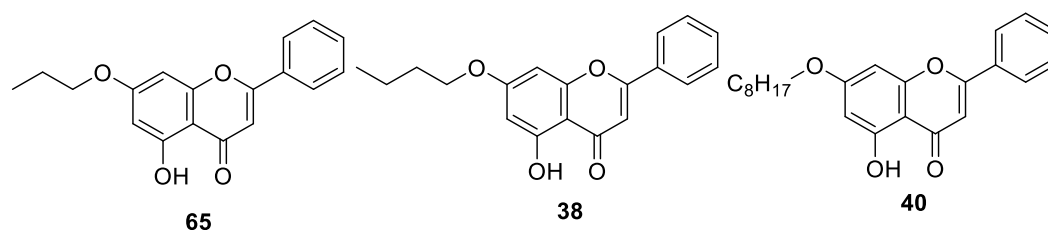


**Figure 3.6** Structures of **65**, **38**, **40**.

In 2014, a study controlled by Cheng's group evaluated the relationship between chrysin (**34**), apigenin (**63**), luteolin (**64**), diosmetin (**66**) and their *O*-alkylated derivatives for the yeast  $\alpha$ -glucosidase inhibitory activity.[44] The synthesized chrysin derivatives displayed a remarkable increasing of inhibition toward  $\alpha$ -glucosidase enzyme comparing to their corresponding flavonoid, and as long as the alkyl were prolonged, up to six carbons of the chain, the  $IC_{50}$  value decreased significantly (**Figure 3.7**). The positive correlation between the length of side-chain and bioactivity showed the efficiency of structural modification on chrysin (**34**).

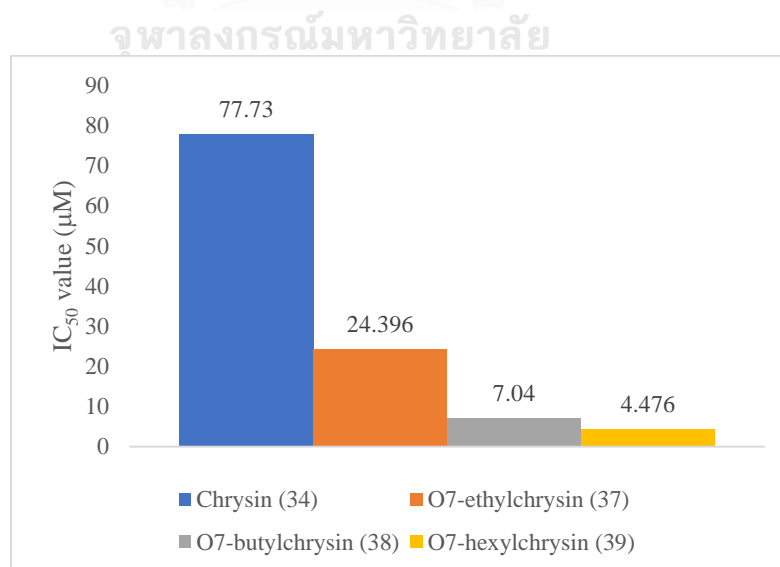


**Figure 3.7**  $IC_{50}$  value of  $\alpha$ -glucosidase inhibitory activity of chrysin and its derivatives.

A noticeable research in 2017 of Nile *et al.* investigated on some natural plant flavonoids, including chrysin (**34**), and their synthesized derivatives for anti-oxidant, anti-inflammatory and enzyme inhibition consolidated the prospect of  $O^7$ -chrysin derivatives.[45] The data obtained from this study implied that  $O^7$ -hexylchrysin (**39**) (**Figure 3.8**) might be used as anti-oxidant and anti-inflammatory candidate with low toxicity.

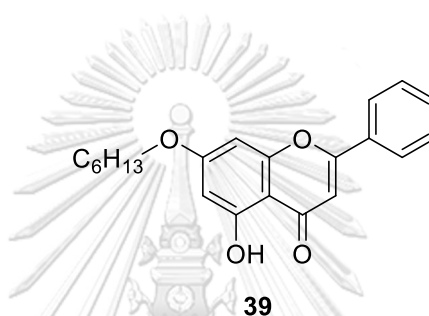


**Figure 3.8** Structure of  $O^7$ -hexylchrysin (**39**).

Lastly, a study of Krongkan *et al.* on chrysin and nine synthesized derivatives with substituent modification on ring A was examined on five strains of pathogenic bacteria *P. acnes*, *S. aureus*, *S. sobrinus*, *S. typhi* and *S. mutans*. [28] Chrysin and its  $O^7$ -ether derivatives showed moderate inhibitory activity with all tested bacteria at 1 mM. Specifically,  $O^7$ -octylchrysin (**40**) exhibited very good effect against *S. sobrinus* (inhibition zone=  $13.33 \pm 0.47$  mm) and good inhibition against *S. mutans* (inhibition zone=  $11.33 \pm 0.47$  mm) and *S. aureus* (inhibition zone=  $10.33 \pm 0.47$  mm);  $O^7$ -hexylchrysin (**39**) displayed good value toward *S. sobrinus* (inhibition zone=  $11.67 \pm 0.47$

mm) and *S. mutans* (inhibition zone= 13.00 ± 0.00 mm). This information suggested the promising bioactivity of  $O^7$ -ether chrysin for further investigation.

Based on the positive results of anti-dengue activity of 6,8-halogenated chrysin and literature reviews about biological potentials of  $O^7$ -ether chrysin, a series of brominated  $O^7$ -ether chrysin with a variety of certain alkyl chains length were generated in order to evaluate the relationship between structure and bioactivity.

### 3.2.2 Synthesis of brominated $O^7$ -ether chrysin

Based on the success of using NaBr/H<sub>2</sub>O<sub>2</sub>/CH<sub>3</sub>COOH for the synthesis of brominated flavonoids, at first, this condition was tested. There were two proposed pathways: bromination of chrysin (**34**) and then etherification at position 7 or reverse (**Figure 3.9**).

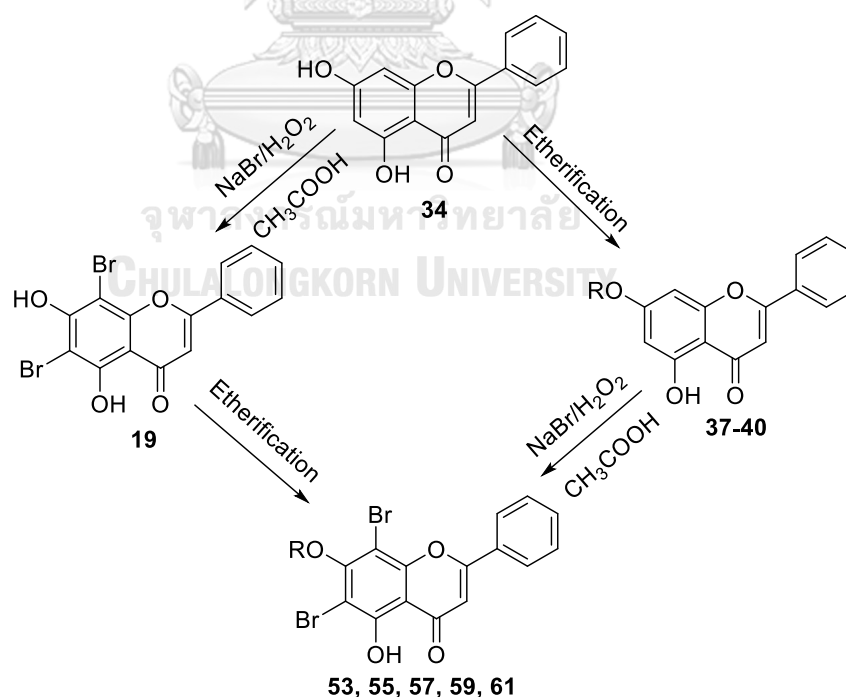
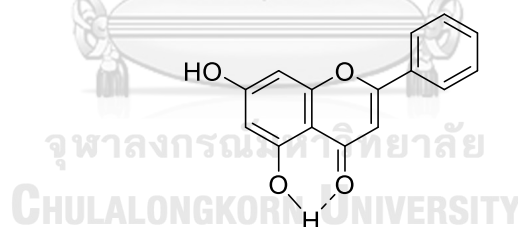


**Figure 3.9** Two proposed synthetic pathways of dibromo  $O^7$ - ether chrysin **53, 55, 57, 59, 61**.

Opposed to expectation, none of the designed routes worked effectively. The first effort to synthesize the ether derivatives from **19** was failed because of the solubility of **19** in the solvent of etherification. Generally, etherification of flavonoids uses alkyl bromide and acetone as solvent with  $K_2CO_3$  as base.[28] However, when applying these conditions, **19** did not dissolve well in acetone and after refluxing in 24 h, the starting material remained. To overcome this problem, the synthetic plan was reversed. Starting from chrysin (**34**), a series of desired ethers were synthesized first and then brominated by  $NaBr/H_2O_2/CH_3COOH$ . The selectivity toward hydroxyl group at position 7 instead of position 5 could be explained by the chelation of proton of 5-hydroxyl with the neighbor carbonyl group (Figure 3.10). This weak hydrogen bonding blocked the hydroxyl group, resulting in etherification occurred at 7-position only.



Hydrogen bonding of 5-hydroxyl group and C=O

**Figure 3.10** Hydrogen bonding of hydroxyl group and adjacent carbonyl group.

This change expected to solve the obstacle since the condition operated smoothly with pinostrobin (**6**), which has the methoxy group at position 7. Once again, the procedure did not occur proficiently because of the solubility of  $O^7$ -ether chrysin (**37-40**) in used solvent. Acetic acid could not dissolve the ether chrysin, so after 24 h,

the reaction did not take place. In addition, the steric effect of the bulky side chains might obviate the attack of brominium ion  $\text{Br}^+$  to positions 6 and 8. In summary, the application of bromination by  $\text{NaBr}/\text{H}_2\text{O}_2/\text{CH}_3\text{COOH}$  was limited in the case of ether chrysin derivatives. Another approach to control the bromination of  $O^7$ -ether chrysin was to change the reagent to NBS, based on a study of Pan *et al.* in 2015.[33]

Synthetic process was followed previous method from a research of Pan and colleagues in 2015 with some modifications.[33] The series of  $O^7$ -ether chrysin were received from Kongkran *et al.* study.[28] The synthetic scheme including reaction conditions was summarized in **Figure 3.11**.

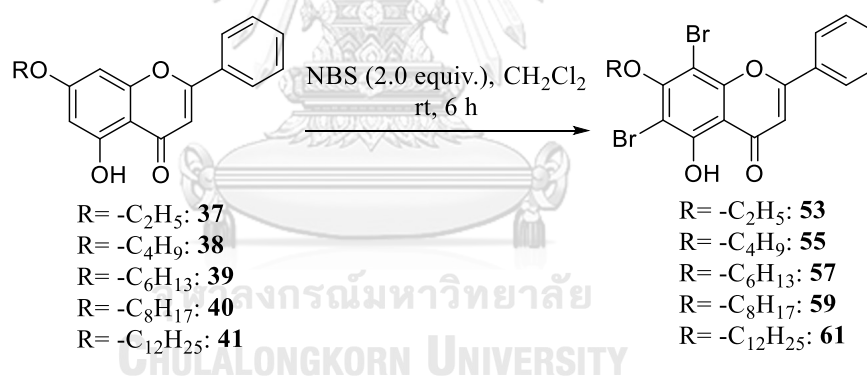


**Figure 3.11** Synthetic scheme of dibromo  $O^7$ - ether chrysin **53**, **55**, **57**, **59**, **61**.

Briefly, in order to get dibromo substituted compounds as major component, the amount of NBS was increased up to 2.0 equiv. and the reaction mixture was checked every hour by TLC. Experiments using 1.0 equiv. of NBS were also carried out to obtain the 6-bromo derivatives for comparison in activity (**Figure 3.12**).



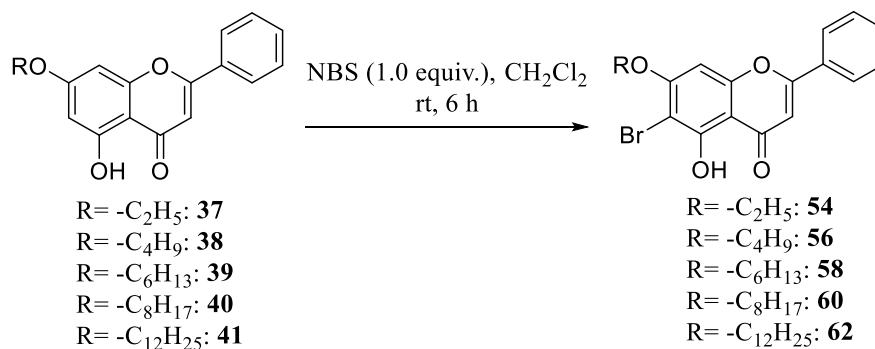


**Figure 3.12** Synthetic scheme of monobromo *O*<sup>7</sup>- ether chrysin **54**, **56**, **58**, **60**, **62**.

The regioselectivity of NBS to position 6 could be interpreted by the interaction of carbonyl group of NBS molecule with the hydroxyl at position 5 of ether derivatives, presenting in **Figure 3.13**.<sup>[39]</sup>

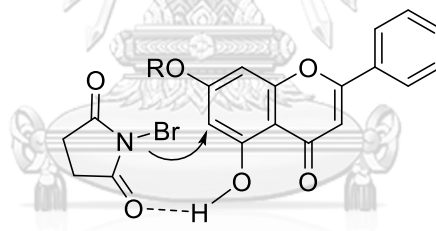


**Figure 3.13** Regioselectivity of NBS to position 6 of *O*<sup>7</sup>- ether chrysin.

This chelation attracted two molecules close to each other in the rigid position, which supports for the specific selectivity. The experimental data is presented in **Table**

**3.5.**

**Table 3.5** Bromination of  $O^7$ - ether chrysin series **53** - **62**.

Entry	R	Compound	NBS	% Yield
1	C <sub>2</sub> H <sub>5</sub>	6,8-dibromo- $O^7$ -ethylchrysin ( <b>53</b> )	2.0 equiv.	86
2		6-bromo- $O^7$ -ethylchrysin ( <b>54</b> )	1.0 equiv.	91
3	C <sub>4</sub> H <sub>9</sub>	6,8-dibromo- $O^7$ -butylchrysin ( <b>55</b> )	2.0 equiv.	82
4		6-bromo- $O^7$ -butylchrysin ( <b>56</b> )	1.0 equiv.	90
5	C <sub>6</sub> H <sub>13</sub>	6,8-dibromo- $O^7$ -hexylchrysin ( <b>57</b> )	2.0 equiv.	87
6		6-bromo- $O^7$ -hexylchrysin ( <b>58</b> )	1.0 equiv.	89
7	C <sub>8</sub> H <sub>17</sub>	6,8-dibromo- $O^7$ -octylchrysin ( <b>59</b> )	2.0 equiv.	90
8		6-bromo- $O^7$ -octylchrysin ( <b>60</b> )	1.0 equiv.	89
9	C <sub>12</sub> H <sub>25</sub>	6,8-dibromo- $O^7$ -dodecylchrysin ( <b>61</b> )	2.0 equiv.	88
10		6-bromo- $O^7$ -dodecylchrysin ( <b>62</b> )	1.0 equiv.	90

Similarly in the case of bromination of chrysin (**34**) to obtain **19**, the series of dibromo  $O^7$ -ether chrysin were confirmed by the missing of signals of two protons at positions 6 and 8 of phenyl ring A around  $\delta_H$  6.3 and 6.8 ppm, comparing to its precursors (Figures A30, A33, A36, *etc.*). On the other hand, the regioselectivity on position 6 was recognized by the missing of the proton signal at position 6, along with the correlation of proton at position 8 with carbon at position 9 on the 2D NMR spectra of monobromo derivatives **56** and **60** (Figures 3.14-3.15).

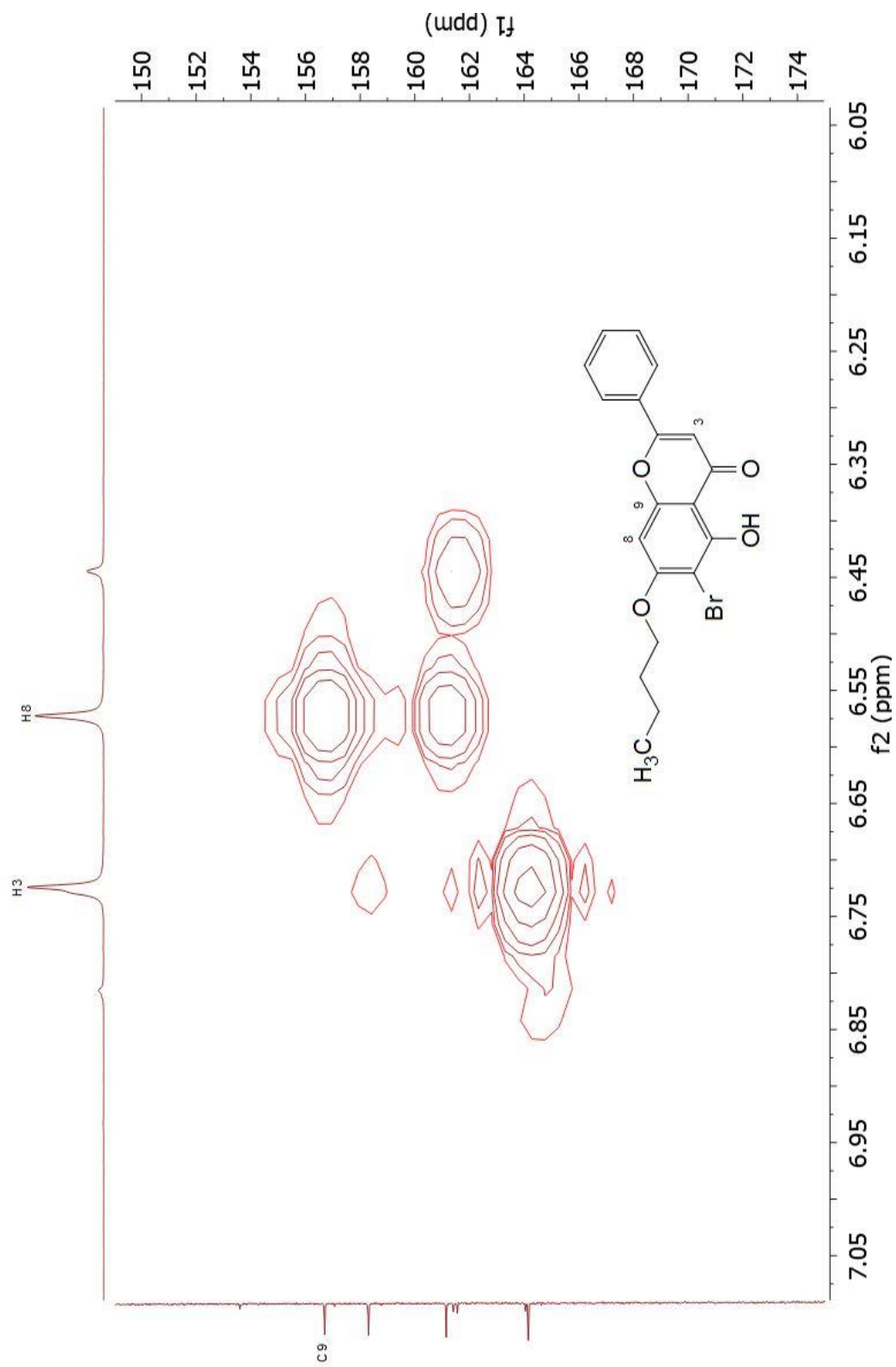


**Figure 3.14** Correlation of proton 8 with carbon 9 on HMBC of **56** (Expansion)

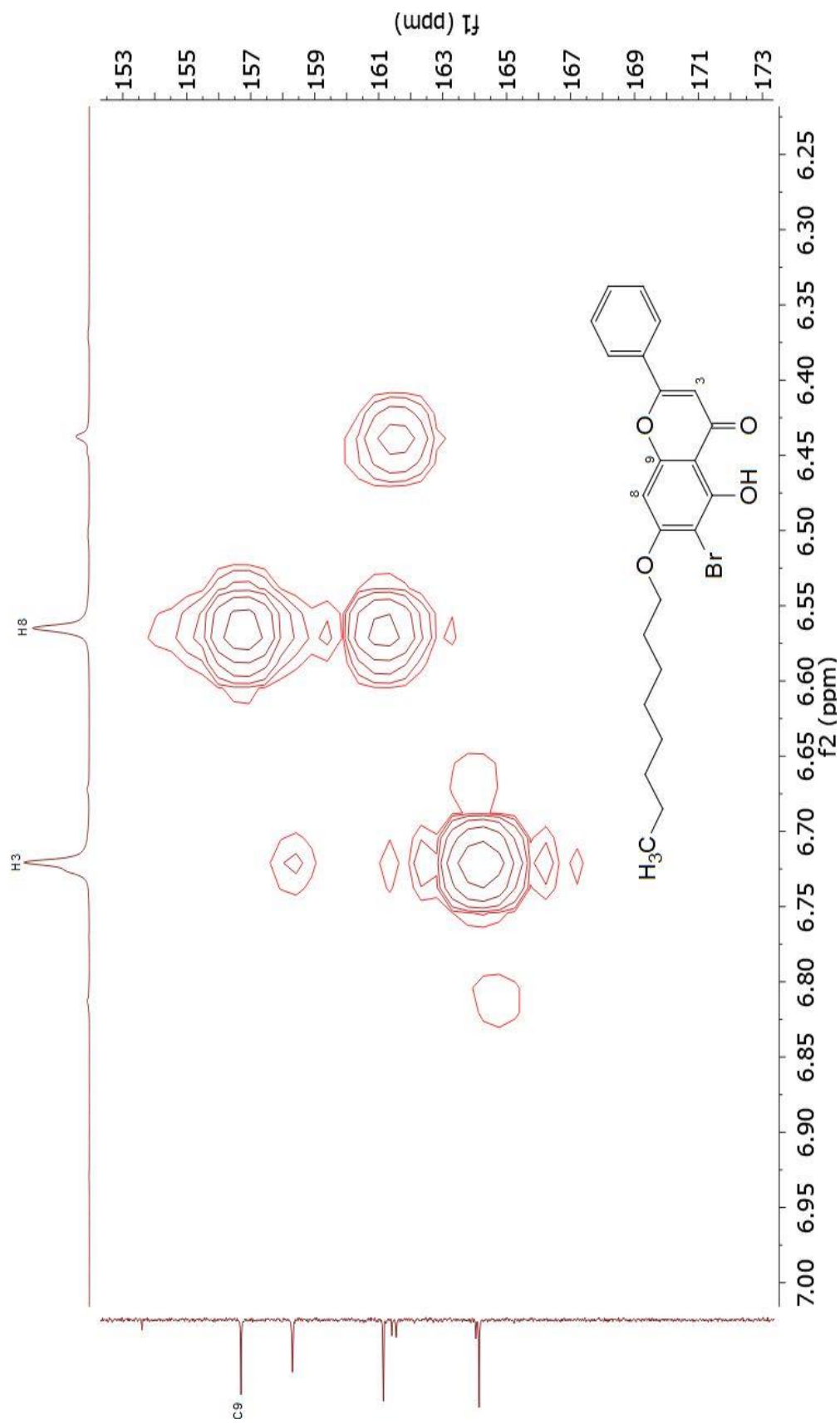


**Figure 3.15** Correlation of proton 8 with carbon 9 on HMBC of **60** (Expansion).

In accordance with previous study,[33] the brominated  $O^7$ -ether chrysin was achieved in excellent yields (>82%). Moreover, the adjustment in ratio of NBS from 1.0 to 2.0 equiv. resulted in the excellent yield of dibromo derivatives indicating the efficiency of this modification. In fact, the bulky side chain at position 7 did not hinder positions 6- and 8- on the phenyl ring A, which implied that the bromination of  $O^7$ -ether flavonoids may not be affected by the steric effect. In addition, the existence of 6-bromo derivatives confirmed the crucial effect of hydroxyl group at 5-position on regioselectivity.[33, 39] Despite of the bulky alkyl side chains on position-7, the supporting of ethereal oxygen of fused heterocycle C and the chelated hydroxyl group activated the reactivity of position 6, as mentioned before.

The brominated ethers have not been synthesized before. The obtained compounds were elucidated by appropriate spectroscopic techniques. The  $^1\text{H}$  NMR assignment and exact mass were displayed in **Table 3.6**.

**Table 3.6** Tentative  $^1\text{H}$  NMR spectral assignment and exact mass of compounds **53-62**.

Cpd	H-3	5-OH	H-6	H-8	H-2', 6'	H-3', 4', 5'	Alkyl chain	Exact mass	
								Calcd.	Found
<b>53</b>	6.83	13.58	-	-	8.02 (dd, $J =$	7.58 (m)	4.24 (q, $J = 7.0$ Hz, 2H), 1.57 (t, $J = 7.0$ Hz,	460.90000	460.90024
	(s)	(s)			8.0, 3.5 Hz)		3H)		
<b>54</b>	6.73	13.46	-	6.56	7.89 (m)	7.41 (m)	4.22 (q, $J = 7.0$ Hz, 2H), 1.55 (t, $J = 7.0$ Hz,	389.98949	389.98970
	(s)	(s)		(s)			3H)		
<b>55</b>	6.82	13.57	-	-	8.01 (m)	7.58 (m)	4.15 (q, $J = 6.5$ Hz, 2H), 1.94 (m, 2H), 1.62	488.93130	488.93206
	(s)	(s)					(m, 2H), 1.03 (t, $J = 6.5$ Hz, 3H)		
<b>56</b>	6.69	13.46	-	6.54	7.88 (m)	7.54 (m)	4.12 (q, $J = 6.4$ Hz, 2H), 1.89 (m, 2H), 1.58		
	(s)	(s)		(s)			(m, 2H), 1.02 (t, $J = 6.4$ Hz, 3H)		
<b>57</b>	6.82	13.57	-	-	8.00 (d, $J =$	7.58 (m)	4.14 (q, $J = 6.6$ Hz, 2H), 1.95 (m, 2H), 1.58	516.96260	516.96247
	(s)	(s)			7.2 Hz)		(s, 6H), 0.93 (t, $J = 6.6$ Hz, 3H)		

**Table 3.6 (Continue)**

Cpd	H-3	5-OH	H-6	H-8	H-2', 6'	H-3', 4', 5'	Alkyl chain	Exact mass	
								Calcd.	Found
58	6.71	-	-	6.55	7.89 (m)	7.54 (m)	4.12 (q, $J = 6.4$ Hz, 2H), 1.91 (m, 2H), 1.53 (m, 2H), 1.38 (m, 4H), 0.93 (t, $J = 6.4$ Hz, 3H)		
	(s)	(s)	(s)						
59	6.82	13.53	-	-	8.00 (m)	7.56 (m)	4.12 (q, $J = 6.6$ Hz, 2H), 1.92 (m, 2H), 1.56 (m, 2H), 1.34 (m, 8H), 0.93 (t, $J = 6.5$ , 3H)		
	(s)	(s)							
60	6.70	-	-	6.55	7.88 (d, $J =$	7.54 (m)	4.11 (q, $J = 6.4$ Hz, 2H), 1.90 (m, 2H), 1.54 (m, 2H), 1.35 (m, 8H), 0.89 (t, $J = 6.4$ , 3H)		
	(s)			(s)	7.4)				
61	6.82	13.58	-	-	8.02 (m)	7.58 (m)	4.14 (q, $J = 6.6$ Hz, 2H), 1.95 (m, 2H), 1.27 (s, 18H), 0.88 (t, $J = 6.5$ Hz, 3H)	601.0564	601.0573
	(s)	(s)							
62	6.73	13.48	-	6.57	7.89 (m)	7.55 (m)	4.13 (q, $J = 6.0$ Hz, 2H), 1.89 (m, 2H), 1.27 (s, 18H), 0.88 (t, $J = 6.0$ Hz, 3H)	501.16405	501.16529
	(s)	(s)		(s)					

### 3.2.3 Anti-dengue activity of brominated $O^7$ -ether chrysin

The percentage of plaque inhibition, percentage of cell viability of brominated  $O^7$ -ether chrysin are shown in **Table 3.7**.

**Table 3.7** % plaque inhibition and % cell viability of brominated  $O^7$ - ether chrysin series.

Entry	Compounds	R	% plaque inhibition (at 10 $\mu$ M)	% cell viability (at 10 $\mu$ M)
1	Chrysin ( <b>34</b> )		86.67 $\pm$ 6.67	79.87 $\pm$ 1.40
2	6,8-dibromochrysin ( <b>19</b> )	H	98.82 $\pm$ 0.42	89.08 $\pm$ 7.62
3	6,8-dibromo- $O^7$ -ethylchrysin ( <b>53</b> )	C <sub>2</sub> H <sub>5</sub>	79.09 $\pm$ 6.86	109.98 $\pm$ 3.86
4	6-bromo- $O^7$ -ethylchrysin ( <b>54</b> )	C <sub>2</sub> H <sub>5</sub>	74.45 $\pm$ 8.18	104.66 $\pm$ 2.49
5	6,8-dibromo- $O^7$ -butylchrysin ( <b>55</b> )	C <sub>4</sub> H <sub>9</sub>	87.27 $\pm$ 6.30	112.27 $\pm$ 3.70
6	6-bromo- $O^7$ -butylchrysin ( <b>56</b> )	C <sub>4</sub> H <sub>9</sub>	In.	In.
7	6,8-dibromo- $O^7$ -hexylchrysin ( <b>57</b> )	C <sub>6</sub> H <sub>13</sub>	90.00 $\pm$ 3.15	98.67 $\pm$ 2.18
8	6-bromo- $O^7$ -hexylchrysin ( <b>58</b> )	C <sub>6</sub> H <sub>13</sub>	In.	In.
9	6,8-dibromo- $O^7$ -octylchrysin ( <b>59</b> )	C <sub>8</sub> H <sub>17</sub>	In.	In.
10	6-bromo- $O^7$ -octylchrysin ( <b>60</b> )	C <sub>8</sub> H <sub>17</sub>	97.11 $\pm$ 0.77	93.83 $\pm$ 1.24
11	6,8-dibromo- $O^7$ -dodecylchrysin ( <b>61</b> )	C <sub>12</sub> H <sub>25</sub>	84.55 $\pm$ 1.57	116.74 $\pm$ 8.86
12	6-bromo- $O^7$ -dodecylchrysin ( <b>62</b> )	C <sub>12</sub> H <sub>25</sub>	In.	In.

In.: Insoluble.

Data represent means  $\pm$  standard error mean (SEM) of three independent experiment.

The results were reported from three independent experiments.



The preliminary screening at 10  $\mu\text{M}$  displayed unpredictable structure-activity relationship of the brominated ether chrysin. Results showed that increasing the length of alkyl chain did not increase the percent viral inhibition as previously hypothesized by docking.[46] To be specific, 6,8-dibromochrysin (**19**) (98.82% of inhibition) was the most efficient dengue inhibitor among dibromo compounds. Among the dibromo ether chrysin, there was an ambiguous trend when increasing the number of carbon in the alkyl chains. From ethyl to hexyl, the percentage of plaque inhibition went up gradually from 79.09% of **53** to 90.00% of **57**. However, since the missing value of **60** made the trend was interrupted, the optimized number of carbons of side chain stimulating the activity could not be given out clearly. The difference of percentage inhibition between **57** and **61** was not remarkable, 90.00% of **57** versus 84.55% of **61**, but the decreasing showed that the longer side chain, the worse activity is. Literature review also showed the suitable side chain to obtain the best activity was normally hexyl.[28, 44, 45] On the other hand, the inhibition pattern was inconclusive in monobromo compounds. Although most of the dibromo derivatives were able to be dissolved in DMSO or DMSO with 1% acetone – solvents used for the bioactive test – more than half of monobromo ether chrysin were insoluble. The monobromo long alkyl side chains were hardly tested therefore results could not be obtained obviously. However, 6-bromo-*O*<sup>7</sup>-octylchrysin (**60**) possessed 97.11% of inhibition could be considered as the best monobromo ether derivative. Moreover, in comparison with other derivatives, **60** was the most active compound in the series, with negligible

distinction in percentage plaque inhibition with **19**, 97.11% and 98.82% respectively. It was speculated that the monobromo series benefited from increasing alkyl chain more than the dibromo series. The bulky nature of dibromo series did not allow addition of another bulky group adjacent to them; whereas the monobromo still allow a room for the bulky hydrocarbon and still fit all additional structures into the binding pocket. However, it was obvious that the side chain  $C_2H_5$  contributed to the lowest inhibition efficiency in both mono and dibromo compounds suggesting steric hindrance (or incompetency) towards the binding pocket.

Cell viability assay was used to confirm that all soluble compounds were relatively non-cytotoxic at the tested concentration (10  $\mu$ M). Despite of the moderate inhibition at examined concentration comparing to **19**, all the synthesized compounds were less toxic with cells than chrysin (**34**) and 6,8-dibromochrysin (**19**). Noticeably, there was a consistence between the inhibitory activity and the toxicity of the series: the more active compound, the more toxic to the cells it is. **60** was observed as the best inhibitor with 97.11% inhibition, but it also had the lowest percentage cell viability among derivatives with 93.83%. To combine the inhibitory efficiency and the toxicity for evaluation, the best candidates for further study were 6,8-dibromo- $O^7$ -butylchrysin (**55**) and 6,8-dibromo- $O^7$ -hexylchrysin (**57**).

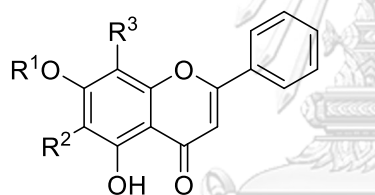
On the other hand, the results also implied the drawback of this modification, as the solubility of the derivatives were significantly decreased. The etherification could not enhance the antiviral activity as assumption.



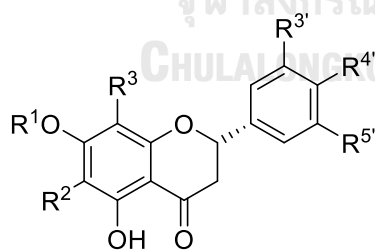
## Chapter 4

### Conclusions

Derived from corresponding flavonoids, twenty-two halogenated derivatives were synthesized and elucidated their structures by appropriate spectroscopic techniques. Among them, eighteen compounds were obtained for the first time. These substrates were characterized by using  $^1\text{H}$ ,  $^{13}\text{C}$  and HR-ESI-MS, and the summary of their structures is displayed below.



- (53)  $\text{R}^1 = \text{C}_2\text{H}_5$ ,  $\text{R}^2 = \text{R}^3 = \text{Br}$
- (54)  $\text{R}^1 = \text{C}_2\text{H}_5$ ,  $\text{R}^2 = \text{Br}$ ,  $\text{R}^3 = \text{H}$
- (55)  $\text{R}^1 = \text{C}_4\text{H}_9$ ,  $\text{R}^2 = \text{R}^3 = \text{Br}$
- (56)  $\text{R}^1 = \text{C}_4\text{H}_9$ ,  $\text{R}^2 = \text{Br}$ ,  $\text{R}^3 = \text{H}$
- (57)  $\text{R}^1 = \text{C}_6\text{H}_{13}$ ,  $\text{R}^2 = \text{R}^3 = \text{Br}$
- (58)  $\text{R}^1 = \text{C}_6\text{H}_{13}$ ,  $\text{R}^2 = \text{Br}$ ,  $\text{R}^3 = \text{H}$
- (59)  $\text{R}^1 = \text{C}_8\text{H}_{17}$ ,  $\text{R}^2 = \text{R}^3 = \text{Br}$
- (60)  $\text{R}^1 = \text{C}_8\text{H}_{17}$ ,  $\text{R}^2 = \text{Br}$ ,  $\text{R}^3 = \text{H}$
- (61)  $\text{R}^1 = \text{C}_{12}\text{H}_{25}$ ,  $\text{R}^2 = \text{R}^3 = \text{Br}$
- (62)  $\text{R}^1 = \text{C}_{12}\text{H}_{25}$ ,  $\text{R}^2 = \text{Br}$ ,  $\text{R}^3 = \text{H}$



- (44)  $\text{R}^1 = \text{R}^3 = \text{R}^4 = \text{R}^5 = \text{H}$ ,  $\text{R}^2 = \text{R}^3 = \text{Br}$
- (45)  $\text{R}^1 = \text{R}^3 = \text{R}^4 = \text{R}^5 = \text{H}$ ,  $\text{R}^2 = \text{I}$
- (46)  $\text{R}^1 = \text{CH}_3$ ,  $\text{R}^3 = \text{R}^4 = \text{R}^5 = \text{H}$ ,  $\text{R}^2 = \text{R}^3 = \text{Br}$
- (47)  $\text{R}^1 = \text{CH}_3$ ,  $\text{R}^3 = \text{R}^4 = \text{R}^5 = \text{H}$ ,  $\text{R}^2 = \text{R}^3 = \text{I}$
- (48)  $\text{R}^1 = \text{CH}_3$ ,  $\text{R}^3 = \text{R}^4 = \text{R}^5 = \text{H}$ ,  $\text{R}^2 = \text{I}$
- (49)  $\text{R}^1 = \text{H}$ ,  $\text{R}^4 = \text{OH}$ ,  $\text{R}^2 = \text{R}^3 = \text{R}^3' = \text{R}^5 = \text{Br}$
- (50)  $\text{R}^1 = \text{H}$ ,  $\text{R}^4 = \text{OH}$ ,  $\text{R}^2 = \text{R}^3 = \text{R}^3' = \text{R}^5 = \text{I}$

To evaluate the potential of halogenated flavonoids as new anti-dengue agents, selected derivatives were examined the inhibitory activity against dengue virus serotype 2 DENV-2 infection. The preliminary screening at 10  $\mu\text{M}$  demonstrated the

efficiency of halogen atom contributing to the bioactivity. New compounds **44**, **46**, **47** displayed competitive % inhibition plaque comparing with the precursors. All the tested compounds also relatively low toxic with cells at 10  $\mu\text{M}$ . When inspecting the  $\text{EC}_{50}$  and  $\text{CC}_{50}$ , 8-bromobaicalein (**42**) was the most active compounds in the series, along with brominated and iodinated pinostrobin and pinocembrin (**44**), (**46**), (**47**) as the promising anti-dengue agents. These halogenated derivatives can be further studied for the interaction mechanism with virus in the future.

#### **Suggestion for future work**

The possible development relating to this study is the conjugation of potent compounds with soluble components such as esters or amines in order to enhance the bioavailability as well as bioactivity of these derivatives. Further study about the mechanism of interaction between the substrates and virus should be considered. On the other hand, the new brominated and iodinated flavonoids in this research are possibly investigated other biological activities such as anticancer or anti-inflammatory.

## REFERENCES

- [1] Henschel, E.A. and Putnak, J.R. The dengue viruses. Clinical Microbiology Reviews 3(4) (1990): 376-396.
- [2] Bhamarapravati, N. Hemostatic defects in dengue hemorrhagic fever. Reviews of Infectious Diseases 11(Supplement\_4) (1989): S826-S829.
- [3] Chawla, P., Yadav, A., and Chawla, V. Clinical implications and treatment of dengue. Asian Pacific Journal of Tropical Medicine 7(3) (2014): 169-178.
- [4] MAMMON, W. Dengue hemorrhagic fever-do we know its cause? American Journal of Tropical Medicine and Hygiene 22(1) (1973): 82-91.
- [5] Halstead, S.B. Dengue haemorrhagic fever—a public health problem and a field for research. Bulletin of the World Health Organization 58(1) (1980): 1-21.
- [6] Ooi, E.-E. and Gubler, D.J. Dengue in Southeast Asia: epidemiological characteristics and strategic challenges in disease prevention. Cadernos de saude Publica 25 (2009): S115-S124.
- [7] Gubler, D.J. Dengue and dengue hemorrhagic fever: its history and resurgence as a global public health problem. Dengue and Dengue Hemorrhagic Fever (1997).
- [8] Limkittikul, K., Brett, J., and L'Azou, M. Epidemiological trends of dengue disease in Thailand (2000–2011): a systematic literature review. PLoS Neglected Tropical Diseases 8(11) (2014): e3241.
- [9] Guzmán, M.G. and Kouri, G. Advances in dengue diagnosis. Clinical and Diagnostic Laboratory Immunology 3(6) (1996): 621-627.
- [10] Panche, A., Diwan, A., and Chandra, S. Flavonoids: an overview. Journal of Nutritional Science 5 (2016): e47.
- [11] Sun, M.-Y., Ye, Y., Xiao, L., Rahman, K., Xia, W., and Zhang, H. Daidzein: A review of pharmacological effects. African Journal of Traditional, Complementary and Alternative Medicines 13(3) (2016): 117-132.
- [12] Mani, R. and Natesan, V. Chrysin: Sources, beneficial pharmacological activities, and molecular mechanism of action. Phytochemistry 145 (2018): 187-196.

- [13] Sanchez, I., Gómez-Garibay, F., Taboada, J., and Ruiz, B. Antiviral effect of flavonoids on the dengue virus. Phytotherapy Research 14(2) (2000): 89-92.
- [14] Kiat, T.S., Phippen, R., Yusof, R., Ibrahim, H., Khalid, N., and Rahman, N.A. Inhibitory activity of cyclohexenyl chalcone derivatives and flavonoids of fingerroot, *Boesenbergia rotunda* (L.), towards dengue-2 virus NS3 protease. Bioorganic & Medicinal Chemistry Letters 16(12) (2006): 3337-3340.
- [15] Zandi, K., Teoh, B.-T., Sam, S.-S., Wong, P.-F., Mustafa, M.R., and AbuBakar, S. Antiviral activity of four types of bioflavonoid against dengue virus type-2. Virology Journal 8(1) (2011): 560-570.
- [16] Keivan, Z., Boon-Teong, T., Sing-Sin, S., Pooi-Fong, W., Mustafa, M.R., and Sazaly, A. In vitro antiviral activity of fisetin, rutin and naringenin against dengue virus type-2. Journal of Medicinal Plants Research 5(23) (2011): 5534-5539.
- [17] Zandi, K., Teoh, B.-T., Sam, S.-S., Wong, P.-F., Mustafa, M.R., and AbuBakar, S. Novel antiviral activity of baicalein against dengue virus. BMC Complementary and Alternative Medicine 12(1) (2012): 214-222.
- [18] Frabasile, S., Koishi, A.-C., Kuczera, D., Silveira, G.-F., Verri-Jr., W.-A., Dos Santos, C.-N.-D., and Bordignon, J. The citrus flavanone naringenin impairs dengue virus replication in human cells. Scientific Reports 7 (2017): 41864.
- [19] Goldberg, Y. and Alper, H. Electrophilic halogenation of aromatics and heteroaromatics with N-halosuccinimides in a solid/liquid system using an H<sup>+</sup> ion exchanger or ultrasonic irradiation. Journal of Molecular Catalysis 88(3) (1994): 377-383.
- [20] Clague, M.J. and Butler, A. On the mechanism of cis-dioxovanadium (V)-catalyzed oxidation of bromide by hydrogen peroxide: evidence for a reactive, binuclear vanadium (V) peroxo complex. Journal of the American Chemical Society 117(12) (1995): 3475-3484.
- [21] Roche, D., Prasad, K., Repic, O., and Blacklock, T.J. Mild and regioselective oxidative bromination of anilines using potassium bromide and sodium perborate. Tetrahedron Letters 41(13) (2000): 2083-2086.

- [22] Bovicelli, P., Bernini, R., Antonioletti, R., and Mincione, E. Selective halogenation of flavanones. Tetrahedron Letters 43(32) (2002): 5563-5567.
- [23] Bernini, R., Pasqualetti, M., Provenzano, G., and Tempesta, S. Ecofriendly synthesis of halogenated flavonoids and evaluation of their antifungal activity. New Journal of Chemistry 39(4) (2015): 2980-2987.
- [24] Suroengrit, A., Yuttithamnon, W., Srivarangkul, P., Pankaew, S., Kingkew, K., Chavasiri, W., and Boonyasuppayakorn, S. Halogenated Chrysin inhibit Dengue and Zika virus infectivity. Scientific Reports 7(1) (2017): 13696.
- [25] Lu, Y.-F., Santostefano, M., Cunningham, B.D., Threadgill, M.D., and Safe, S. Substituted flavones as aryl hydrocarbon (Ah) receptor agonists and antagonists. Biochemical Pharmacology 51(8) (1996): 1077-1087.
- [26] Park, H., Dao, T.T., and Kim, H.P. Synthesis and inhibition of PGE2 production of 6, 8-disubstituted chrysin derivatives. European Journal of Medicinal Chemistry 40(9) (2005): 943-948.
- [27] Tran, T.-D., Vo, P.-N., and Do, T.-H. Synthesis and comparison of anti-inflammatory activity of chrysin derivatives. in Proceedings of The 13th International Electronic Conference on Synthetic Organic Chemistry, p. 1: Molecular Diversity Preservation International, 2009.
- [28] Kingkaew, K., Ruga, R., and Chavasiri, W. 6, 8-Dibromo- and 6, 8-Diiodo-5, 7-dihydroxyflavones as New Potent Antibacterial Agents. Chemistry Letters 47(3) (2018): 358-361.
- [29] Zhang, X., Khalidi, O., Kim, S.-Y., Wang, R., Schultz, V., Cress, B.-F., Gross, R.-A., Koffas, M.-AG., and Linhardt, R.-J. Synthesis and biological evaluation of 5, 7-dihydroxyflavanone derivatives as antimicrobial agents. Bioorganic & Medicinal Chemistry Letters 26(13) (2016): 3089-3092.
- [30] Evseeva, O., Andreeva, O., and Oganessian, É. Studies of the hydrolysis of hesperidin. Pharmaceutical Chemistry Journal 47(11) (2014): 606-609.
- [31] Zhang, W., Yi, D., Gao, K., Liu, M., Yang, J., Liao, X., and Yang, B. Hydrolysis of scutellarin and related glycosides to scutellarein and the corresponding aglycones. Journal of Chemical Research 38(7) (2014): 396-398.



- [32] Lee, Y., Yeo, H., Liu, S.-H., Jiang, Z., Savizky, R.-M., Austin, D.-J., and Cheng, Y.-C. Increased anti-P-glycoprotein activity of baicalein by alkylation on the A ring. Journal of Medicinal Chemistry 47(22) (2004): 5555-5566.
- [33] Pan, G., Yang, K., Ma, Y., Zhao, X., Lu, K., and Yu, P. Synthesis of 6-or 8-Bromo Flavonoids by Regioselective Mono-Bromination and Deprotection Protocol from Flavonoid Alkyl Ethers. Bulletin of the Korean Chemical Society 36(5) (2015): 1460-1466.
- [34] Foti, M.C. and Rocco, C. Unveiling the chemistry behind bromination of quercetin: the 'violet chromogen'. Tetrahedron Letters 55(9) (2014): 1602-1607.
- [35] Yaipakdee, P. and Robertson, L.W. Enzymatic halogenation of flavanones and flavones. Phytochemistry 57(3) (2001): 341-347.
- [36] Zhu, Z.-Y., Wang, W.-X., Wang, Z.-Q., Chen, L.-J., Zhang, J.-Y., Liu, X.-C., Wu, S.-P., and Zhang, Y.-M. Synthesis and antitumor activity evaluation of chrysin derivatives. European Journal of Medicinal Chemistry 75 (2014): 297-300.
- [37] During, A. and Larondelle, Y. The O-methylation of chrysin markedly improves its intestinal anti-inflammatory properties: structure-activity relationships of flavones. Biochemical Pharmacology 86(12) (2013): 1739-1746.
- [38] Dong, X., Liu, T., Yan, J., Wu, P., Chen, J., and Hu, Y. Synthesis, biological evaluation and quantitative structure-activities relationship of flavonoids as vasorelaxant agents. Bioorganic & Medicinal Chemistry 17(2) (2009): 716-726.
- [39] Lu, K., Chu, J., Wang, H., Fu, X., Quan, D., Ding, H., Yao, Q., and Yu, P. Regioselective iodination of flavonoids by N-iodosuccinimide under neutral conditions. Tetrahedron Letters 54(47) (2013): 6345-6348.
- [40] Neubig, R.R., Spedding, M., Kenakin, T., and Christopoulos, A. International Union of Pharmacology Committee on Receptor Nomenclature and Drug Classification. XXXVIII. Update on terms and symbols in quantitative pharmacology. Pharmacological Reviews 55(4) (2003): 597-606.
- [41] Abid, N.B.S., Rouis, Z., Lassoued, M.A., Sfar, S., and Aouni, M. Assessment of the cytotoxic effect and in vitro evaluation of the anti-enteroviral activities of plants rich in flavonoids. Journal of Applied Pharmaceutical Science 2(5) (2012): 74.

- [42] Lv, P.-C., Wang, K.-R., Li, Q.-S., Chen, J., Sun, J., and Zhu, H.-L. Design, synthesis and biological evaluation of chrysin long-chain derivatives as potential anticancer agents. Bioorganic & Medicinal Chemistry 18(3) (2010): 1117-1123.
- [43] Shin, J.-S., Kim, K.-S., Kim, M.-B., Jeong, J.-H., and Kim, B.-K. Synthesis and hypoglycemic effect of chrysin derivatives. Bioorganic & Medicinal Chemistry Letters 9(6) (1999): 869-874.
- [44] Cheng, N., Yi, W.-B., Wang, Q.-Q., Peng, S.-M., and Zou, X.-Q. Synthesis and  $\alpha$ -glucosidase inhibitory activity of chrysin, diosmetin, apigenin, and luteolin derivatives. Chinese Chemical Letters 25(7) (2014): 1094-1098.
- [45] Nile, S.H., Keum, Y.S., Nile, A.S., Jalde, S.S., and Patel, R.V. Antioxidant, anti-inflammatory, and enzyme inhibitory activity of natural plant flavonoids and their synthesized derivatives. Journal of Biochemical and Molecular Toxicology 32(1) (2018): e22002.
- [46] Unpublished paper.



APPENDIX

จุฬาลงกรณ์มหาวิทยาลัย  
**CHULALONGKORN UNIVERSITY**

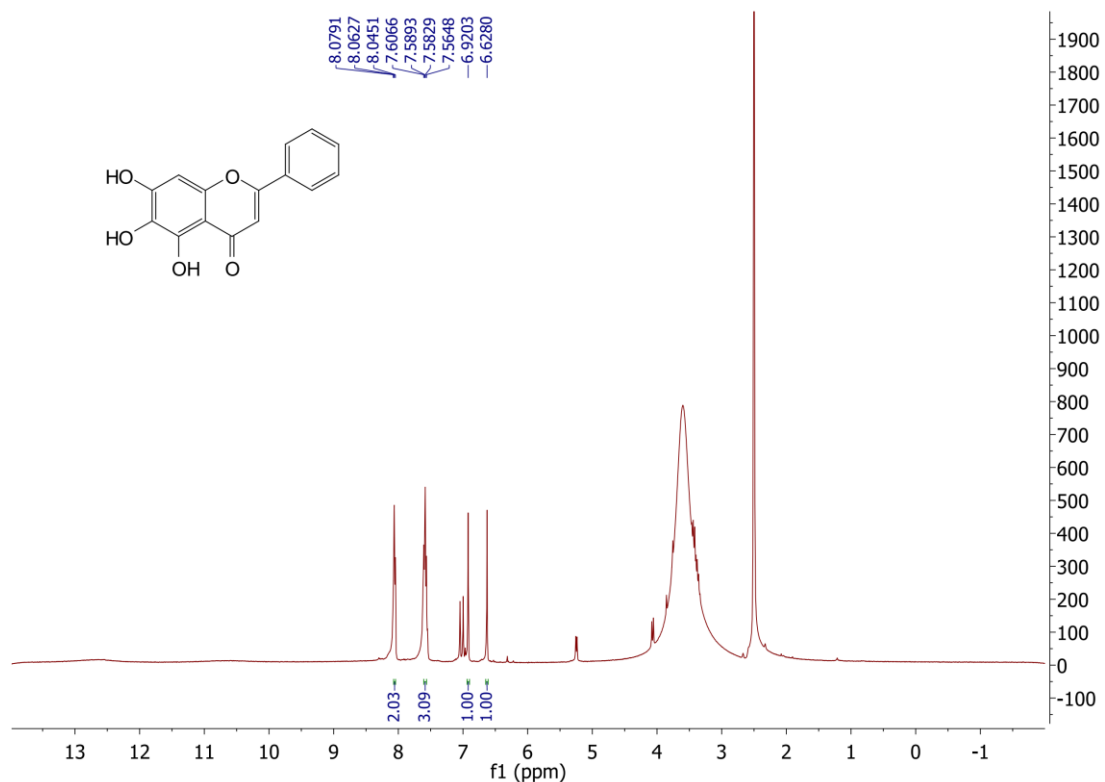


Figure A1 The <sup>1</sup>H NMR spectrum (DMSO-d<sub>6</sub>, 400 MHz) of 18.

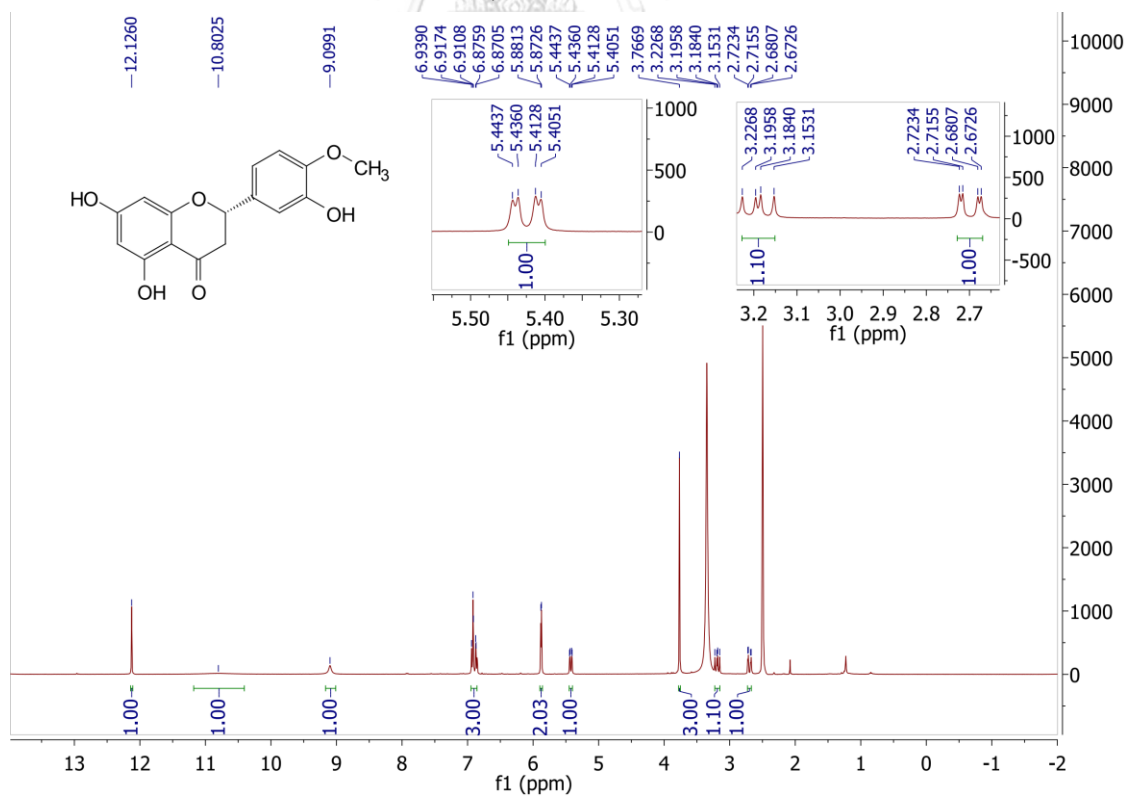


Figure A2 The <sup>1</sup>H NMR spectrum (DMSO-d<sub>6</sub>, 400 MHz) of 15.

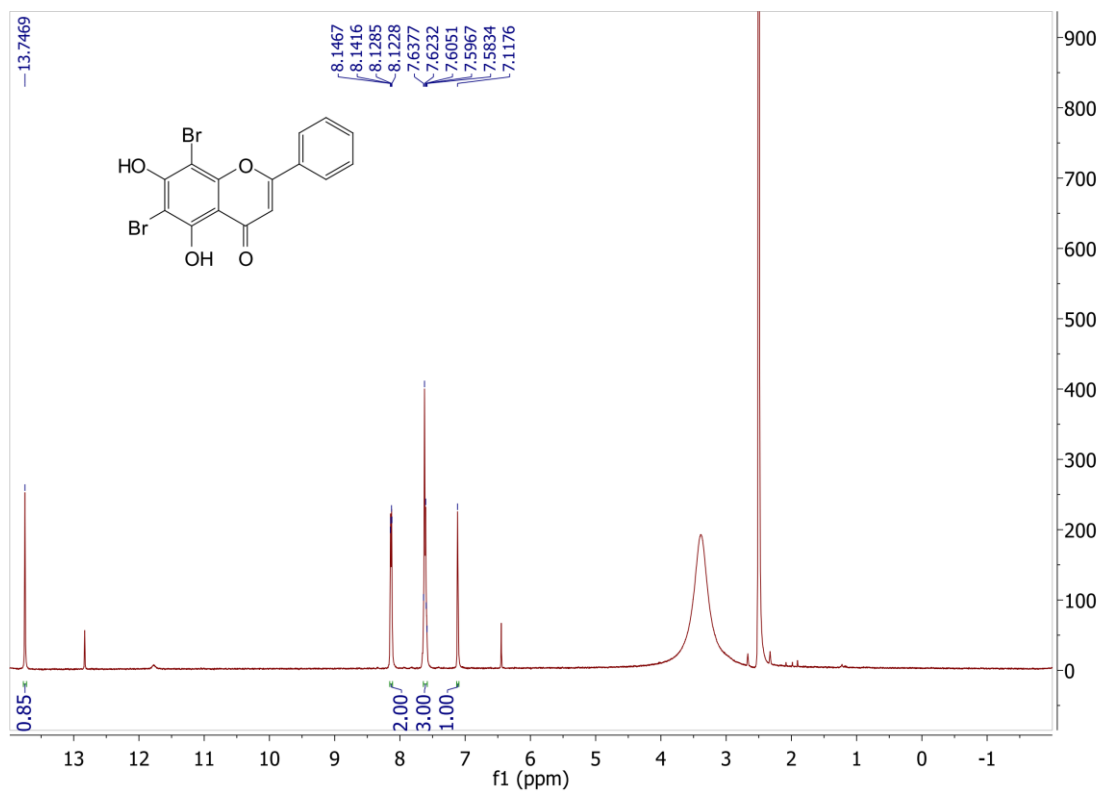


Figure A3 The  $^1\text{H}$  NMR spectrum (DMSO- $d_6$ , 400 MHz) of 19.

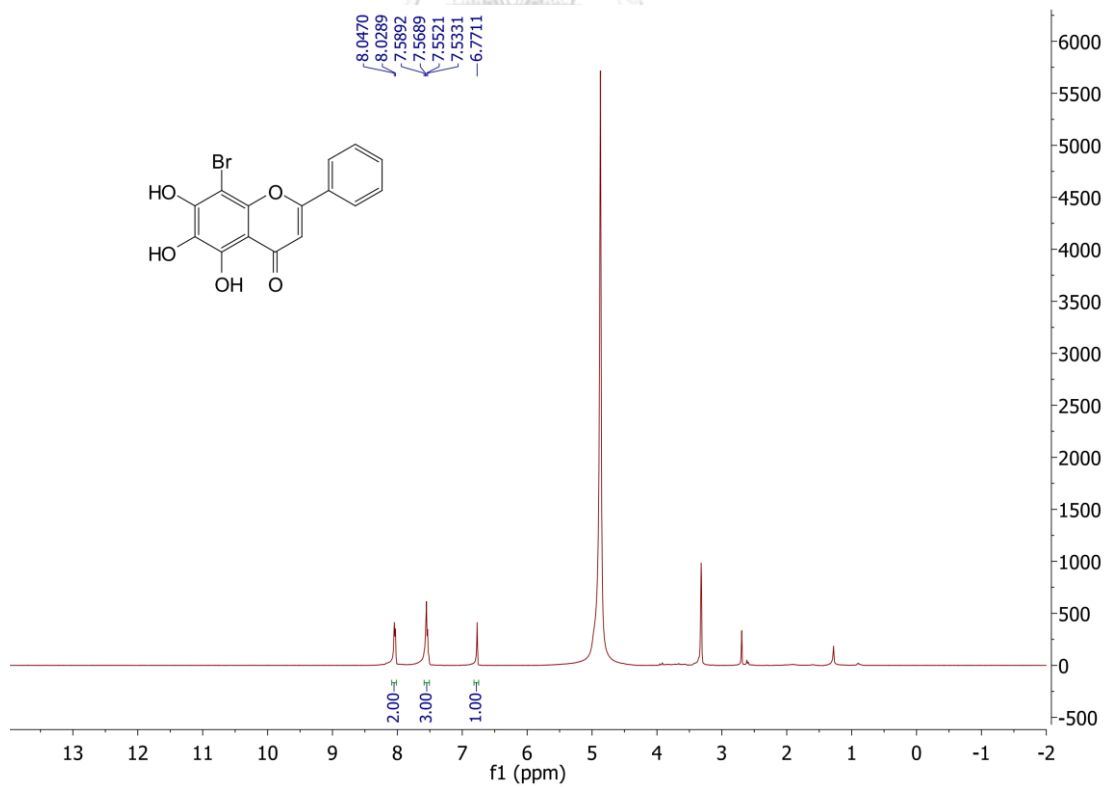


Figure A4 The  $^1\text{H}$  NMR spectrum (MeOD, 400 MHz) of 42.

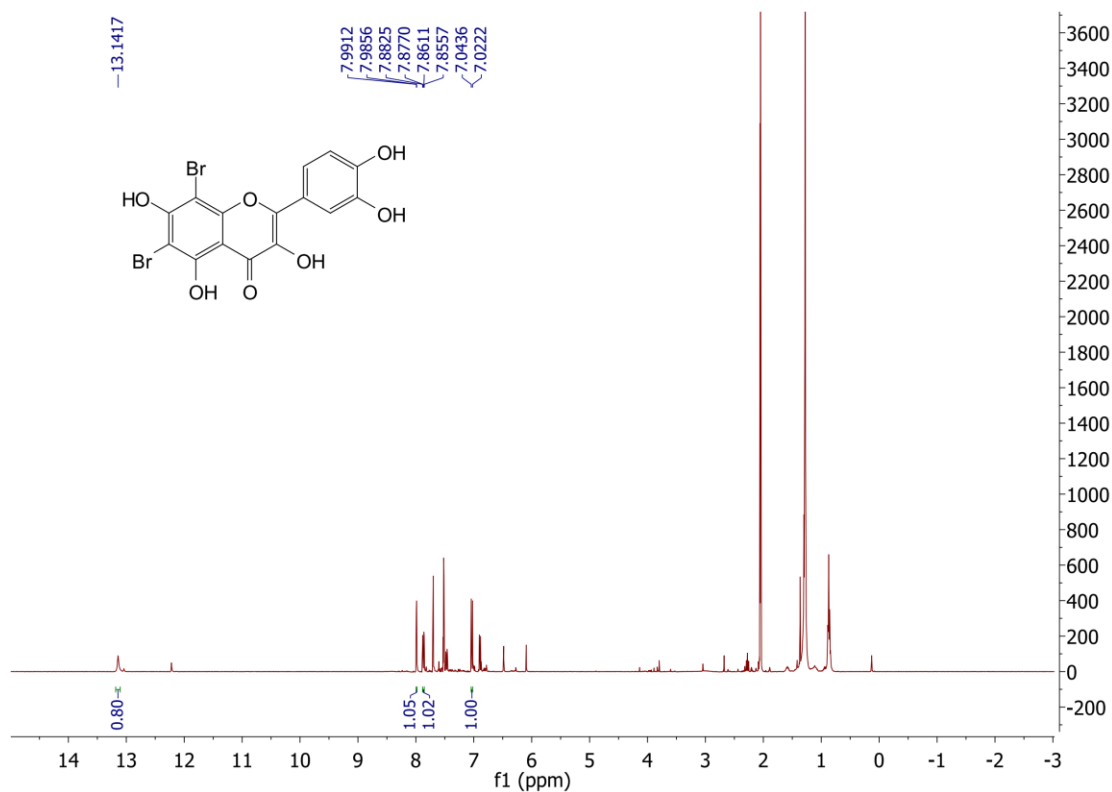


Figure A5 The  $^1\text{H}$  NMR spectrum(Acetone- $d_6$ ) of 43.

### Mass Spectrum List Report

#### Analysis Info

Analysis Name D:\Data\Data Service\190401\T70\_RC4\_01\_2444.d  
 Method nv\_pos\_5min\_profile\_190214.m  
 Sample Name T70  
 Comment

Acquisition Date 4/1/2019 7:49:59 PM

Operator CU.  
 Instrument / Ser# micrOTOF-Q II 10335

#### Acquisition Parameter

Source Type	ESI	Ion Polarity	Positive	Set Nebulizer	3.0 Bar
Focus	Not active	Set Capillary	4000 V	Set Dry Heater	200 °C
Scan Begin	100 m/z	Set End Plate Offset	-500 V	Set Dry Gas	8.0 l/min
Scan End	1500 m/z	Set Collision Cell RF	250.0 Vpp	Set Divert Valve	Waste

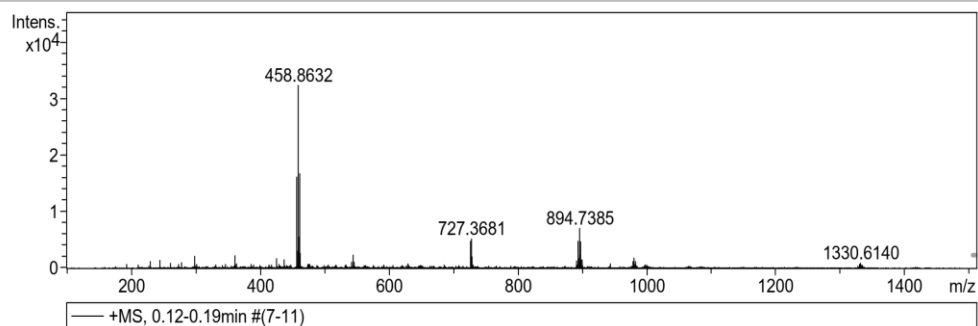
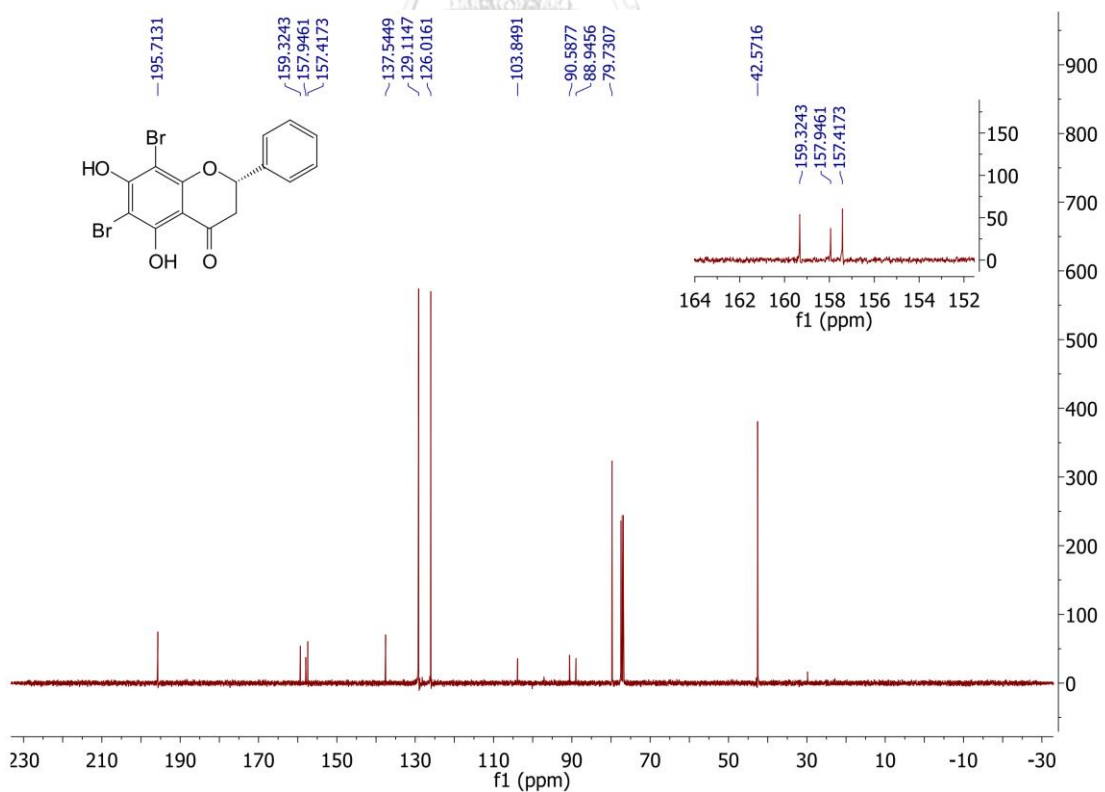
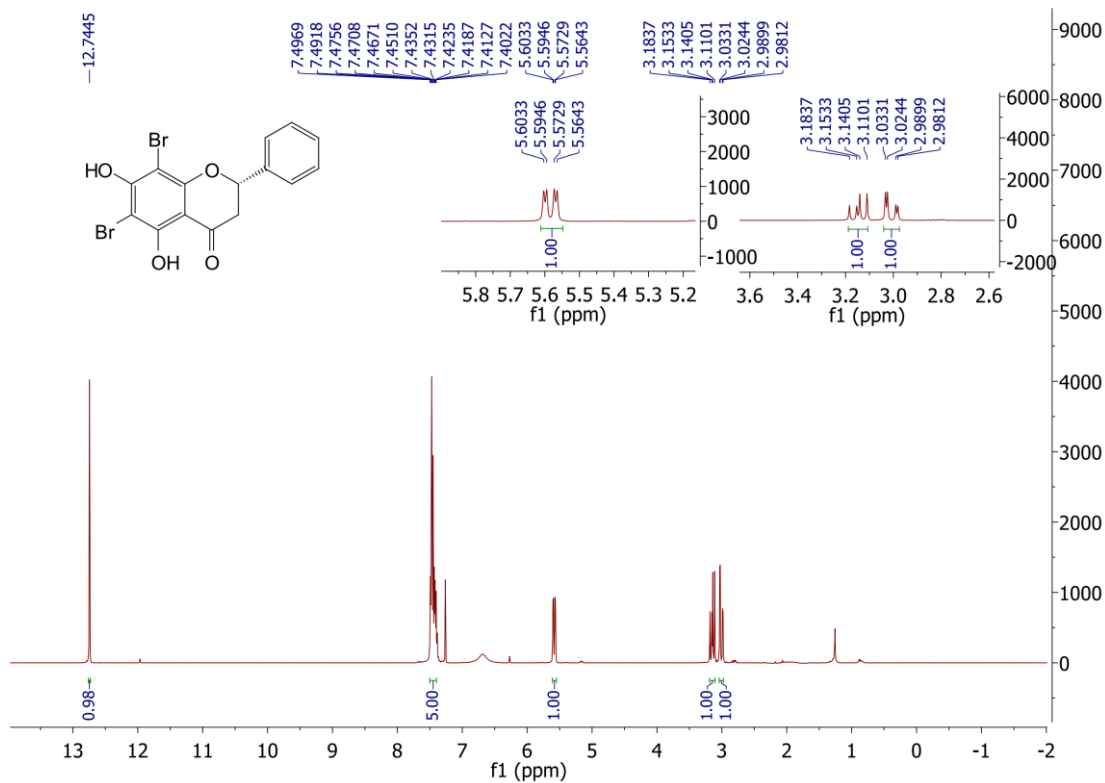


Figure A6 The HR-ESI-MS of 44.



**Figure A8** The  $^{13}\text{C}$  NMR spectrum (Acetone- $\text{d}_6$ , 100 MHz) of **44**.

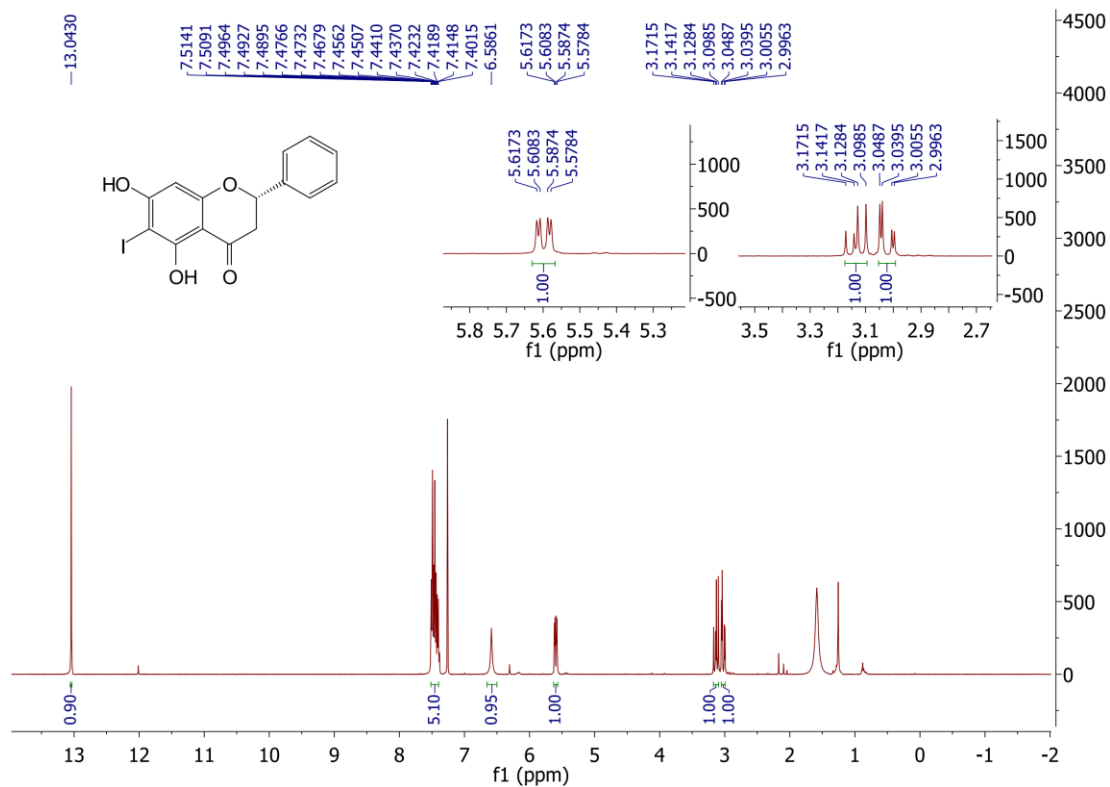


Figure A9 The  $^1\text{H}$  NMR spectrum (CDCl<sub>3</sub>, 400 MHz) of 45.

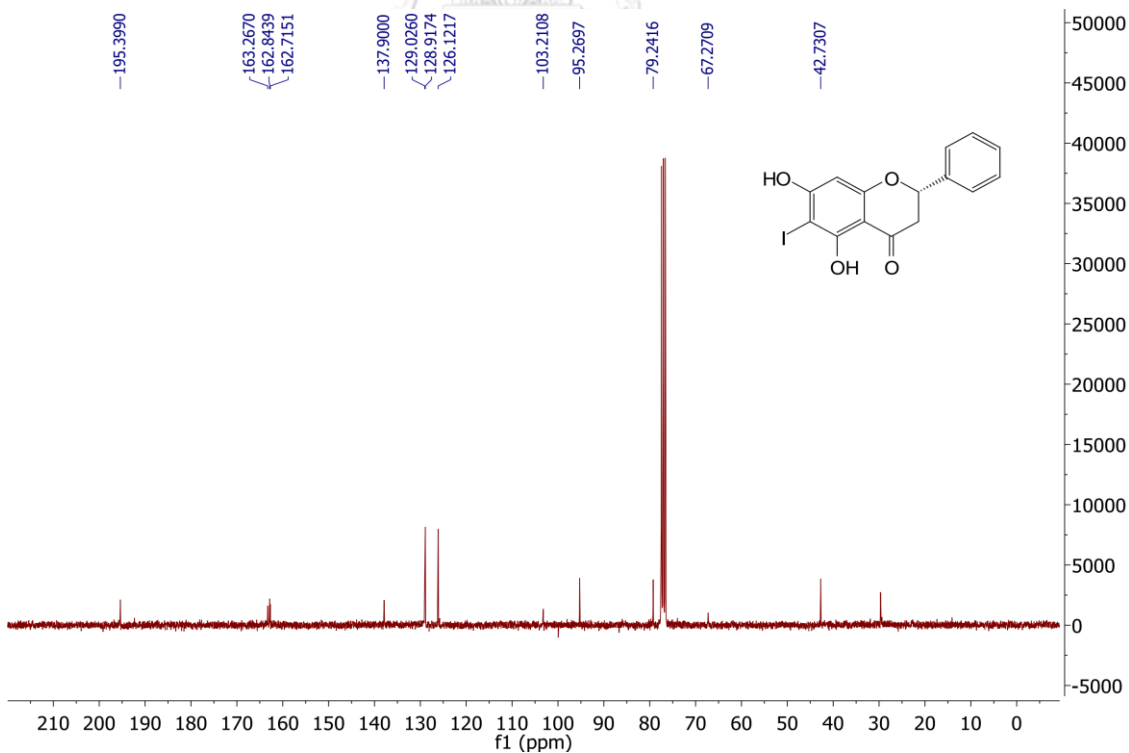


Figure A10 The  $^{13}\text{C}$  NMR spectrum (CDCl<sub>3</sub>, 100 MHz) of 45.



## Mass Spectrum List Report

### Analysis Info

Analysis Name	D:\Data\Data Service\180924_pos_T9.d	Acquisition Date	9/24/2018 1:20:00 PM
Method	NV_pos_0.3min_profile_1segment_lowNubulizerDrygas.m	Operator	CU.
Sample Name	180924_pos_T9	Instrument / Ser#	micrOTOF-Q II 10335
Comment			

### Acquisition Parameter

Source Type	ESI	Ion Polarity	Positive	Set Nebulizer	0.4 Bar
Focus	Not active	Set Capillary	4000 V	Set Dry Heater	200 °C
Scan Begin	50 m/z	Set End Plate Offset	-500 V	Set Dry Gas	4.0 l/min
Scan End	1500 m/z	Set Collision Cell RF	150.0 Vpp	Set Divert Valve	Waste

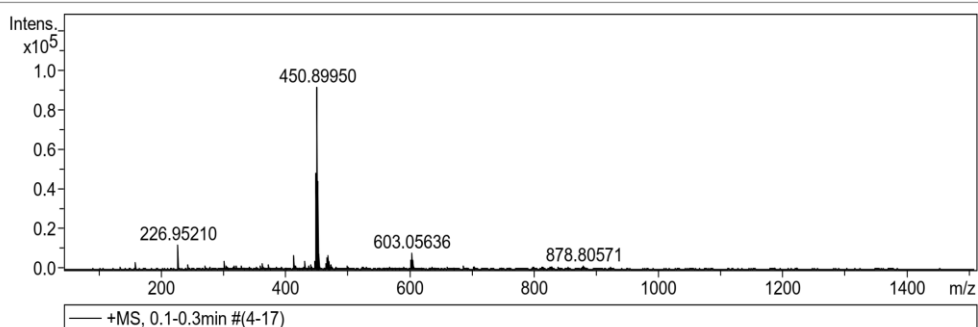


Figure A11 The HR-ESI-MS of 46.

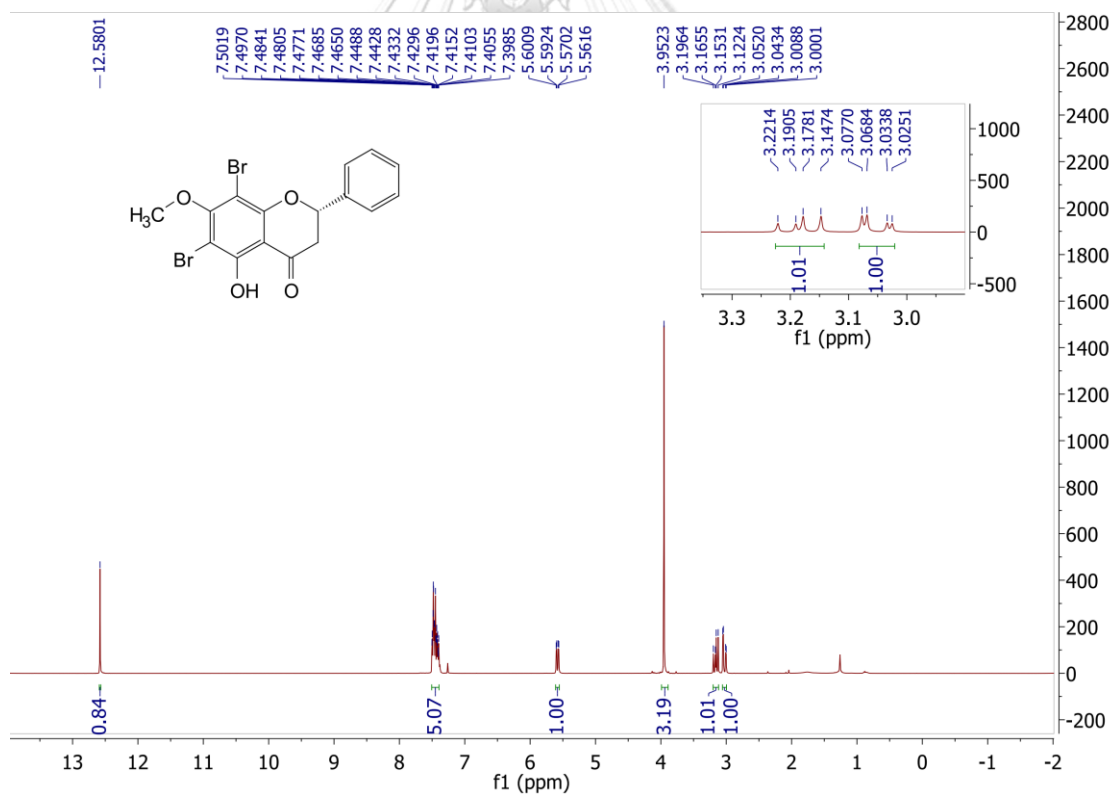


Figure A12 The  $^1\text{H}$  NMR spectrum ( $\text{CDCl}_3$ , 400 MHz) of 46.

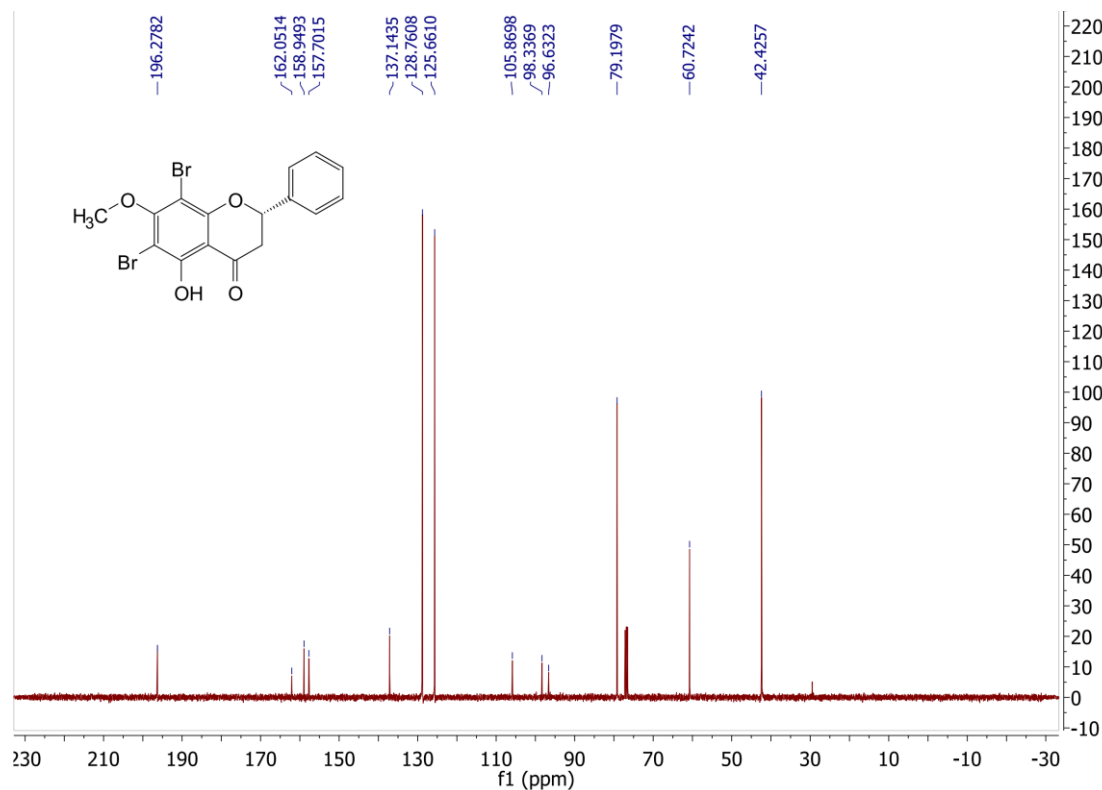


Figure A13 The  $^{13}\text{C}$  NMR spectrum ( $\text{CDCl}_3$ , 100 MHz) of 46.

## Mass Spectrum List Report

Analysis Info		Acquisition Date	
Analysis Name	D:\Data\Data Service\190401\T61_RC3_01_2443.d	4/1/2019 7:43:32 PM	
Method	nv_pos_5min_profile_190214.m	Operator	CU.
Sample Name	T61	Instrument / Ser#	micrOTOF-Q II 10335
Comment			

Acquisition Parameter					
Source Type	ESI	Ion Polarity	Positive	Set Nebulizer	3.0 Bar
Focus	Not active	Set Capillary	4000 V	Set Dry Heater	200 °C
Scan Begin	100 m/z	Set End Plate Offset	-500 V	Set Dry Gas	8.0 l/min
Scan End	1500 m/z	Set Collision Cell RF	250.0 Vpp	Set Divert Valve	Waste

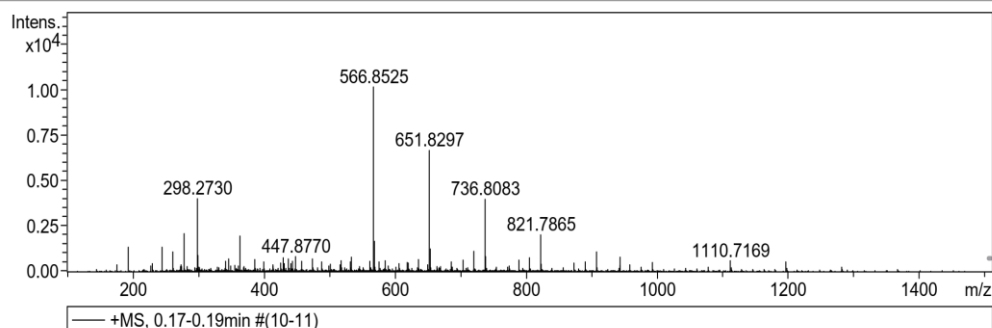


Figure A14 The HR-ESI-MS of 47.

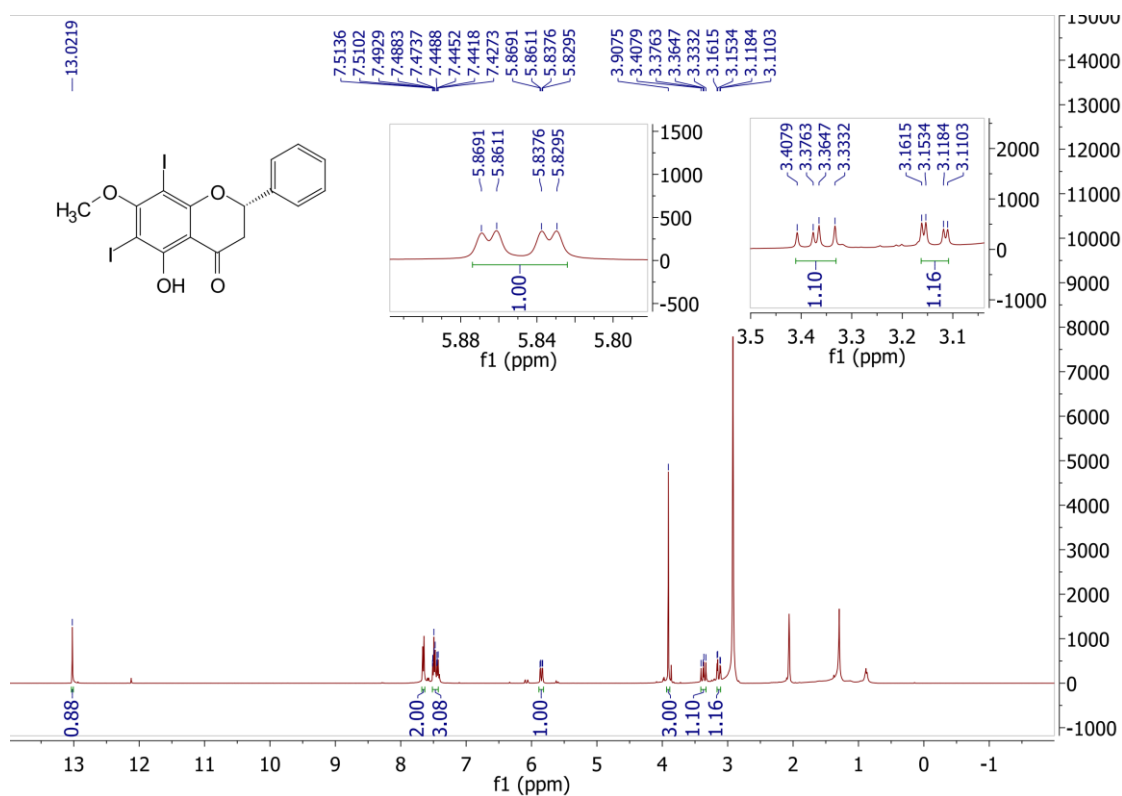


Figure A15 The <sup>1</sup>H NMR spectrum (Acetone-d<sub>6</sub>, 400 MHz) of 47.

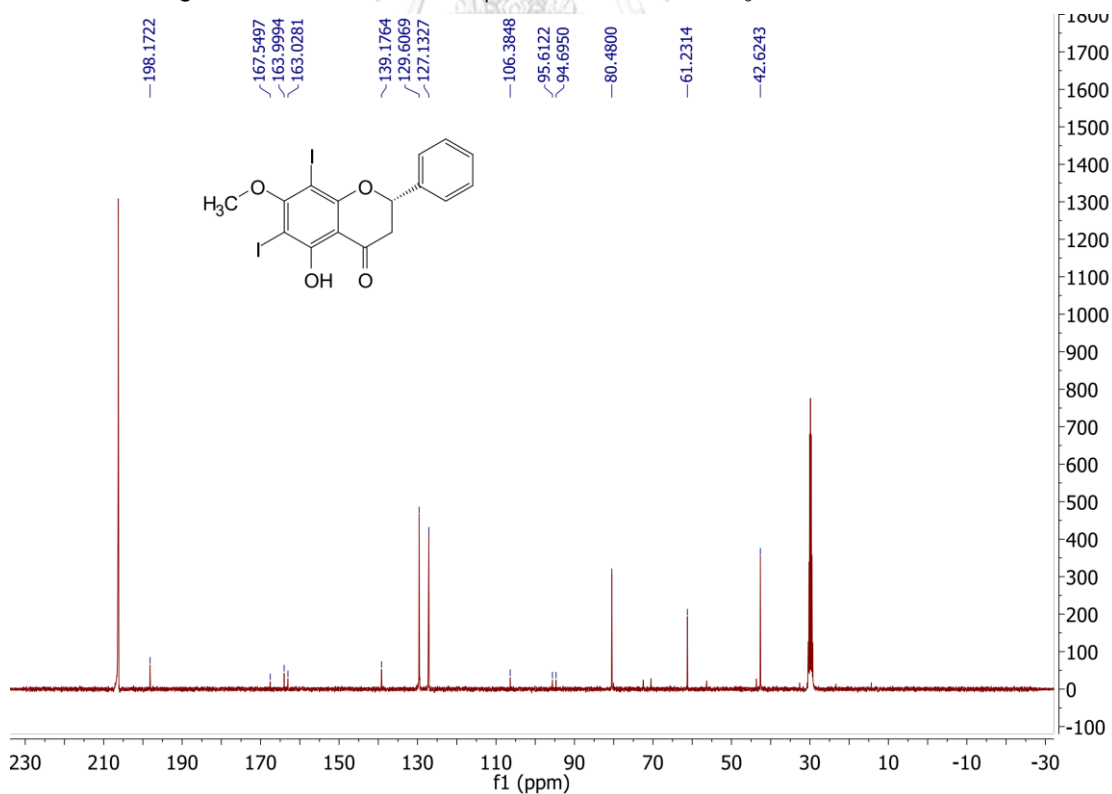


Figure A16 The <sup>13</sup>C NMR spectrum (Acetone-d<sub>6</sub>, 100 MHz) of 47.

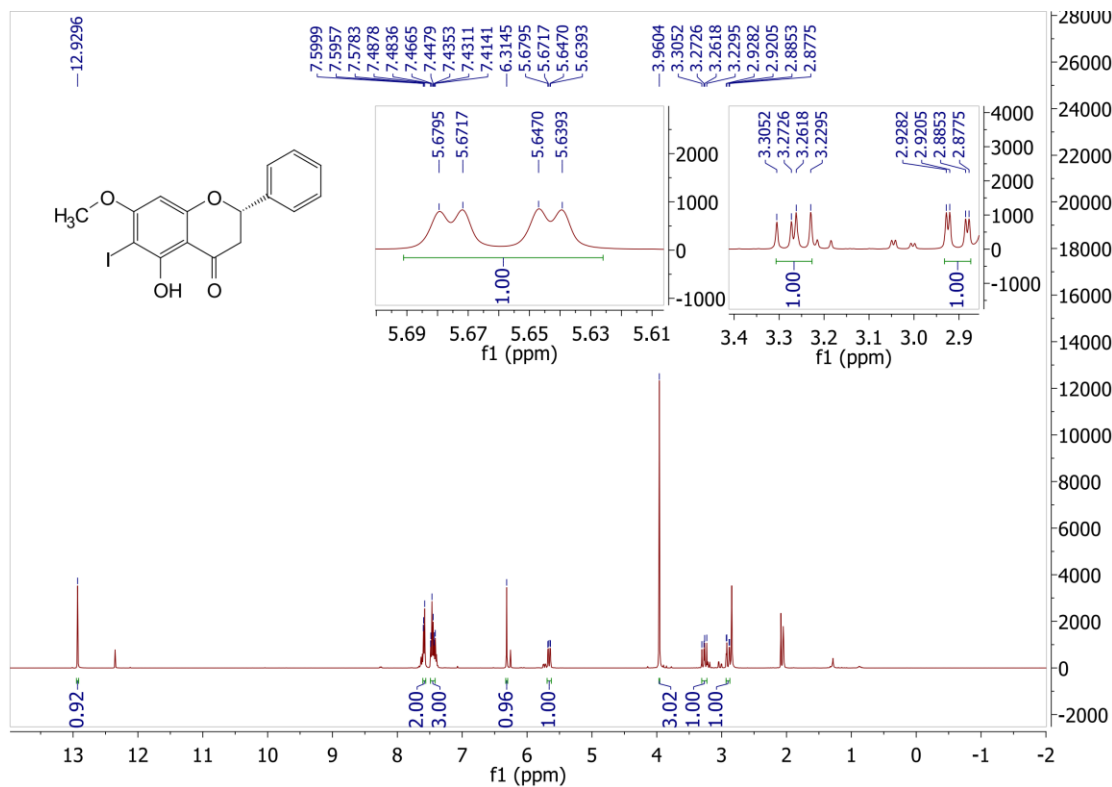


Figure A17 The <sup>1</sup>H NMR (Acetone-d<sub>6</sub>, 400 MHz) of 48.

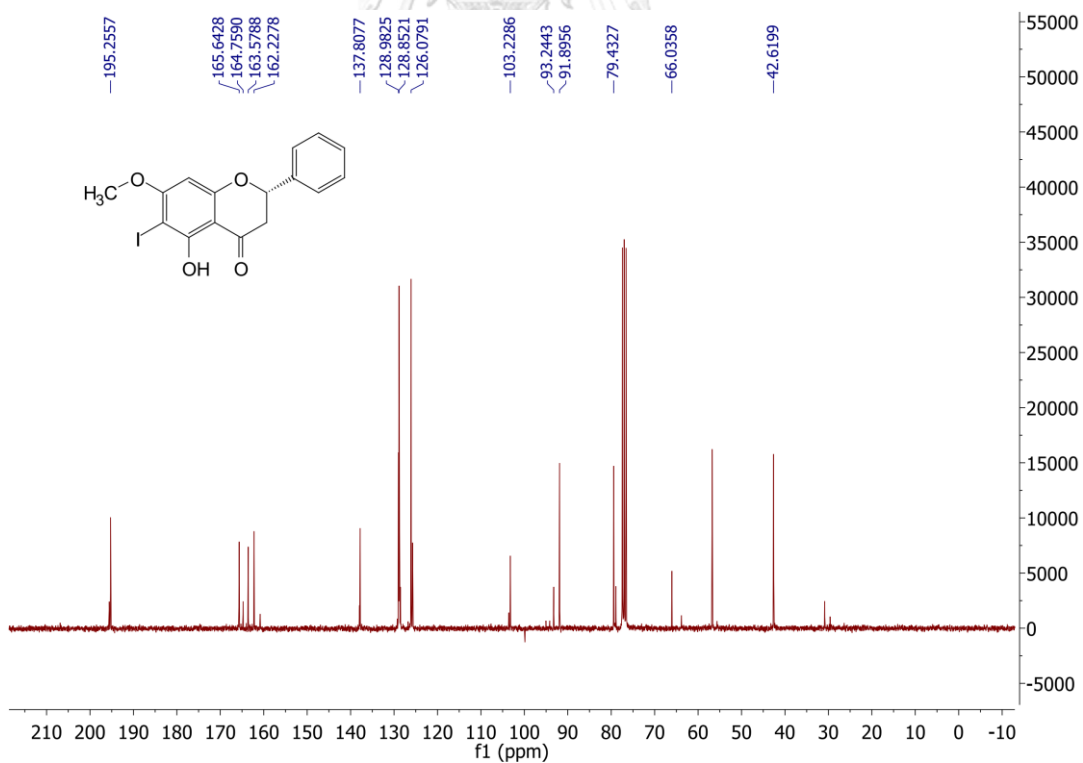


Figure A18 The <sup>13</sup>C NMR (Acetone-d<sub>6</sub>, 100 MHz) of 48.

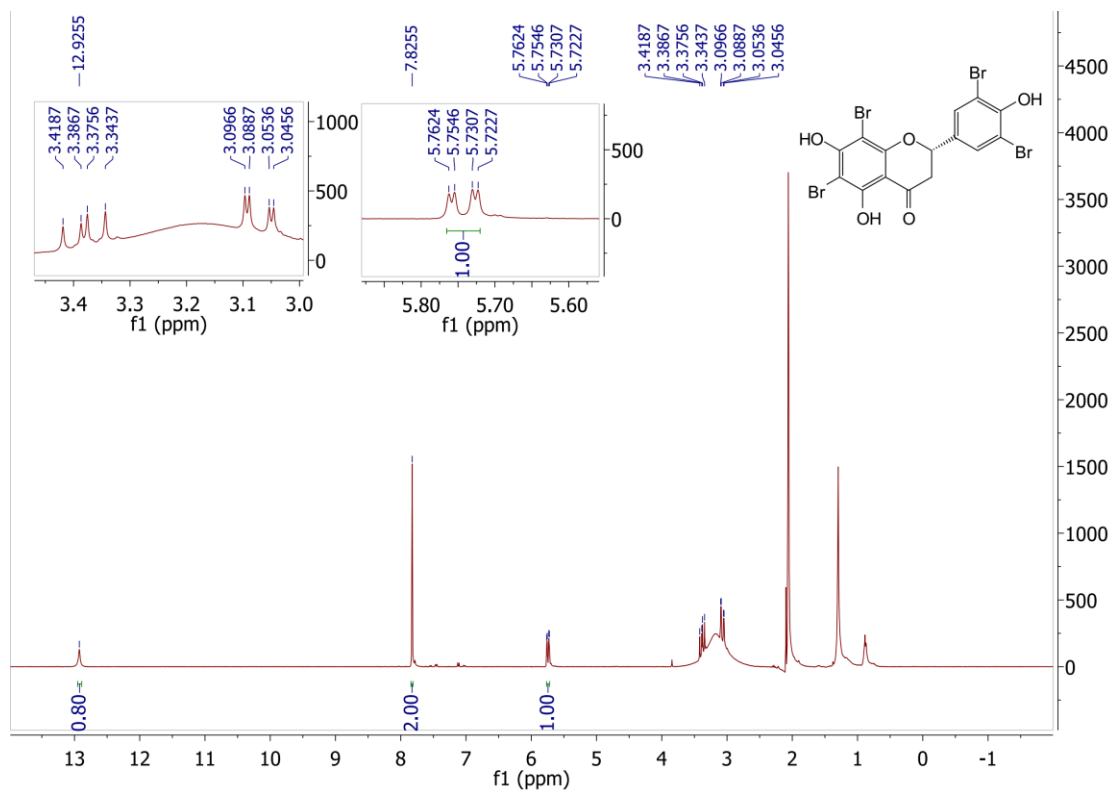


Figure A19 The <sup>1</sup>H NMR spectrum (Acetone-d<sub>6</sub>, 400 MHz) of **49**.

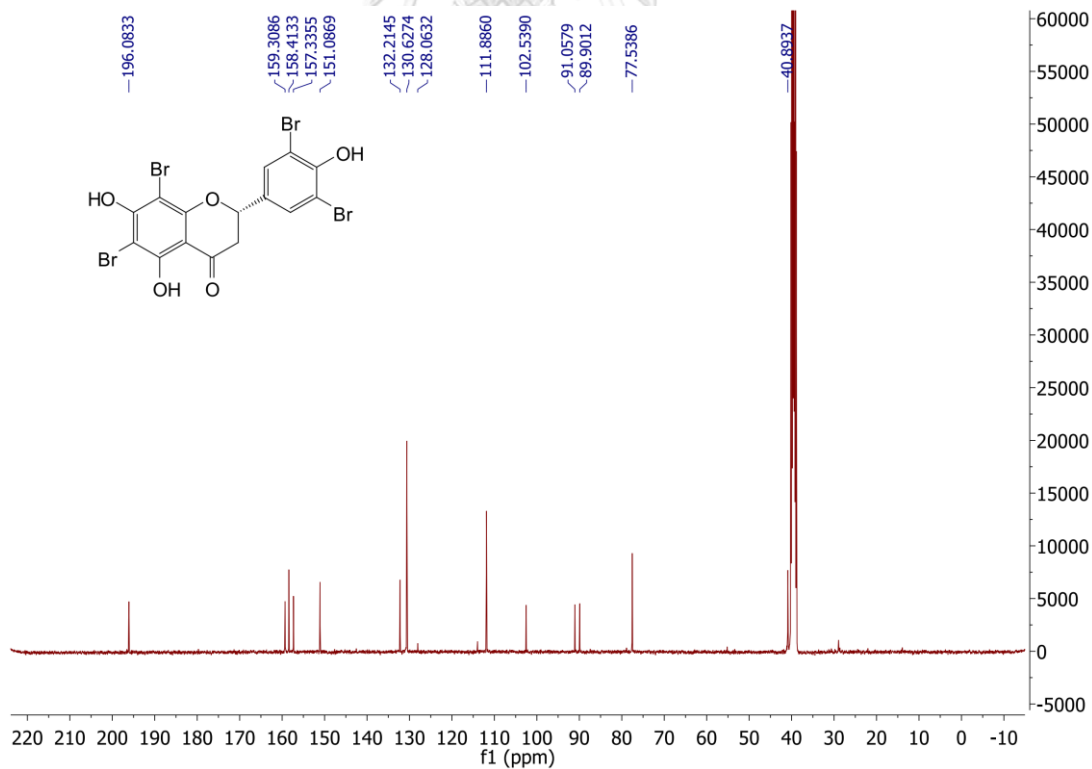
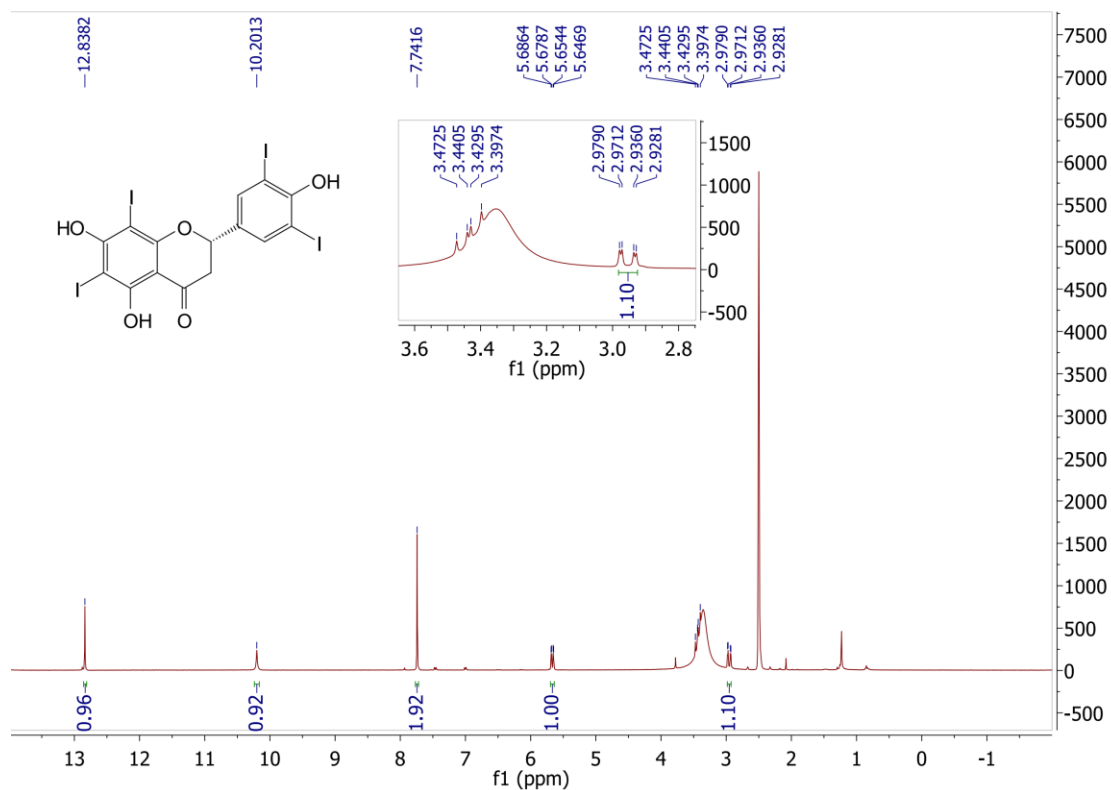
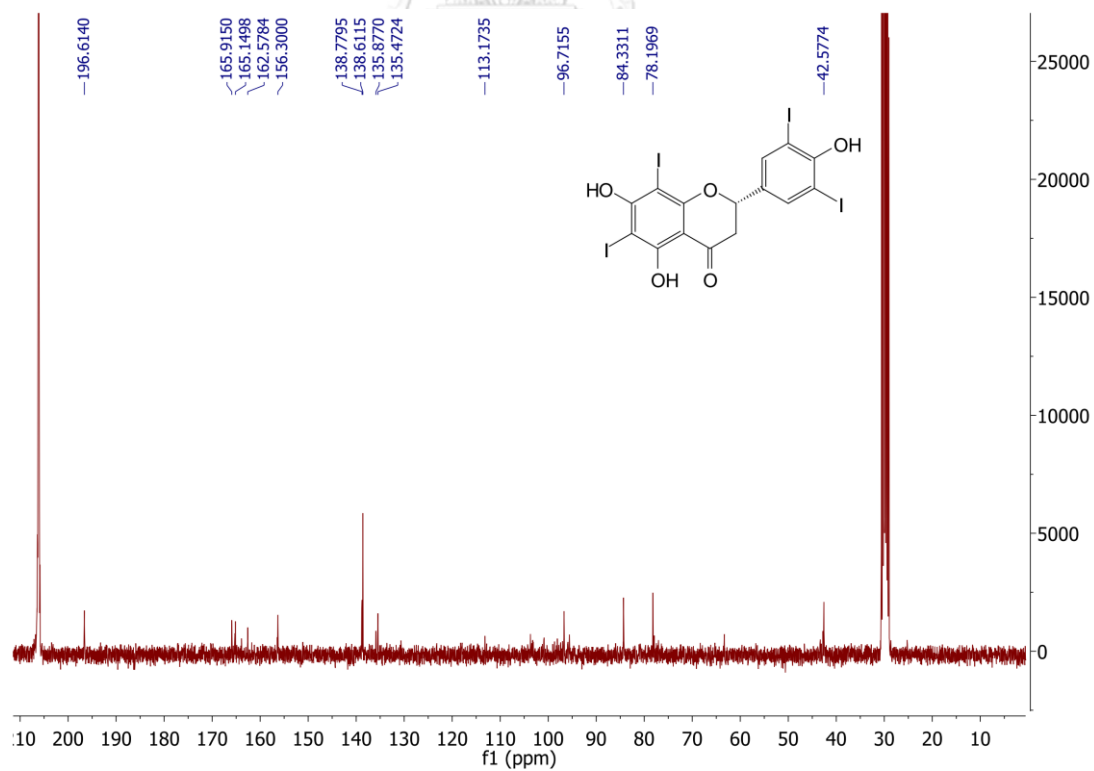


Figure A20 The <sup>13</sup>C NMR spectrum (Acetone-d<sub>6</sub>, 100 MHz) of **49**.



**Figure A21** The  $^1\text{H}$  NMR spectrum (DMSO- $d_6$ , 400 MHz) of **50**.



**Figure A22** The  $^{13}\text{C}$  NMR spectrum (DMSO- $d_6$ , 100 MHz) of **50**.

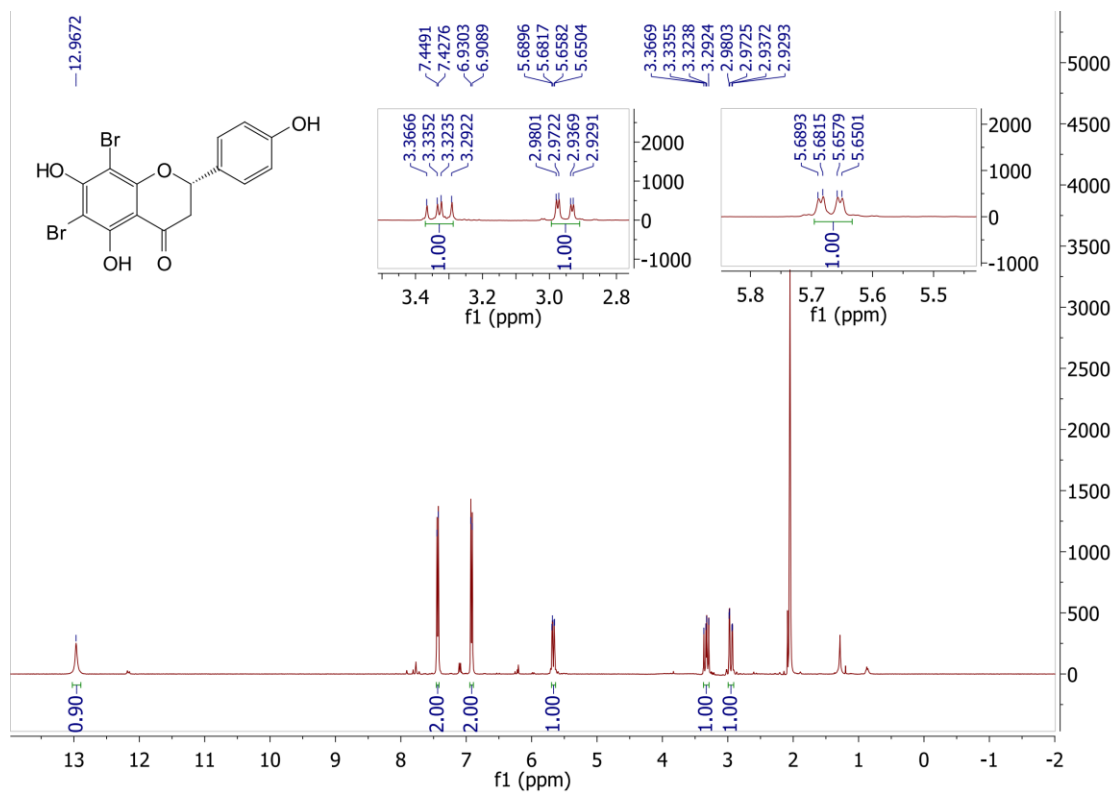


Figure A23 The  $^1\text{H}$  NMR spectrum (Acetone- $d_6$ , 400 MHz) of 51.

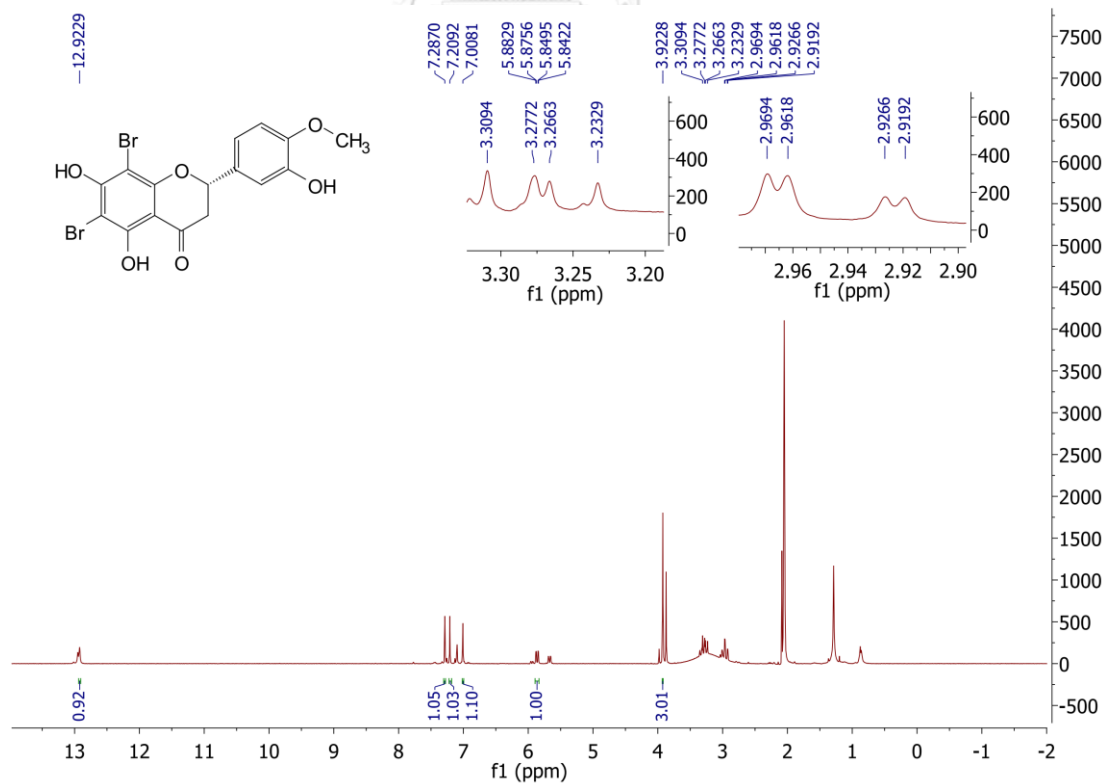


Figure A24 The  $^1\text{H}$  NMR spectrum (Acetone- $d_6$ , 400 MHz) of 52.

## Mass Spectrum List Report

<b>Analysis Info</b>		Acquisition Date	9/24/2018 2:10:33 PM	
Analysis Name	D:\Data\Data Service\180924_pos_T44.d		Operator	CU.
Method	NV_pos_0.3min_profile_1segment_lowNbulizerDrygas.m		Instrument / Ser#	micrOTOF-Q II 10335
Sample Name	180924_pos_T44		Comment	

### Acquisition Parameter

Source Type	ESI	Ion Polarity	Positive	Set Nebulizer	0.4 Bar
Focus	Not active	Set Capillary	4000 V	Set Dry Heater	200 °C
Scan Begin	50 m/z	Set End Plate Offset	-500 V	Set Dry Gas	4.0 l/min
Scan End	1500 m/z	Set Collision Cell RF	150.0 Vpp	Set Divert Valve	Waste

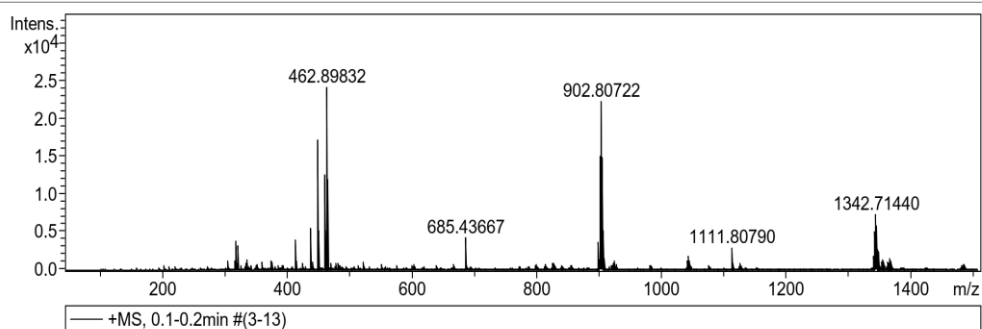


Figure A25 The HR-ESI-MS of 53.

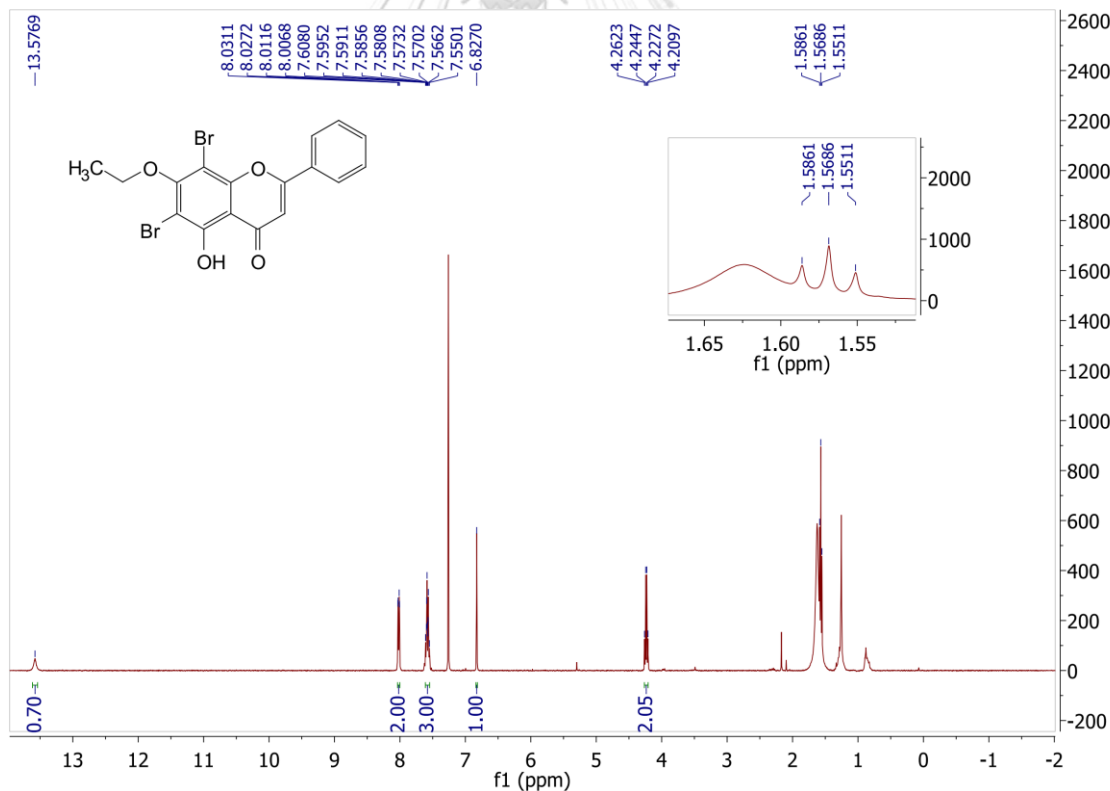


Figure A26 The  $^1\text{H}$  NMR spectrum ( $\text{CDCl}_3$ , 400 MHz) of 53.



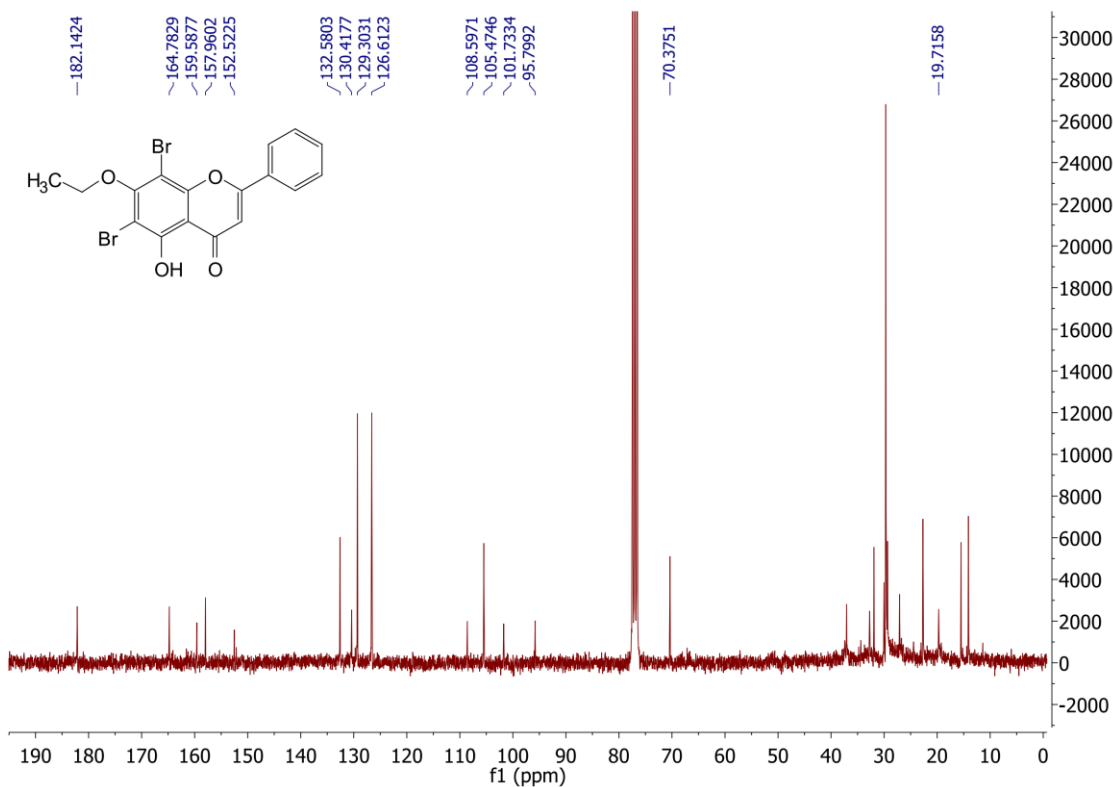


Figure A27 The  $^{13}\text{C}$  NMR spectrum ( $\text{CDCl}_3$ , 100 MHz) of **53**.

### Mass Spectrum List Report

Analysis Info		Acquisition Date	
Analysis Name	D:\Data\Data Service\180924_pos_T45.d	9/24/2018 2:45:23 PM	
Method	NV_pos_0.3min_profile_1segment_lowNubulizerDrygas.m	Operator	CU.
Sample Name	180924_pos_T45	Instrument / Ser#	micrOTOF-Q II 10335
Comment			

Acquisition Parameter			
Source Type	ESI	Ion Polarity	Positive
Focus	Not active	Set Capillary	4000 V
Scan Begin	50 m/z	Set End Plate Offset	-500 V
Scan End	1500 m/z	Set Collision Cell RF	150.0 Vpp
		Set Nebulizer	0.4 Bar
		Set Dry Heater	200 °C
		Set Dry Gas	4.0 l/min
		Set Divert Valve	Waste

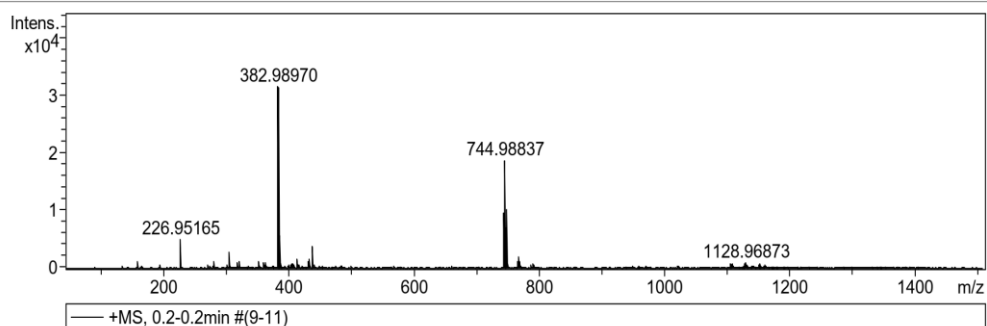


Figure A28 The HR-ESI-MS of **54**.

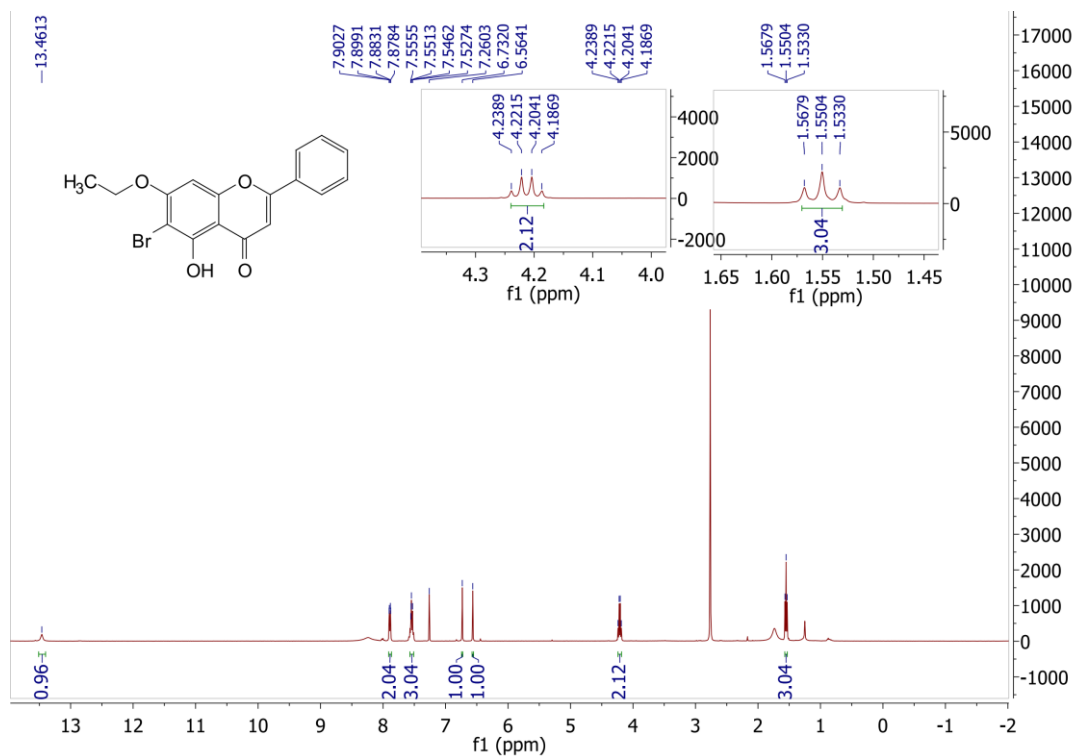


Figure A29 The  $^1\text{H}$  NMR spectrum (CDCl<sub>3</sub>, 400 MHz) of 54.

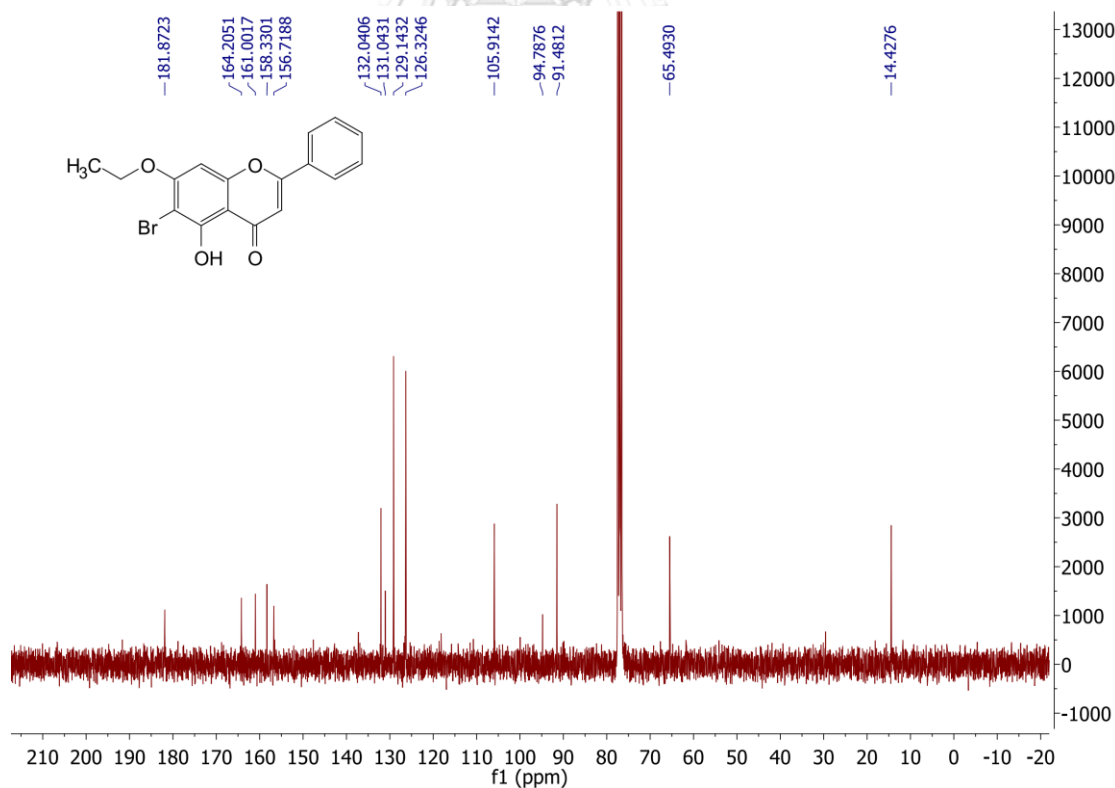


Figure A30 The  $^{13}\text{C}$  NMR spectrum (CDCl<sub>3</sub>, 100 MHz) of 54.

## Mass Spectrum List Report

**Analysis Info**

Analysis Name	D:\Data\Data Service\180924_pos_T59.d	Acquisition Date	9/24/2018 3:58:13 PM
Method	NV_pos_0.3min_profile_1segment_lowNbulizerDrygas.m	Operator	CU.
Sample Name	180924_pos_T59	Instrument / Ser#	micrOTOF-Q II 10335
Comment			

**Acquisition Parameter**

Source Type	ESI	Ion Polarity	Positive	Set Nebulizer	0.4 Bar
Focus	Not active	Set Capillary	4000 V	Set Dry Heater	200 °C
Scan Begin	50 m/z	Set End Plate Offset	-500 V	Set Dry Gas	4.0 l/min
Scan End	1500 m/z	Set Collision Cell RF	150.0 Vpp	Set Divert Valve	Waste

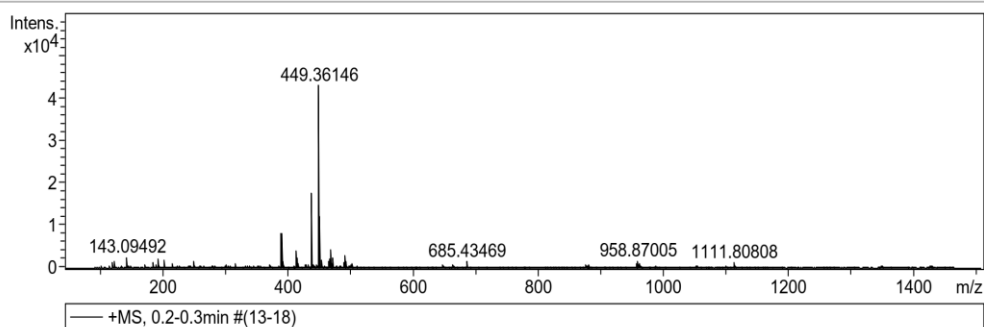


Figure A31 The HR-ESI-MS of **55**.

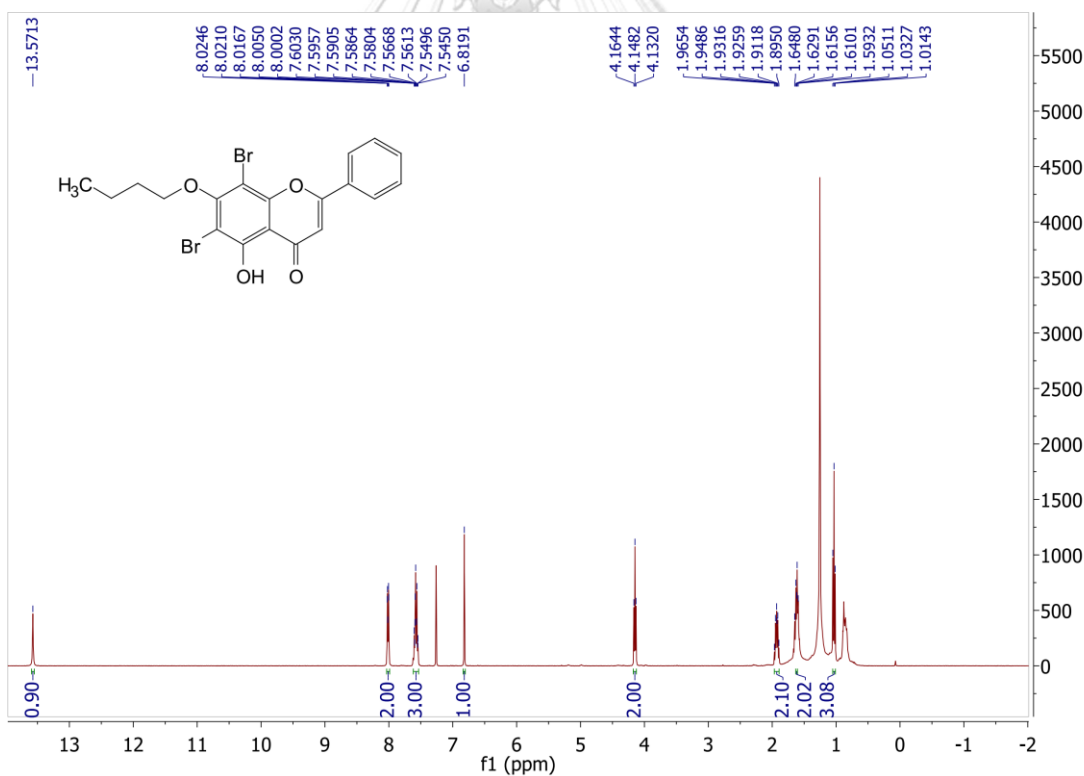


Figure A32 The  $^1\text{H}$  NMR spectrum ( $\text{CDCl}_3$ , 400 MHz) of **55**.

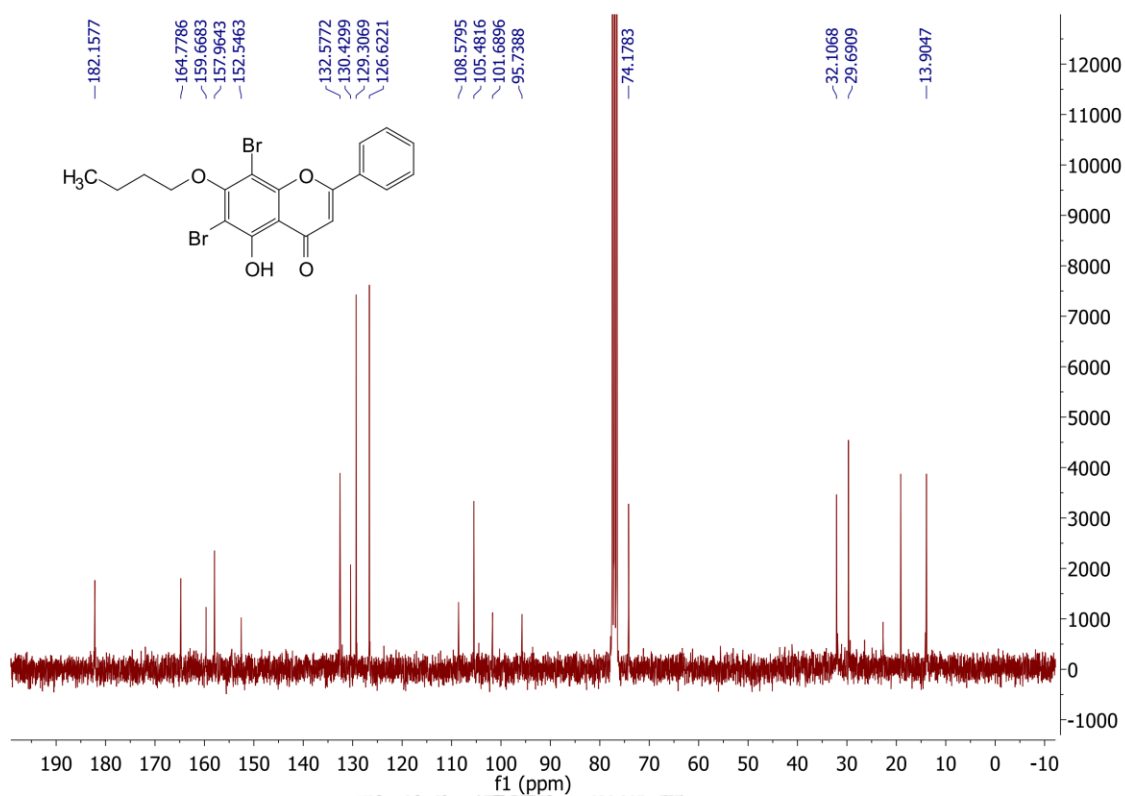


Figure A33 The  $^{13}\text{C}$  NMR spectrum ( $\text{CDCl}_3$ , 100 MHz) of 55.

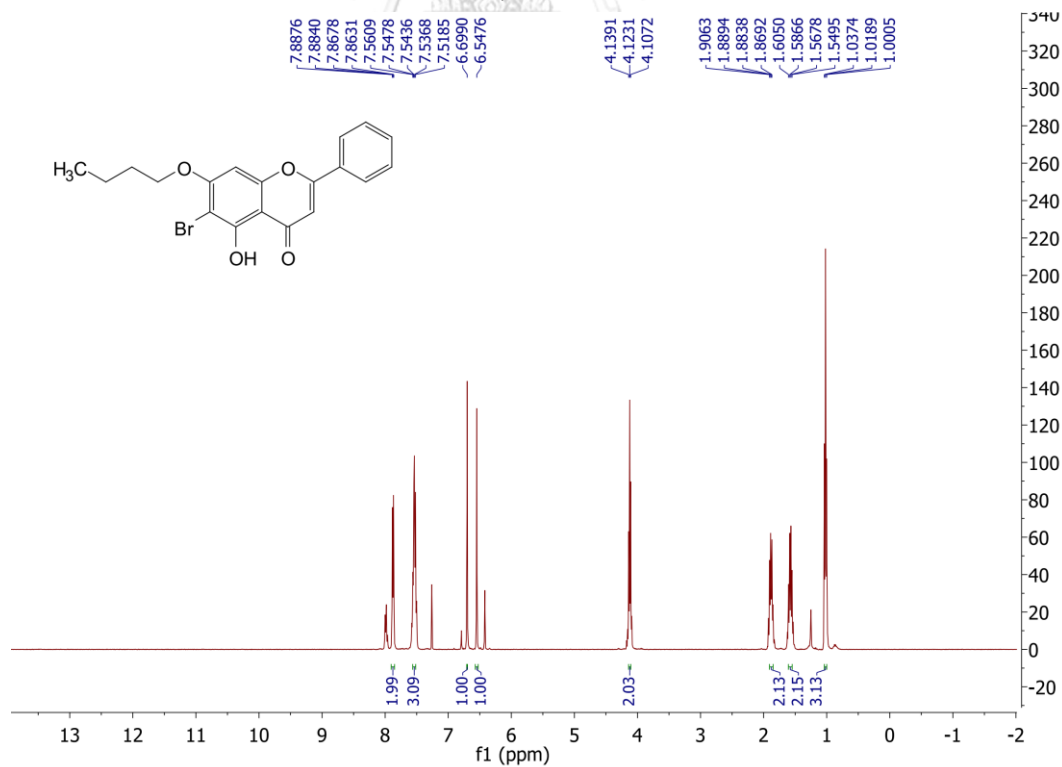


Figure A34 The  $^1\text{H}$  NMR spectrum ( $\text{CDCl}_3$ , 400 MHz) of 56.

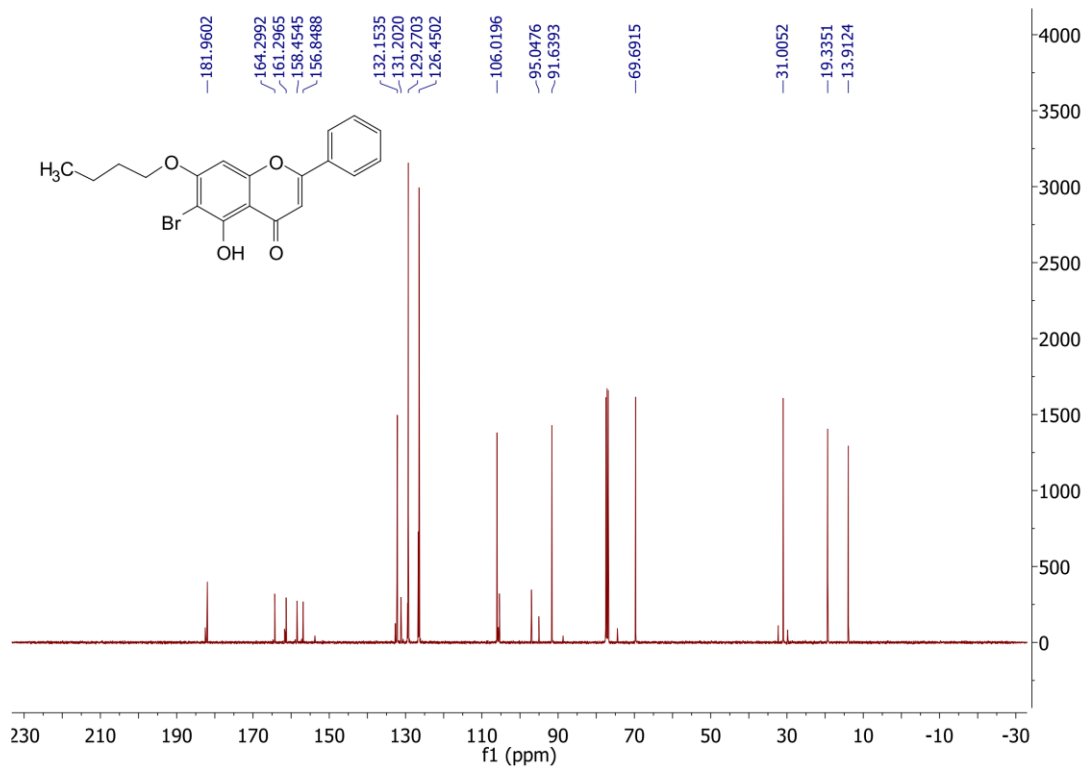


Figure A35 The  $^{13}\text{C}$  NMR spectrum ( $\text{CDCl}_3$ , 100 MHz) of **56**.

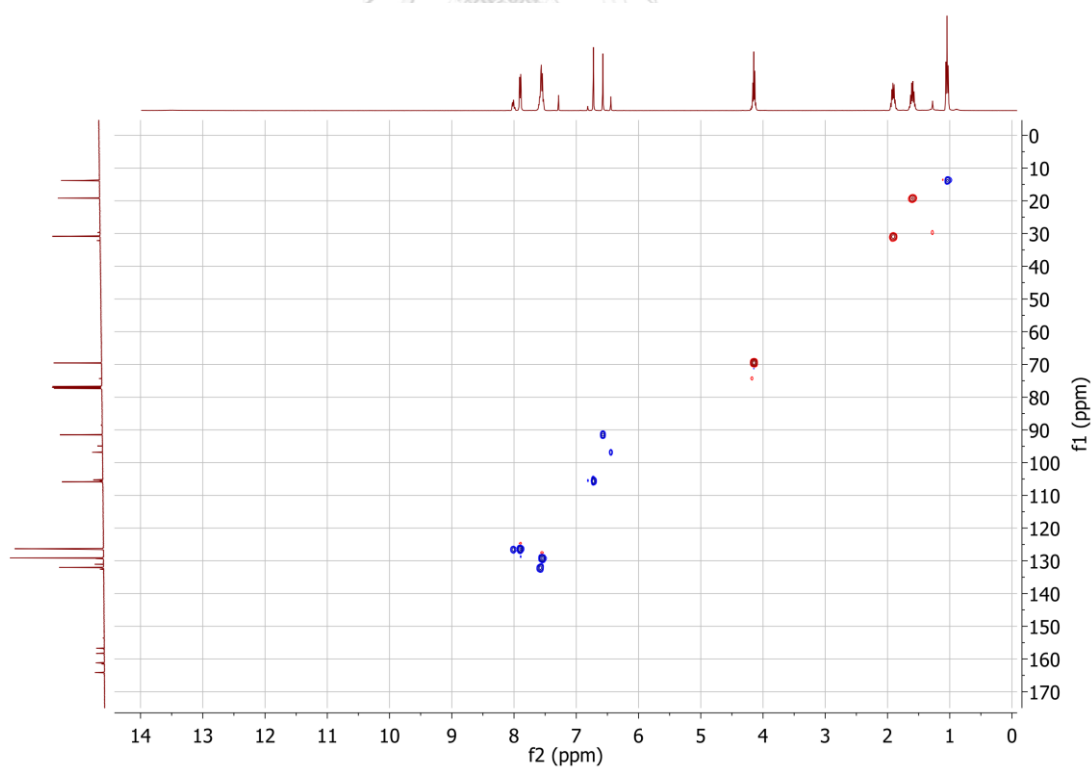


Figure A36 The HSQC correlation ( $\text{CDCl}_3$ ) of **56**.

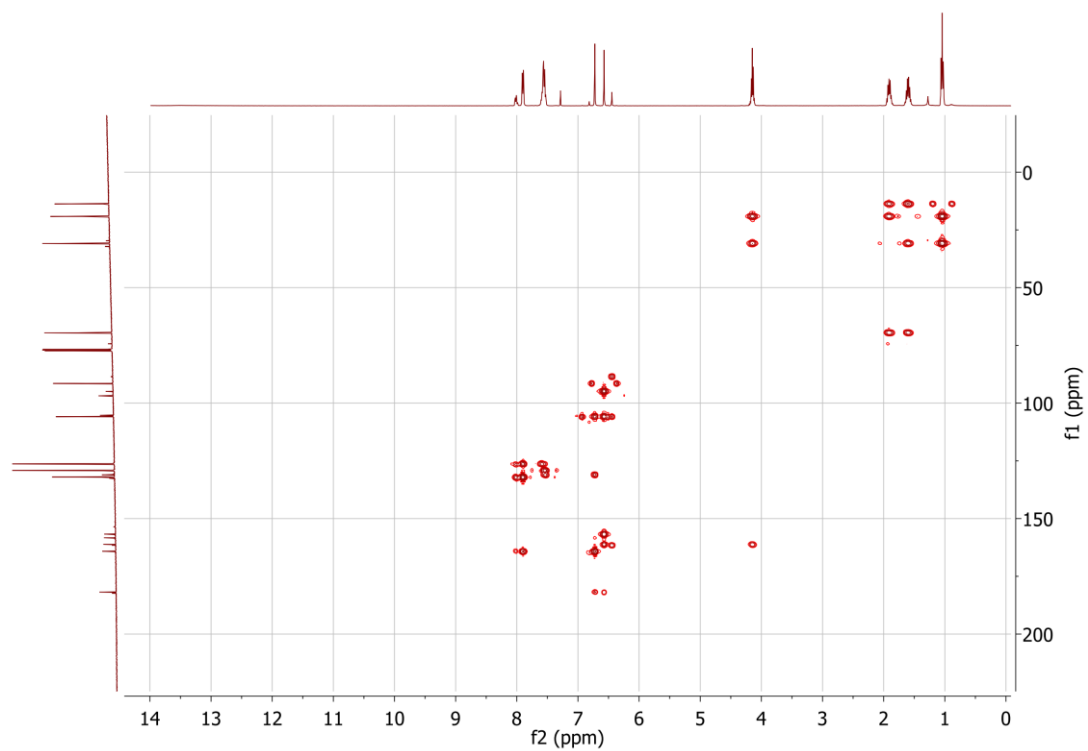


Figure A37 The HMBC correlation ( $\text{CDCl}_3$ ) of **56**.

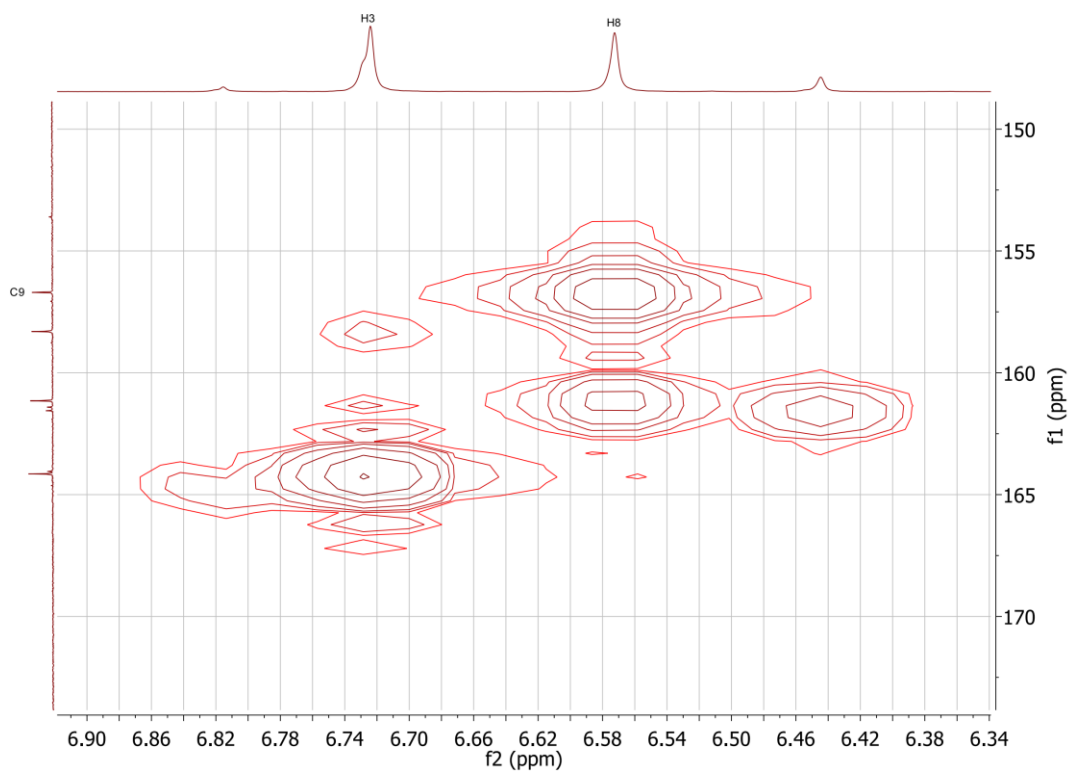


Figure A38 The HMBC (expansion) correlation ( $\text{CDCl}_3$ ) of **56**.

## Mass Spectrum List Report

### Analysis Info

Analysis Name D:\Data\Data Service\180924\_pos\_T52.d  
 Method NV\_pos\_0.3min\_profile\_1segment\_lowNubulizerDrygas.m  
 Sample Name 180924\_pos\_T52  
 Comment

Acquisition Date 9/24/2018 3:24:22 PM

Operator CU.  
 Instrument / Ser# micrOTOF-Q II 10335

### Acquisition Parameter

Source Type	ESI	Ion Polarity	Positive	Set Nebulizer	0.4 Bar
Focus	Not active	Set Capillary	4000 V	Set Dry Heater	200 °C
Scan Begin	50 m/z	Set End Plate Offset	-500 V	Set Dry Gas	4.0 l/min
Scan End	1500 m/z	Set Collision Cell RF	150.0 Vpp	Set Divert Valve	Waste

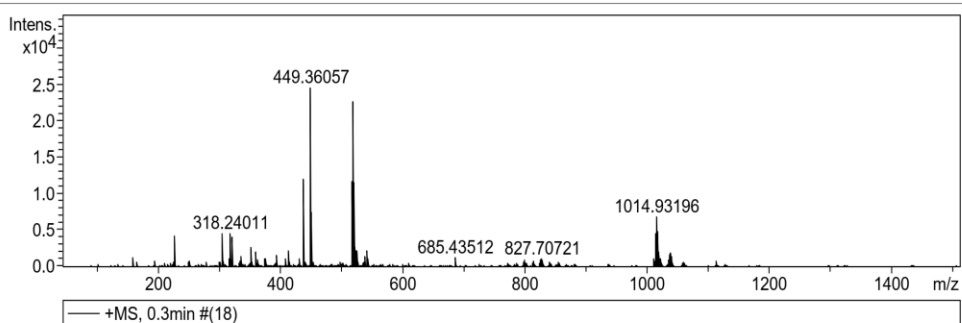


Figure A39 The HR-ESI-MS of 57.

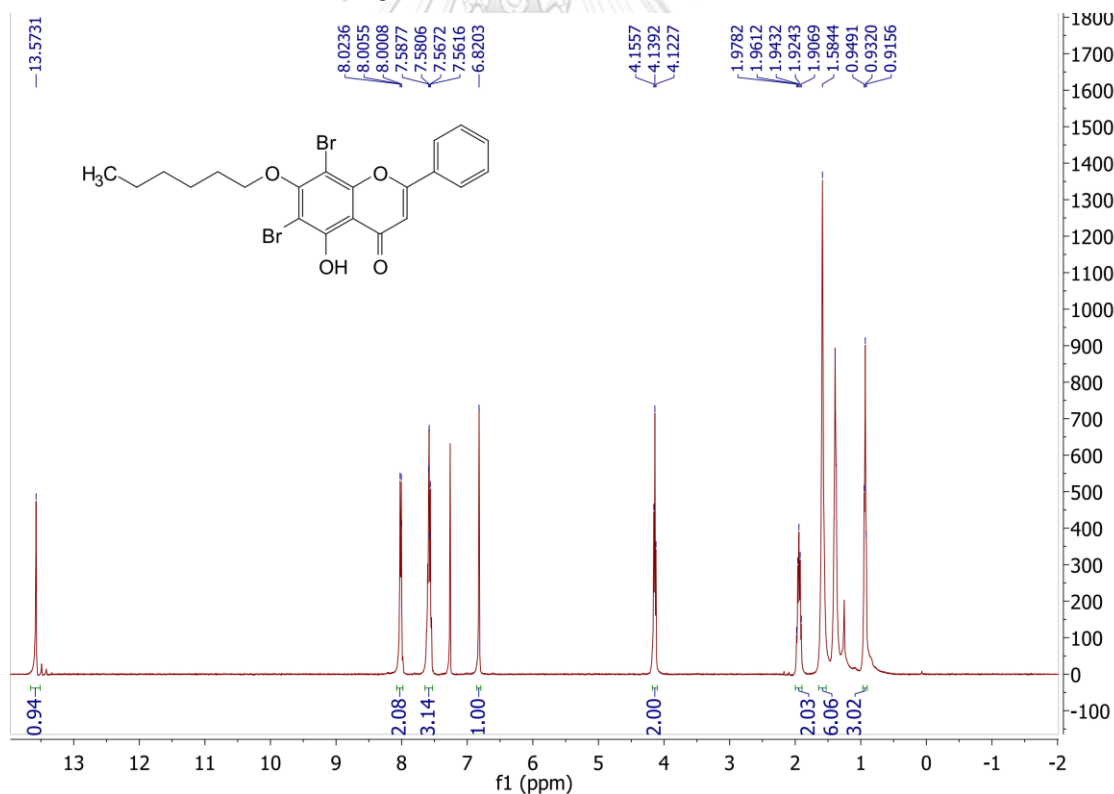


Figure A40 The  $^1\text{H}$  NMR spectrum ( $\text{CDCl}_3$ , 400 MHz) of 57.

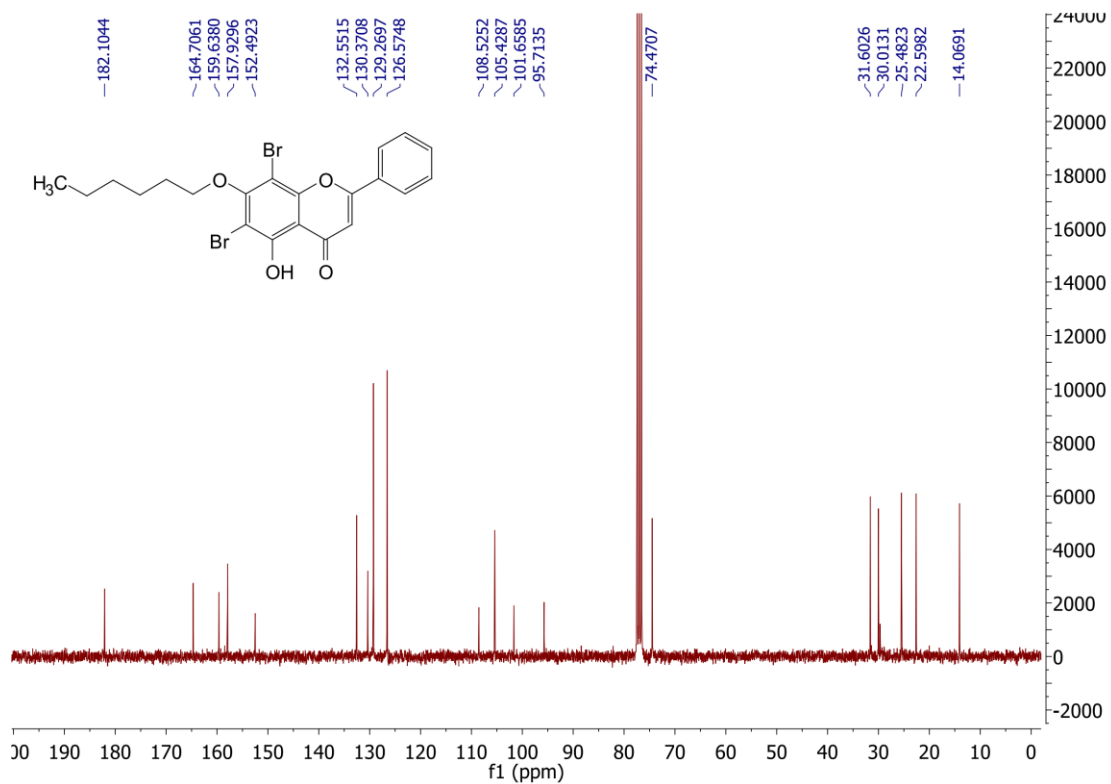


Figure A41 The  $^{13}\text{C}$  NMR spectrum ( $\text{CDCl}_3$ , 100 MHz) of 57.

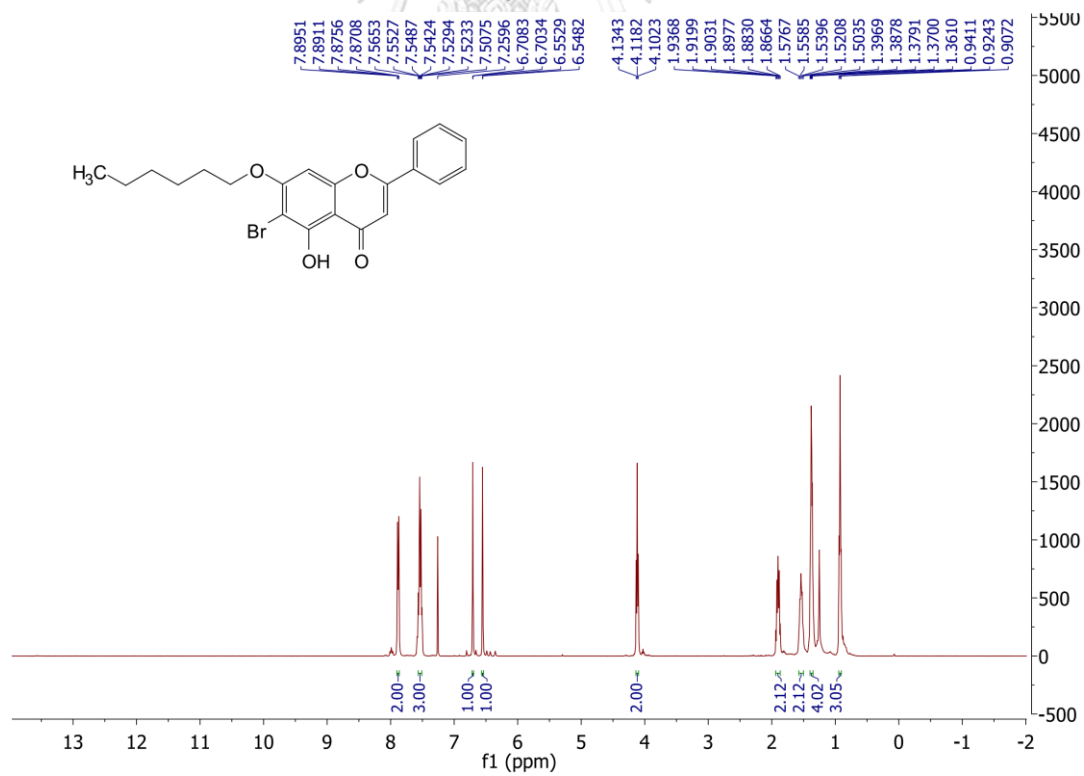


Figure A42 The  $^1\text{H}$  NMR spectrum ( $\text{CDCl}_3$ , 400 MHz) of 58.



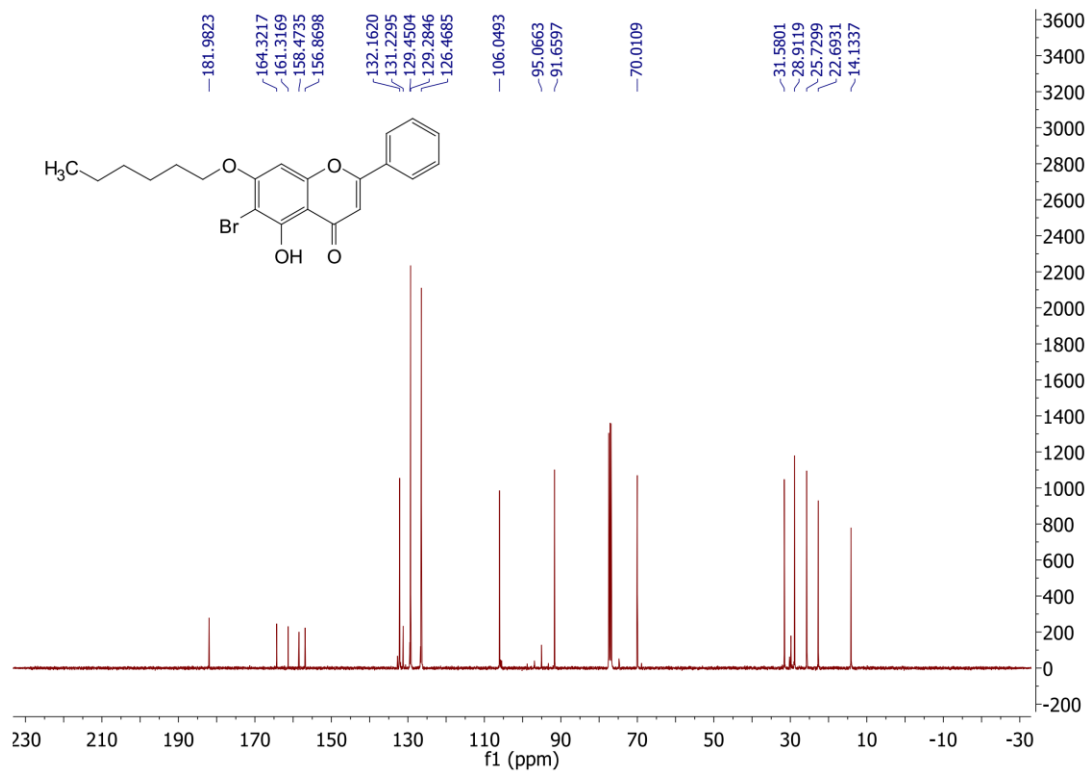


Figure A43 The  $^{13}\text{C}$  NMR spectrum ( $\text{CDCl}_3$ , 100 MHz) of **58**.

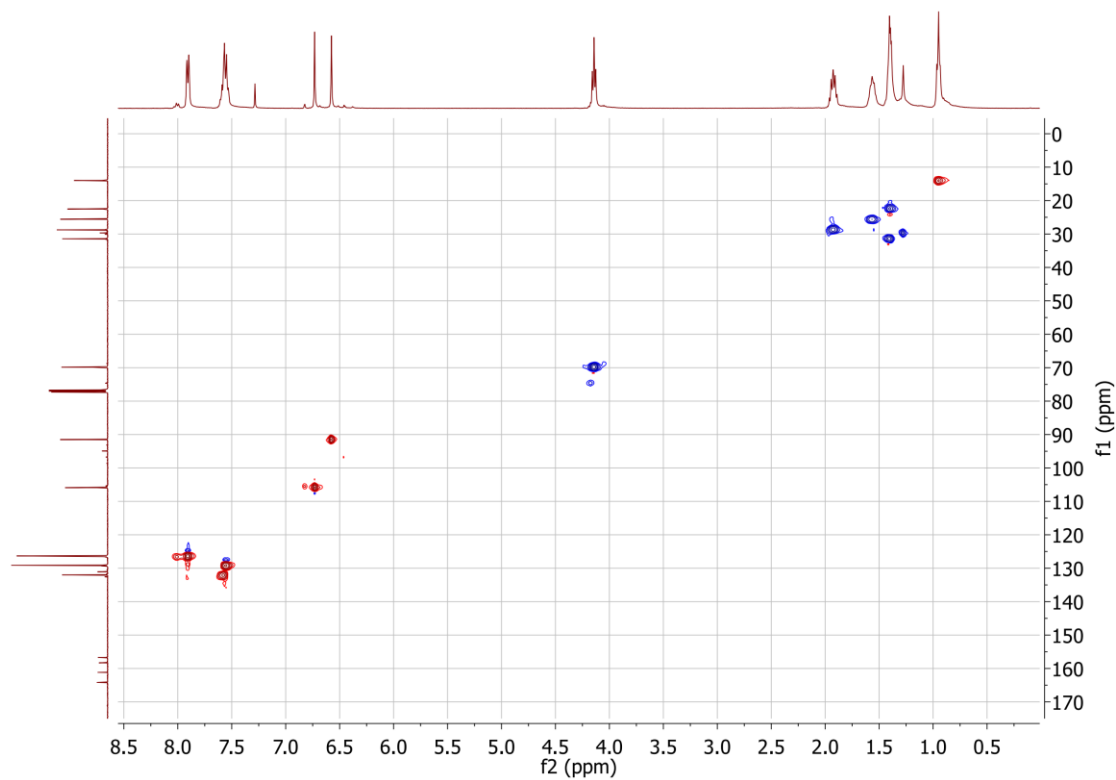


Figure A44 The HSQC correlation ( $\text{CDCl}_3$ ) of **58**.

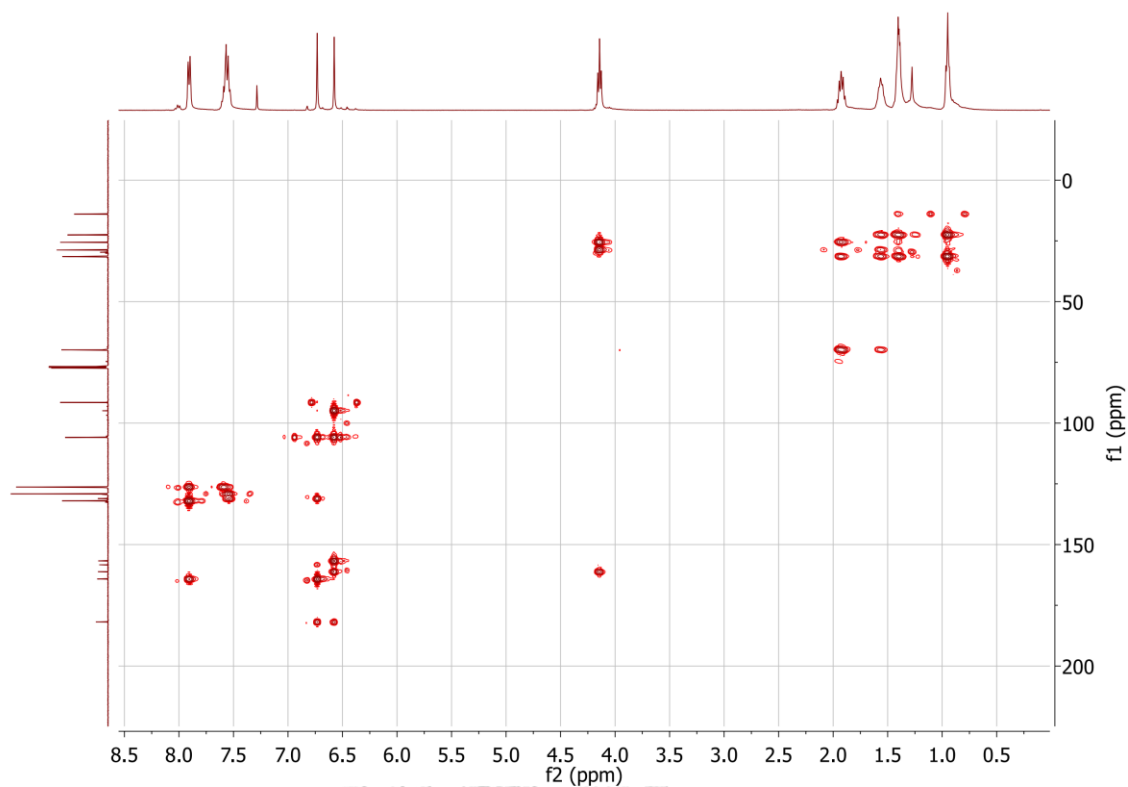


Figure A45 The HMBC correlation (CDCl<sub>3</sub>) of 58.

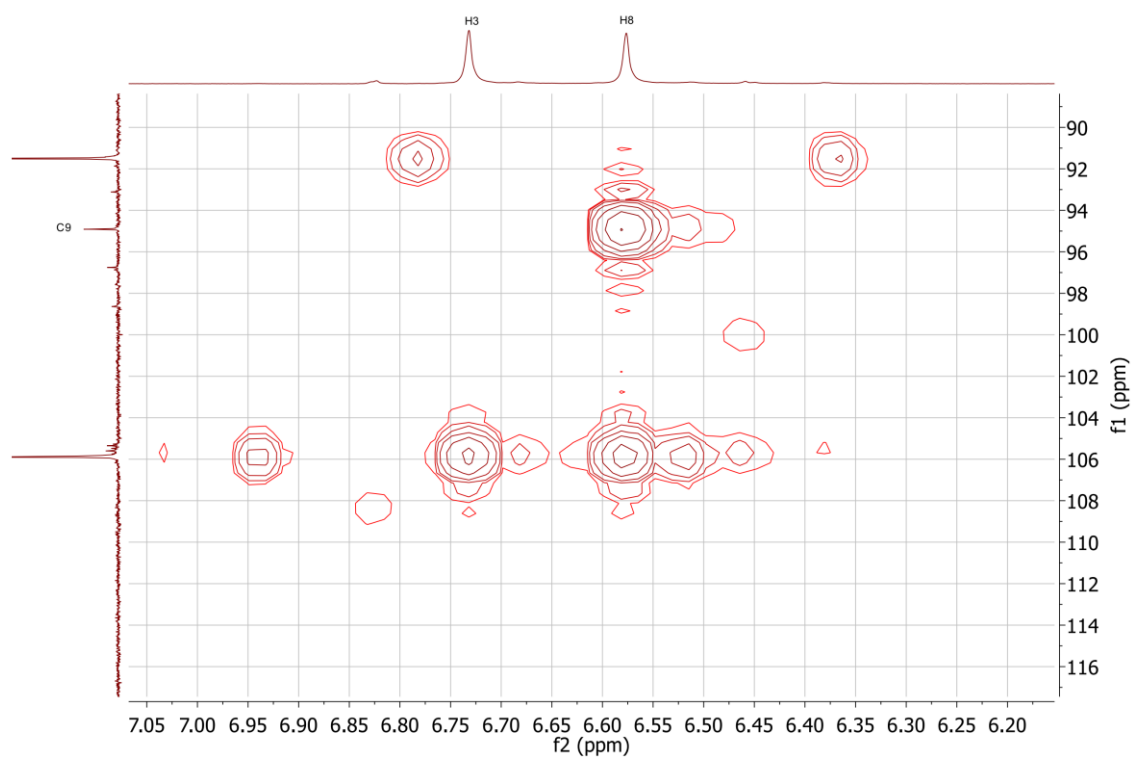


Figure A46 The HMBC (expansion) correlation (CDCl<sub>3</sub>) of 58.

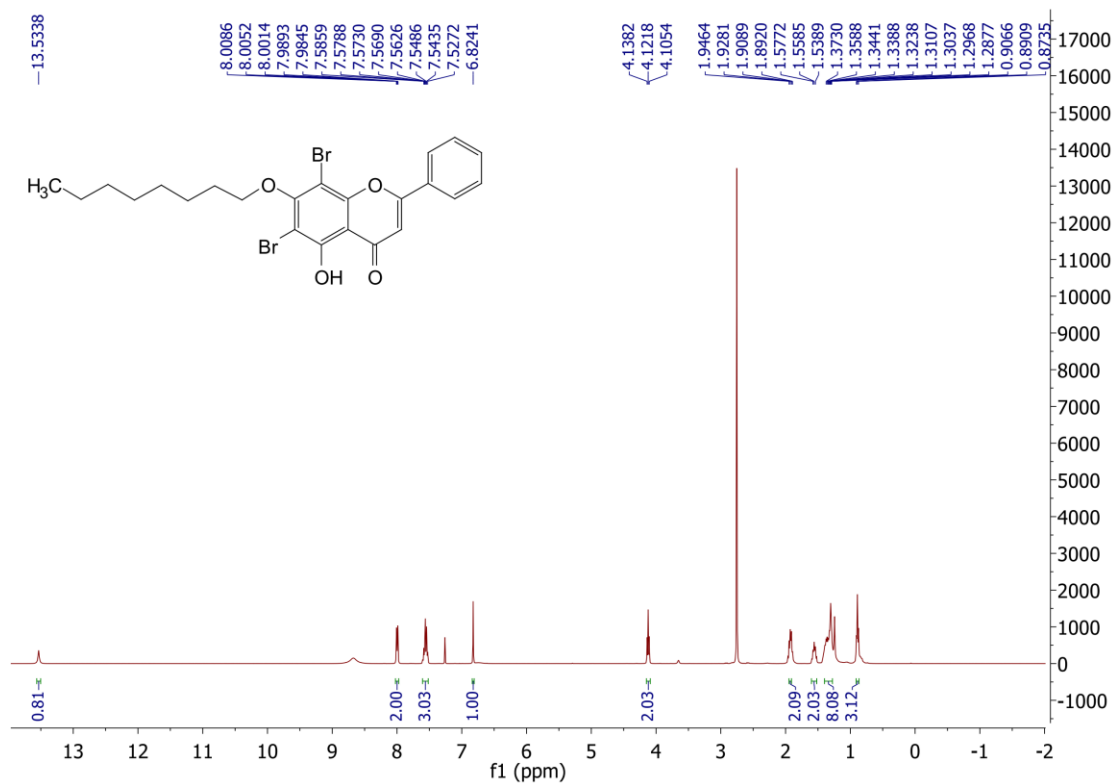


Figure A47 The  $^1\text{H}$  NMR spectrum ( $\text{CDCl}_3$ , 400 MHz) of **59**.

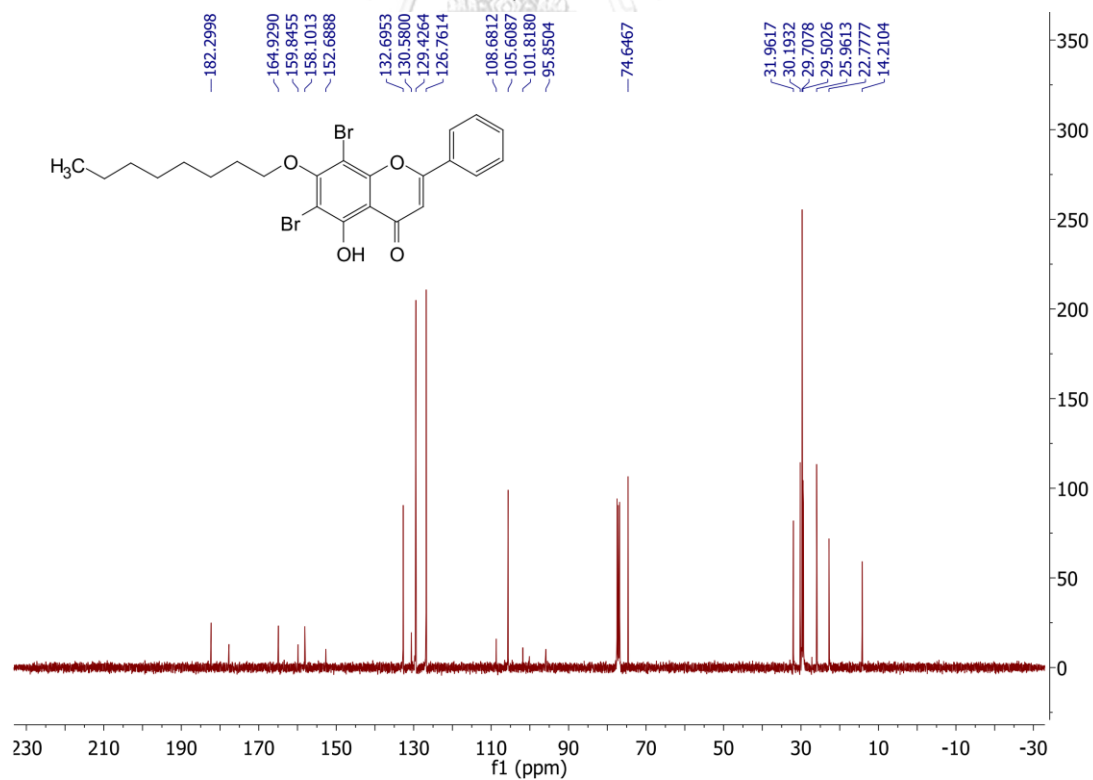


Figure A48 The  $^{13}\text{C}$  NMR spectrum ( $\text{CDCl}_3$ , 100 MHz) of **59**.

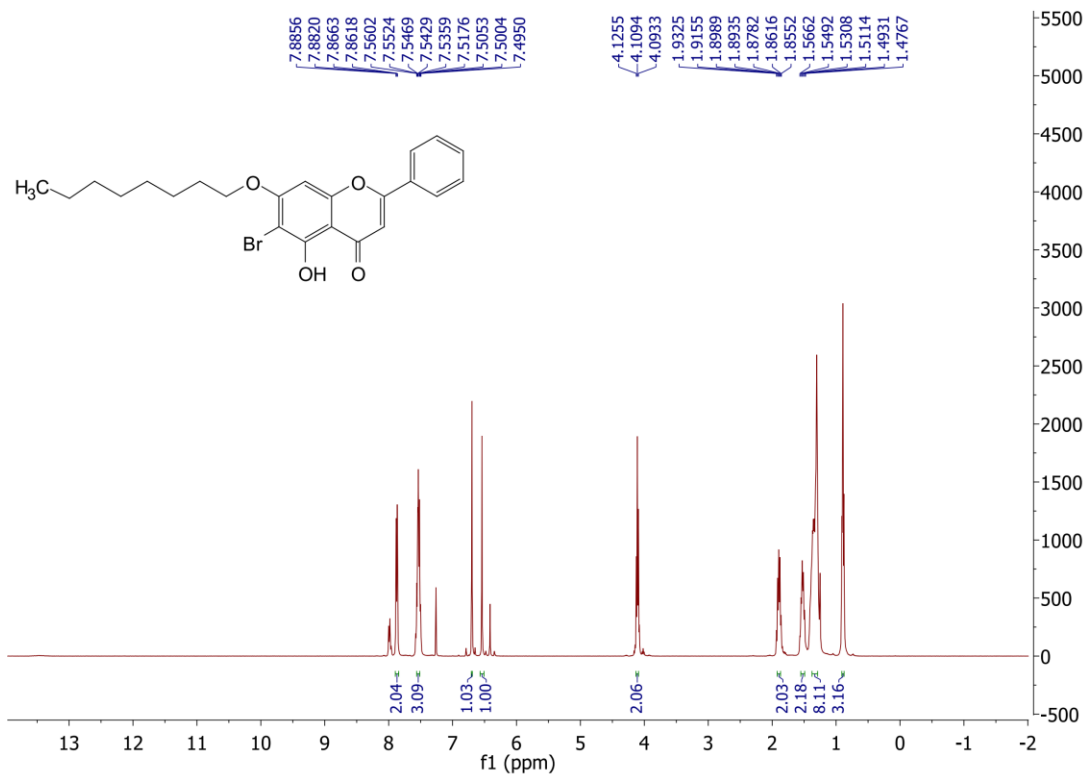


Figure A49 The <sup>1</sup>H NMR spectrum (CDCl<sub>3</sub>, 400 MHz) of **60**.

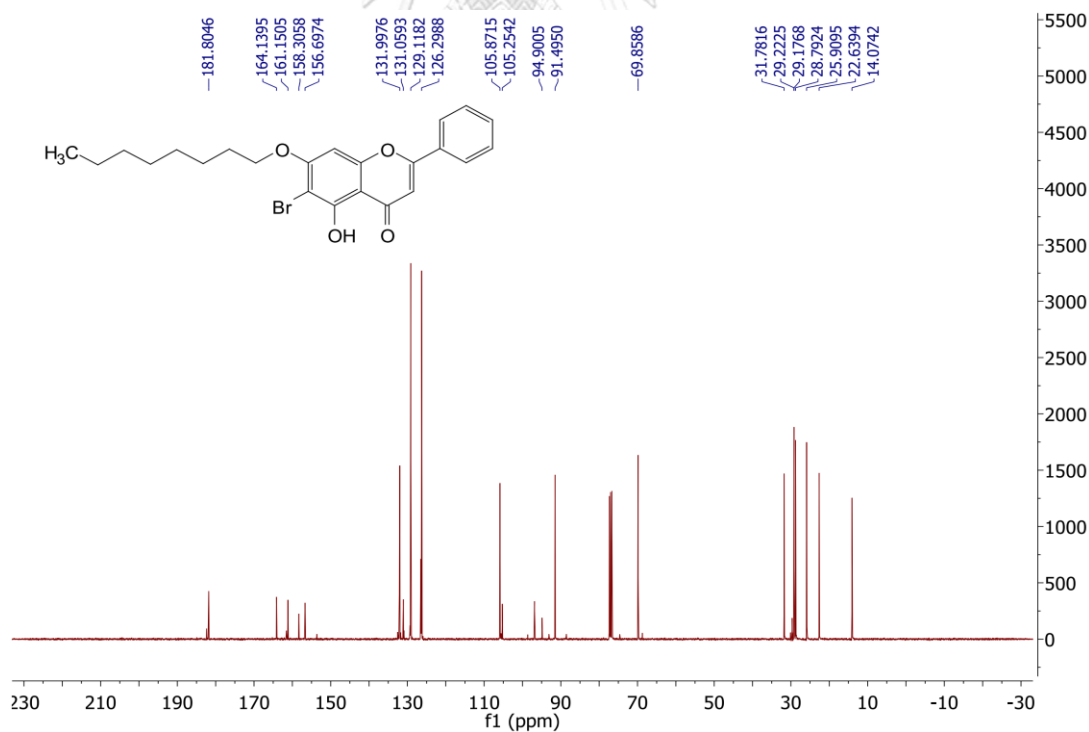


Figure A50 The <sup>13</sup>C NMR spectrum (CDCl<sub>3</sub>, 100 MHz) of **60**.



Figure A51 The HSQC correlation ( $\text{CDCl}_3$ ) of **60**.

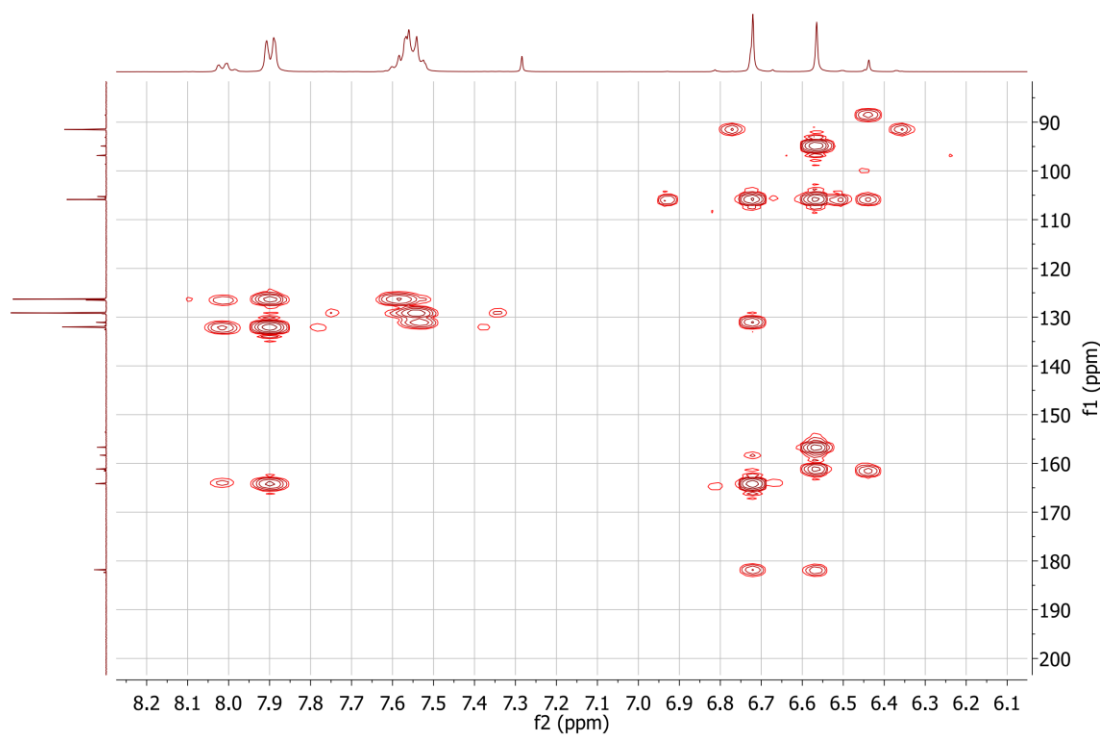


Figure A52 The HMBC correlation ( $\text{CDCl}_3$ ) of **60**.

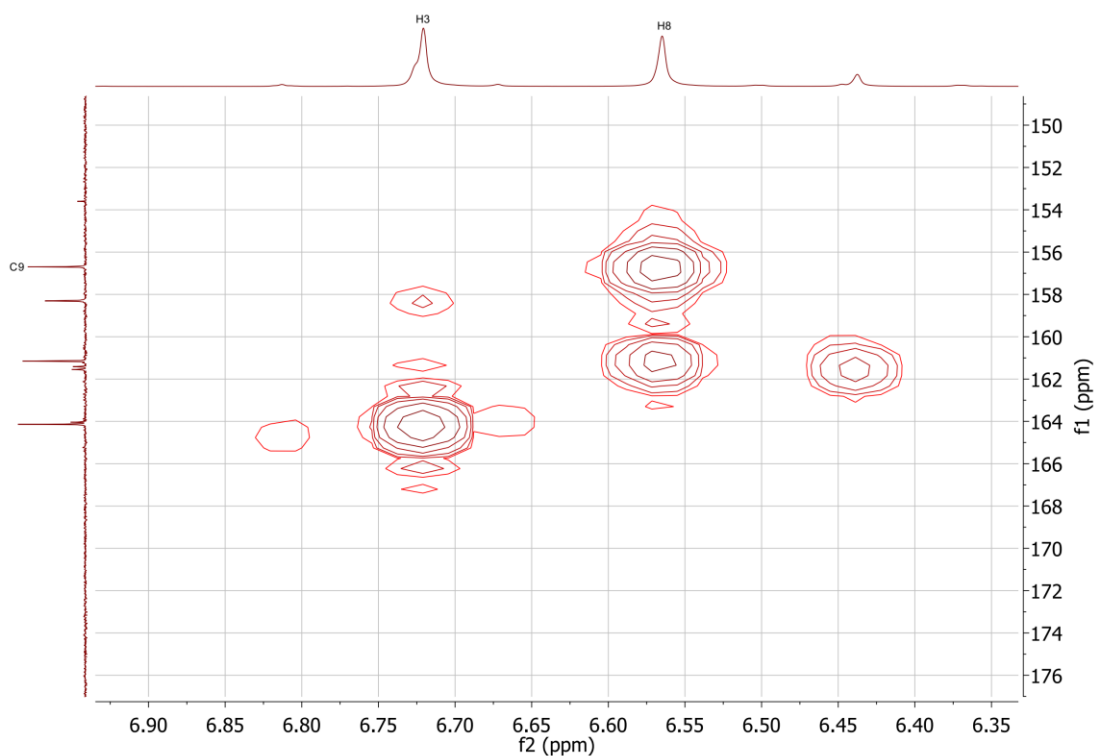


Figure A53 The HMBC (expansion) correlation ( $\text{CDCl}_3$ ) of **60**.

## Mass Spectrum List Report

### Analysis Info

Analysis Name D:\Data\Data Service\180917\_pos\_T46..d  
 Method NV\_pos\_0.3min\_profile\_1segment\_lowNubulizerDrygas.m  
 Sample Name 180917\_pos\_T46.  
 Comment

Acquisition Date 9/17/2018 3:12:45 PM

Operator CU.  
 Instrument / Ser# micrOTOF-Q II 10335

### Acquisition Parameter

Source Type	ESI	Ion Polarity	Positive	Set Nebulizer	0.4 Bar
Focus	Not active	Set Capillary	4000 V	Set Dry Heater	200 °C
Scan Begin	50 m/z	Set End Plate Offset	-500 V	Set Dry Gas	4.0 l/min
Scan End	1500 m/z	Set Collision Cell RF	150.0 Vpp	Set Divert Valve	Waste

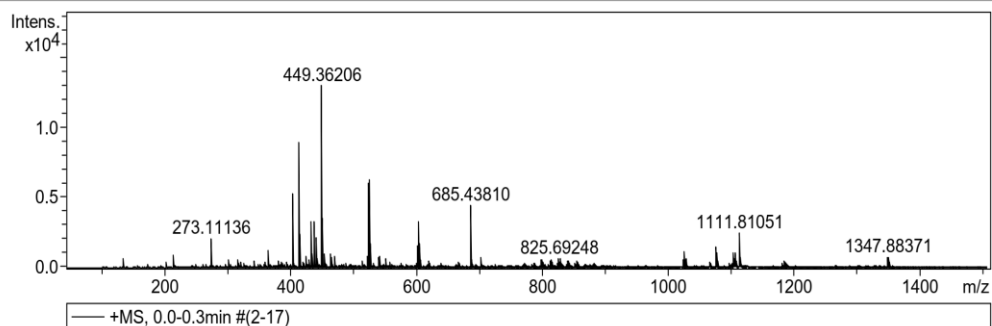


Figure A54 The HR-ESI-MS of **61**.

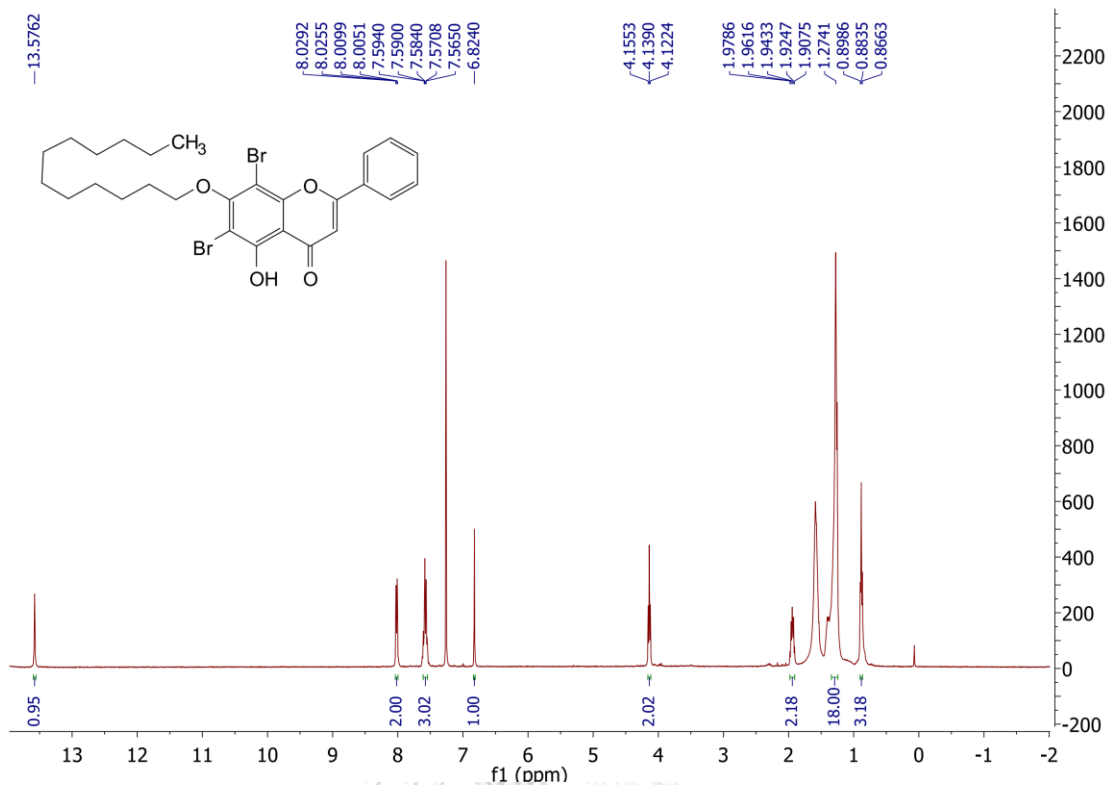


Figure A55 The  $^1\text{H}$  NMR spectrum ( $\text{CDCl}_3$ , 400 MHz) of **61**.

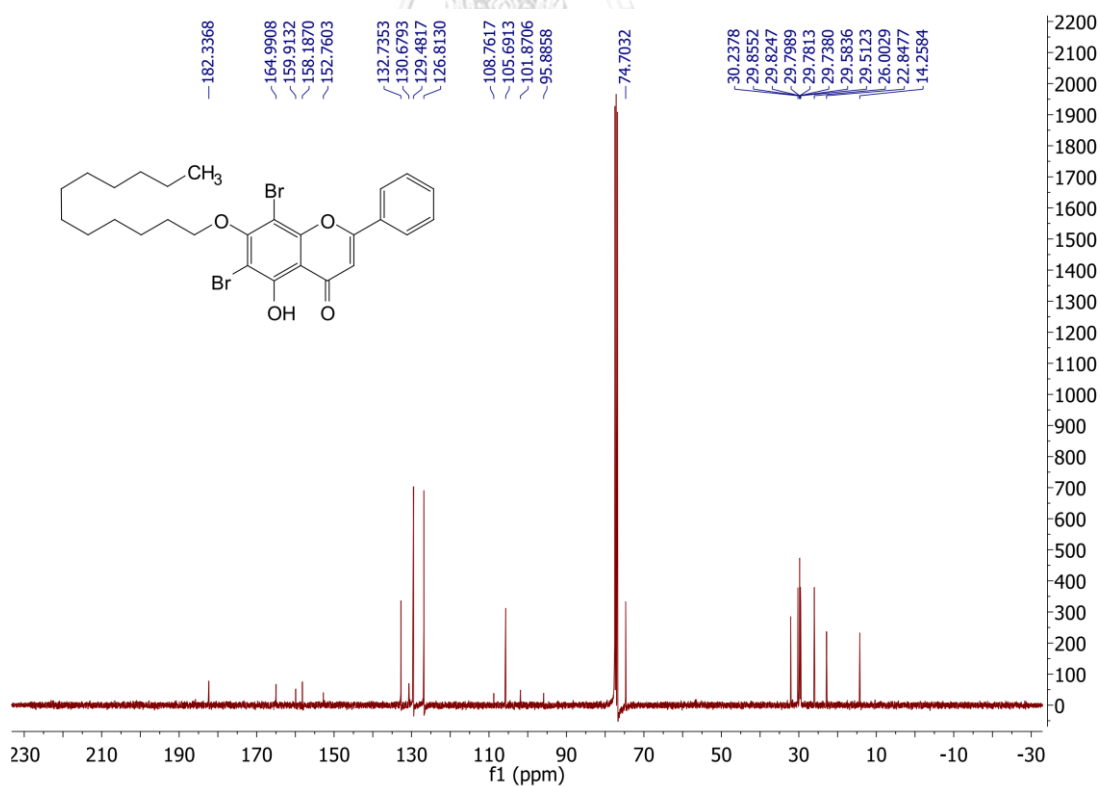


Figure A56 The  $^{13}\text{C}$  NMR spectrum ( $\text{CDCl}_3$ ) of **61**.

## Mass Spectrum List Report

### Analysis Info

Analysis Name	D:\Data\Data Service\180924_pos_T47.d	Acquisition Date	9/24/2018 3:01:16 PM
Method	NV_pos_0.3min_profile_1segment_lowNubulizerDrygas.m	Operator	CU.
Sample Name	180924_pos_T47	Instrument / Ser#	microTOF-Q II 10335
Comment			

### Acquisition Parameter

Source Type	ESI	Ion Polarity	Positive	Set Nebulizer	0.4 Bar
Focus	Not active	Set Capillary	4000 V	Set Dry Heater	200 °C
Scan Begin	50 m/z	Set End Plate Offset	-500 V	Set Dry Gas	4.0 l/min
Scan End	1500 m/z	Set Collision Cell RF	150.0 Vpp	Set Divert Valve	Waste

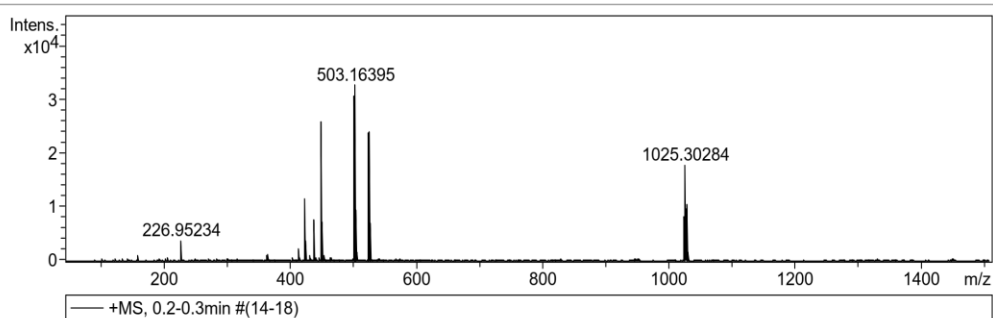


Figure A57 The HR-ESI-MS of **62**.

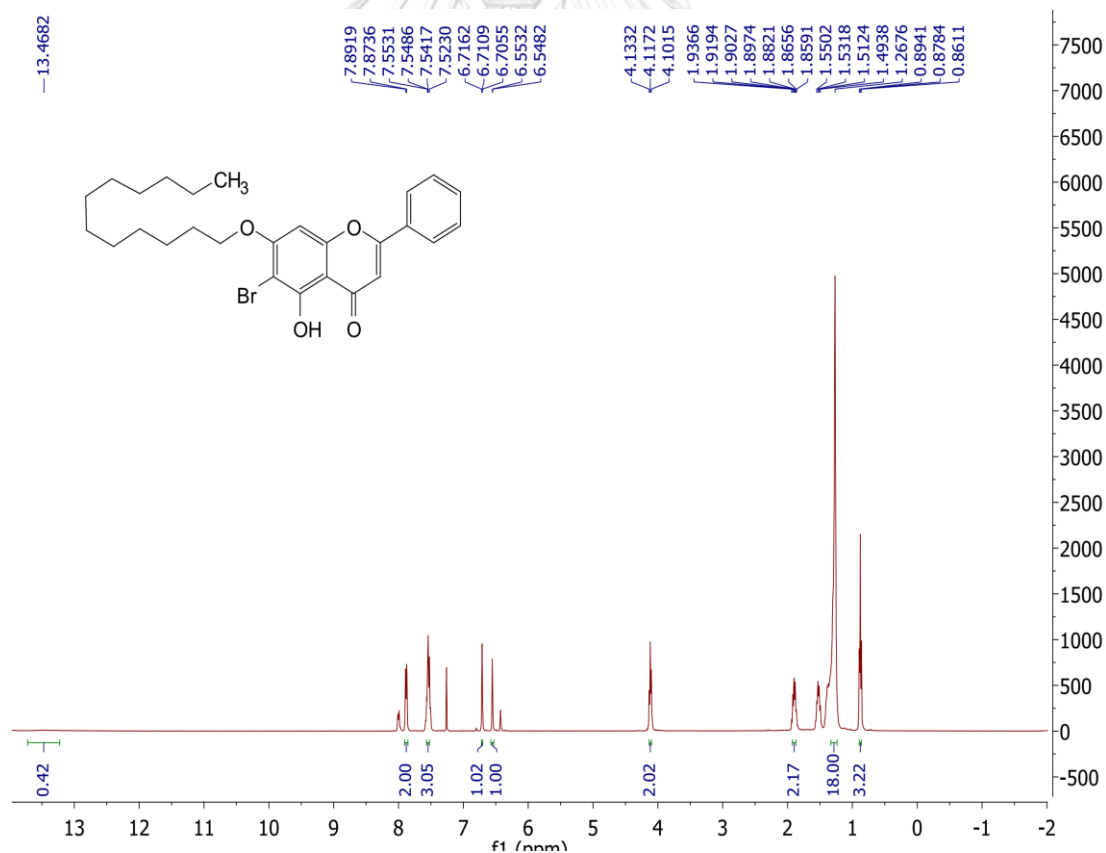


Figure A58 The  $^1\text{H}$  NMR spectrum ( $\text{CDCl}_3$ ) of **62**.



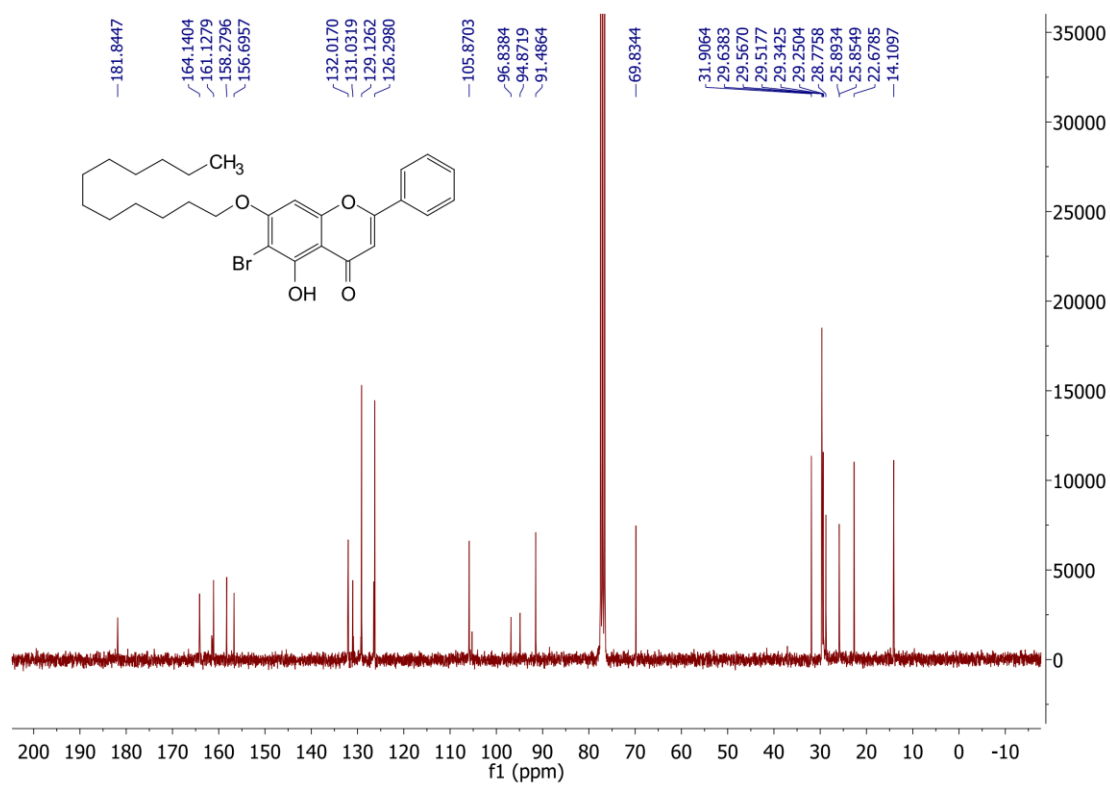


Figure A59 The  $^{13}\text{C}$  NMR spectrum ( $\text{CDCl}_3$ ) of 62.

## VITA

**NAME** Thao Nguyen Thanh Huynh

**DATE OF BIRTH** 09 April 1994

**PLACE OF BIRTH** Ho Chi Minh city, Viet Nam

**INSTITUTIONS ATTENDED** Department of Chemistry, University of Education, HCMC,  
Viet Nam

**HOME ADDRESS** Room 1503, Chula International House, Chulalongkorn  
University, Bangkok, Thailand

